Numerical simulations of relativistic jets emission and dynamics

Petar Mimica [1, @]

1 : Department of Astronomy and Astrophysics, University of Valencia (UV-DAA) - ***Website***

C/ Dr. Moliner 50 46100 Burjassot (Valencia) - Spain

In the recent decades simulations have become an indispensable tool for modeling and understanding many of the jet aspects. After introducing modern numerical methods used to perform relativistic jet simulations, I give an overview of selected topics where numerically computing an observational signature of a relativistic jet simulation is very important.

Subject :	:	oral
Topics	:	Astrophysics
Topics	:	Numerical simulations

Numerical simulations of relativistic jet emission and dynamics

Petar Mimica

Department of Astronomy and Astrophysics

University of Valencia

in collaboration with:

Miguel-Ángel Aloy (Valencia)

Carlos Cuesta-Martínez (Valencia)

Dimitrios Giannios (Purdue)

Brian Metzger (Columbia)

Outline

- Introduction: simulating jet dynamics and emission
- Jets in blackbody-dominated gamma-ray bursts
- Jets from tidal disruption events
- Conclusions

Hydrodynamic simulation: an indispensable tool

- events taking place in jets extraordinarily dynamic and complex
- jet physics: interplay of processes on a large range of length and time scales
- (magneto)hydrodynamical viewpoint accurate enough
- jets modelled as fluids: relativistic generalisation of Euler equations appropriate
- most commonly used systems of equations:
  - relativistic hydrodynamics (RHD)
  - relativistic magnetohydrodynamics (RMHD)
  - general relativistic hydrodynamics (GRHD)
  - general relativistic magnetohydrodynamics (GRMHD)
  - resistive relativistic magnetohydrodynamics (RRMHD)
  - ...
- advances in numerical techniques and supporting hardware and software make it possible to simultaneously perform *HD simulations *and* compute corresponding synthetic images, spectra and light curves *and* compare to observations

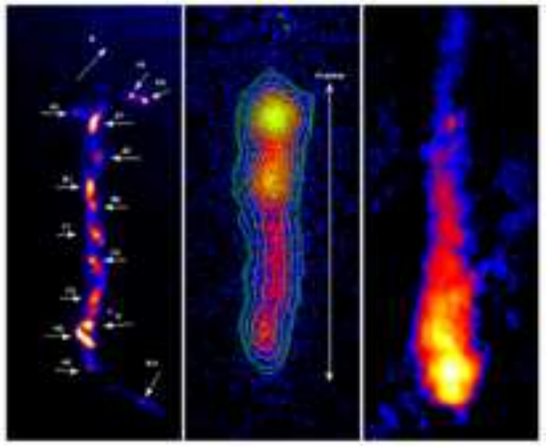

Simulating Relativistic Jets

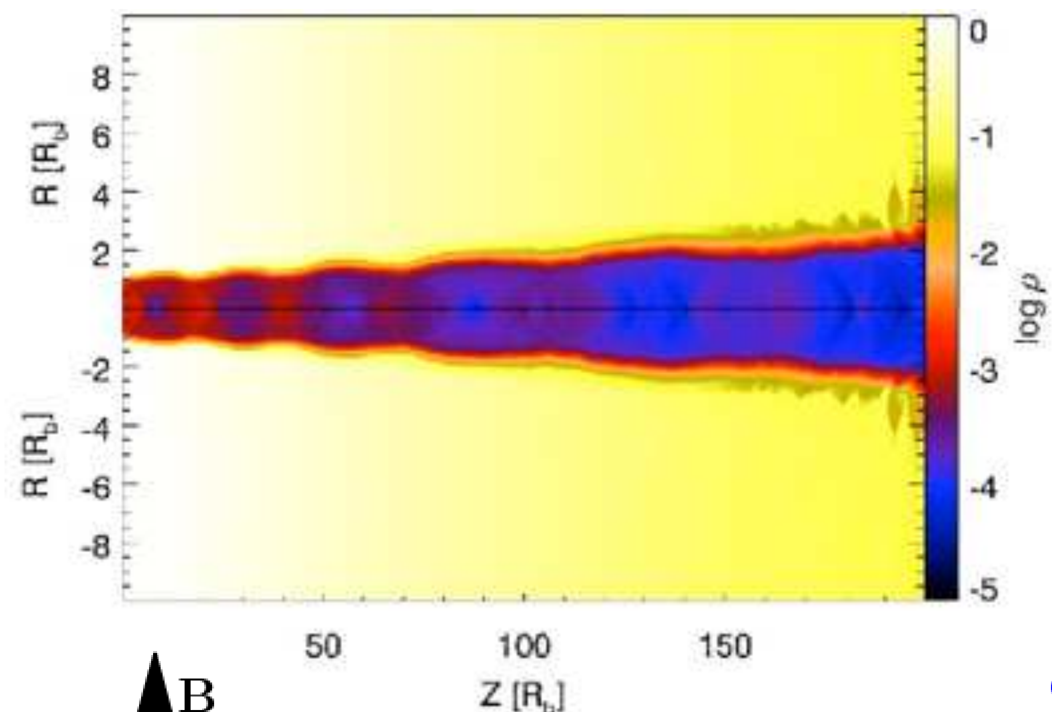

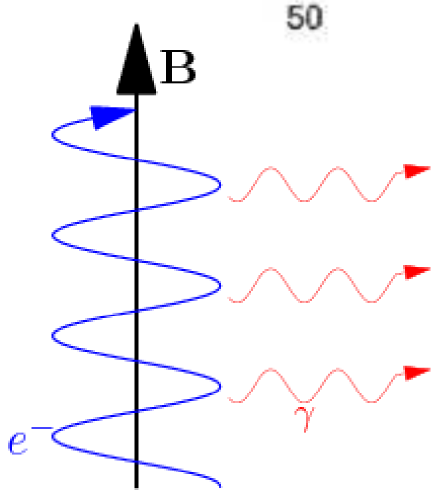

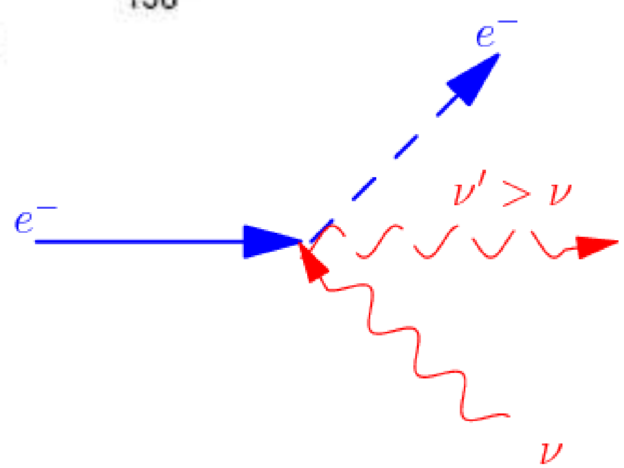

1. relativistic (magneto) hydrodynamics simulation
   - finite-volumes
   - method of lines
   - shock-capturing
   - approximate Riemann solver

2. non-thermal particle evolution and emission
   - phenomenological shock acceleration
   - radiative and adiabatic loses
   - semi-analytic electron-kinetic eq. solver
   - spatial advection

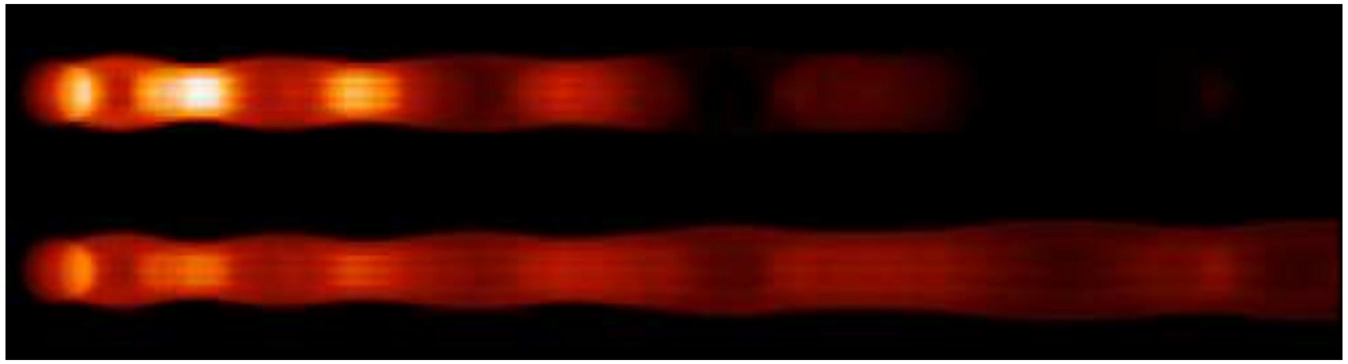

3. radiative transfer
   - time-dependent emission and absorption
   - relativistic effects (beaming, Doppler)
   - light-travel times
   - synchrotron, inverse-Compton scattering

1. Hydrodynamic Simulations

MRGENESIS (Aloy *et al.* '99 ApJS , Leismann *et al.* '05, A&A, Mimica *et al.* '07, '09 A&A)

- finite volume approach
- method of lines: separate semi-discretization of space and time
- time advance: TVD Runge-Kutta methods of 2nd and 3rd order
- high-resolution shock-capturing scheme
- inter-cell reconstruction: PPM
- numerical fluxes: Marquina, HLLE, HLLC
- RMHD: constraint transport to conserve $\nabla \mathbf{B}$
- orthogonal coordinate systems: Cartesian, cylindrical, spherical
- MPI + OpenMP: scales up to 10K cores
- HDF5 library for parallel I/O

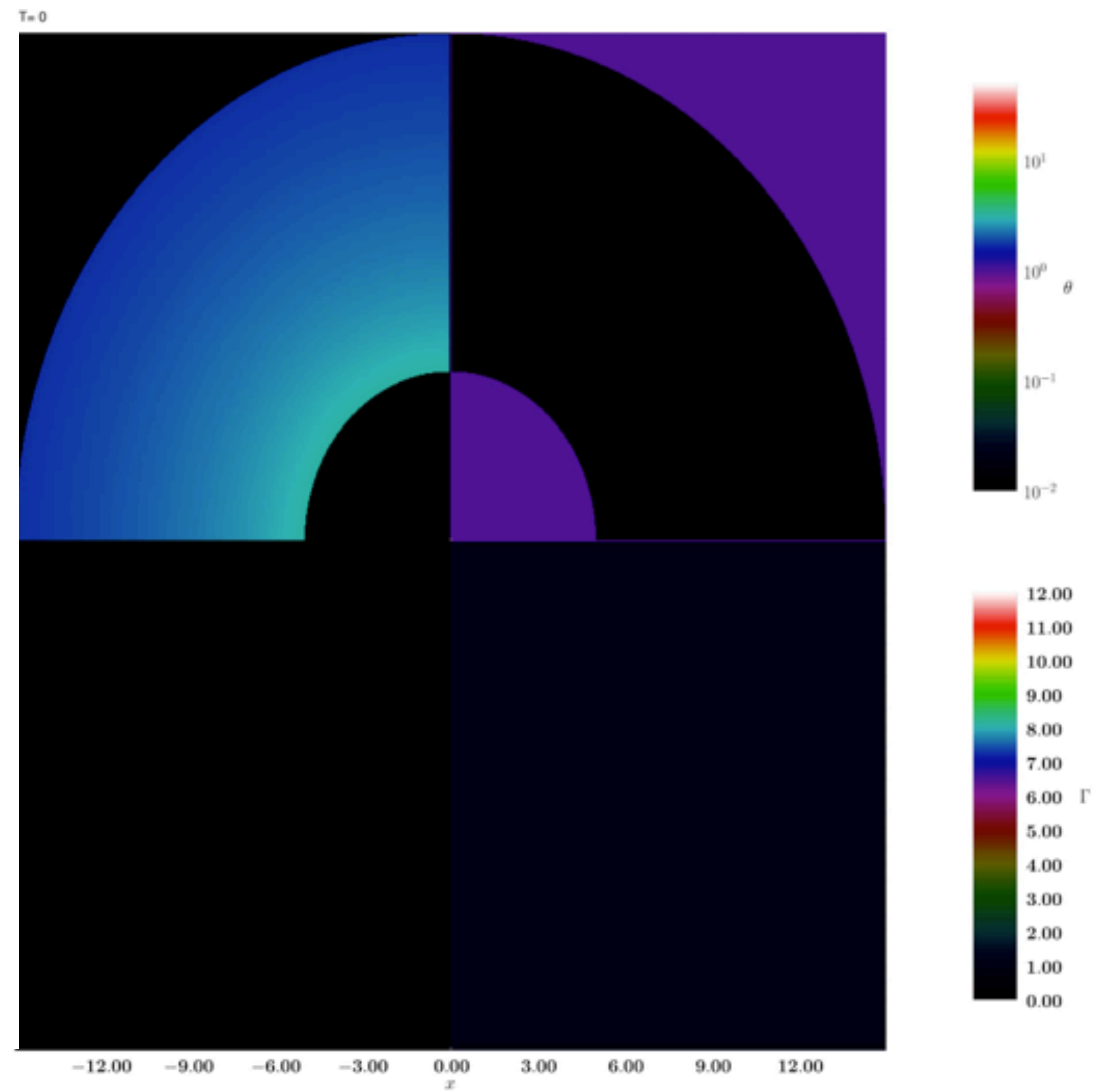

Our scheme is compatible with other codes: *Ratpenat* (M. Perucho), *Aenus* (M. Obergaulinger)

1. Hydrodynamic Simulations

MRGENESIS (Aloy *et al.* '99 ApJS , Leismann *et al.* '05, A&A, Mimica *et al.* '07, '09 A&A)

- finite volume approach
- method of lines: separate semi-discretization of space and time
- time advance: TVD Runge-Kutta methods of 2nd and 3rd order
- high-resolution shock-capturing scheme
- inter-cell reconstruction: PPM
- numerical fluxes: Marquina, HLLE, HLLC
- RMHD: constraint transport to conserve ∇**B**
- orthogonal coordinate systems: Cartesian, cylindrical, spherical
- MPI + OpenMP: scales up to 10K cores
- HDF5 library for parallel I/O

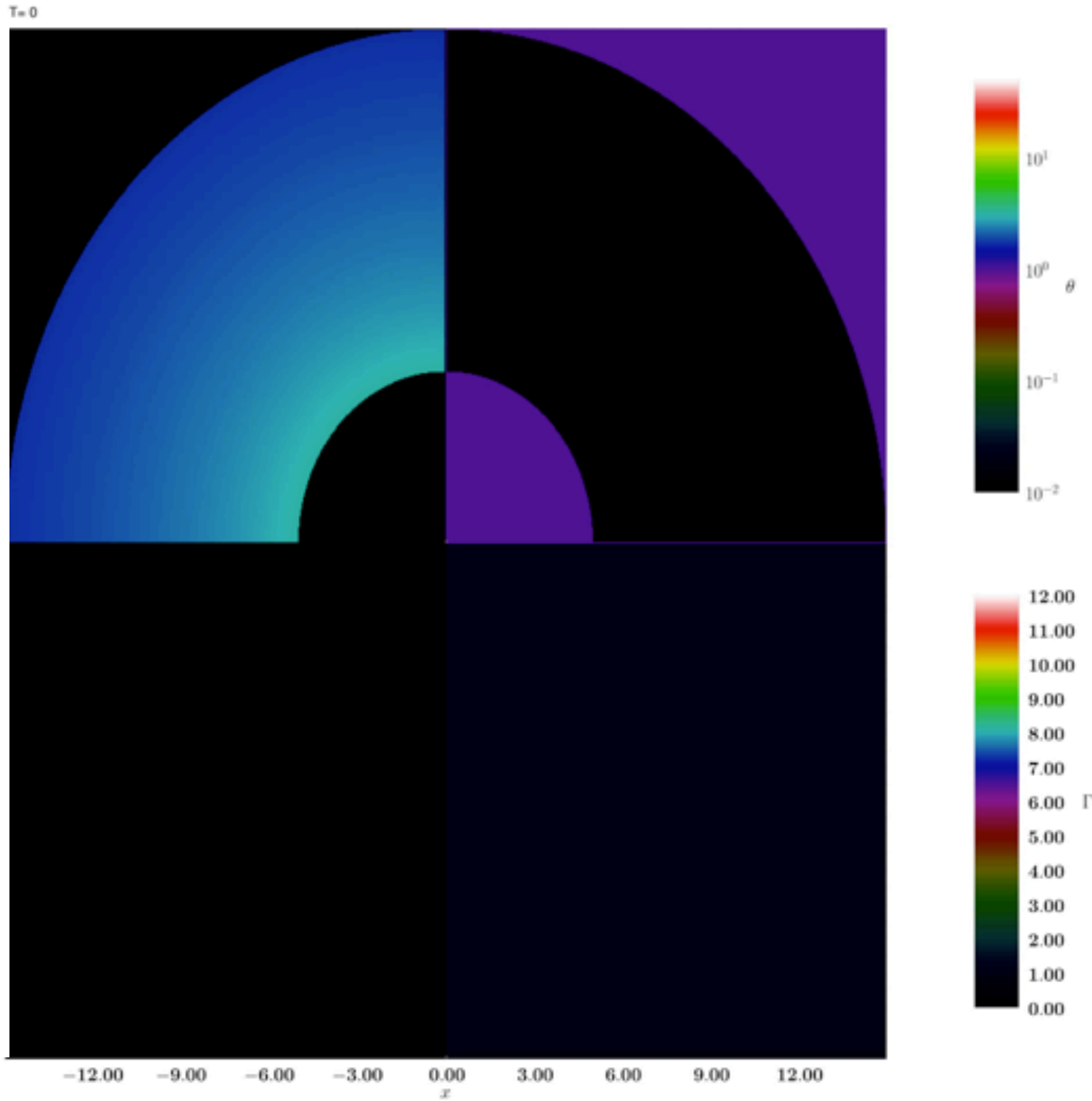

Our scheme is compatible with other codes: *Ratpenat* (M. Perucho), *Aenus* (M. Obergaulinger)

2. Non-thermal Particles

- underlying jet fluid ("thermal plasma") not directly observable from Earth
- population of high-energy non-thermal particles in the jet responsible for observed emission

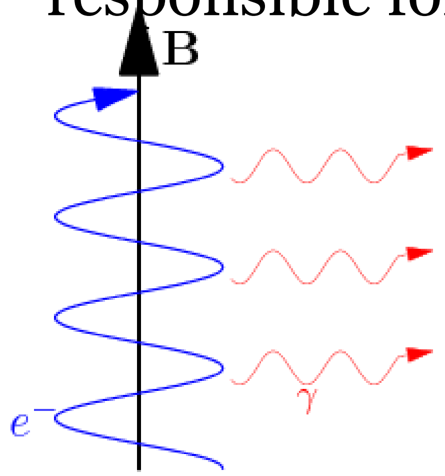

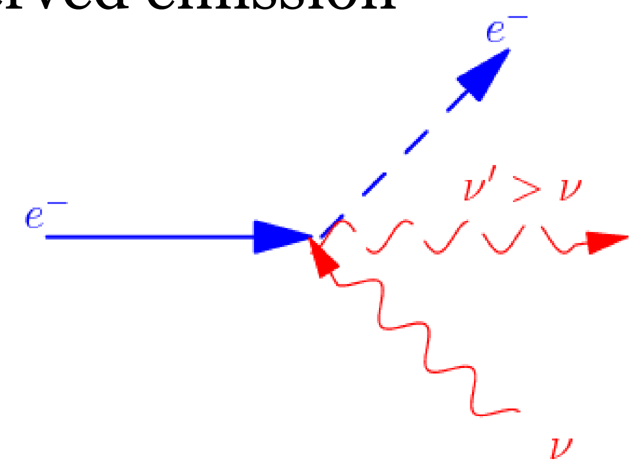

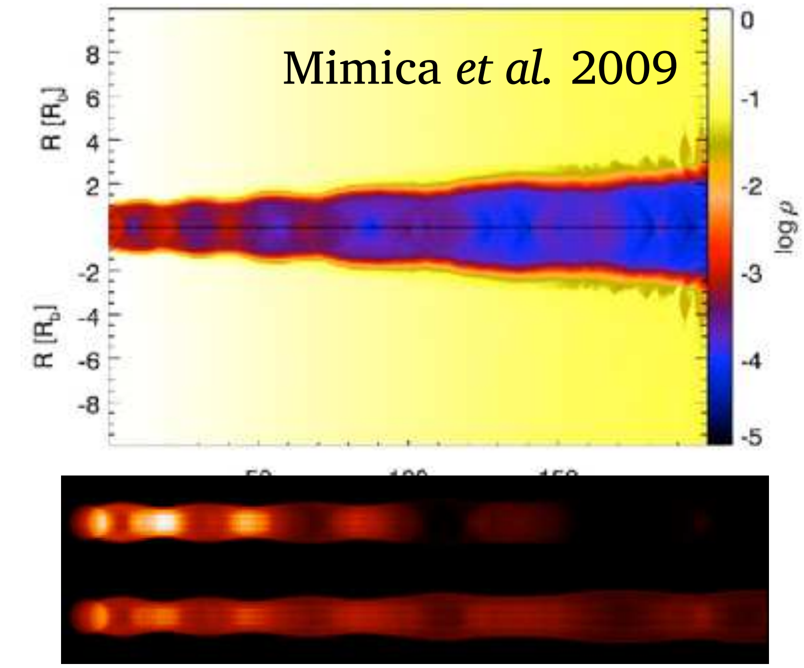

Mimica *et al.* 2009

Non-Thermal Particle Algorithms Classification

	$\tau \ll 1$	$\tau \gtrsim 1$
local	• X & γ-ray afterglows • blazars emission	• stationary radio emission
transport	• opt. & UV afterglows • X-ray TDE jets	• radio jets • late-time radio afterglows

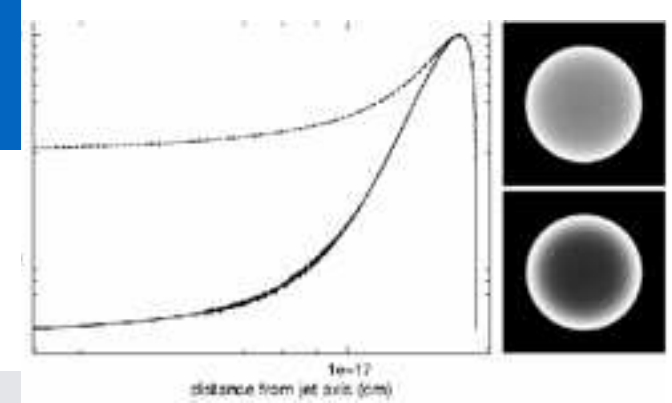

van Eerten *et al.* 2011

3. Radiative Transfer

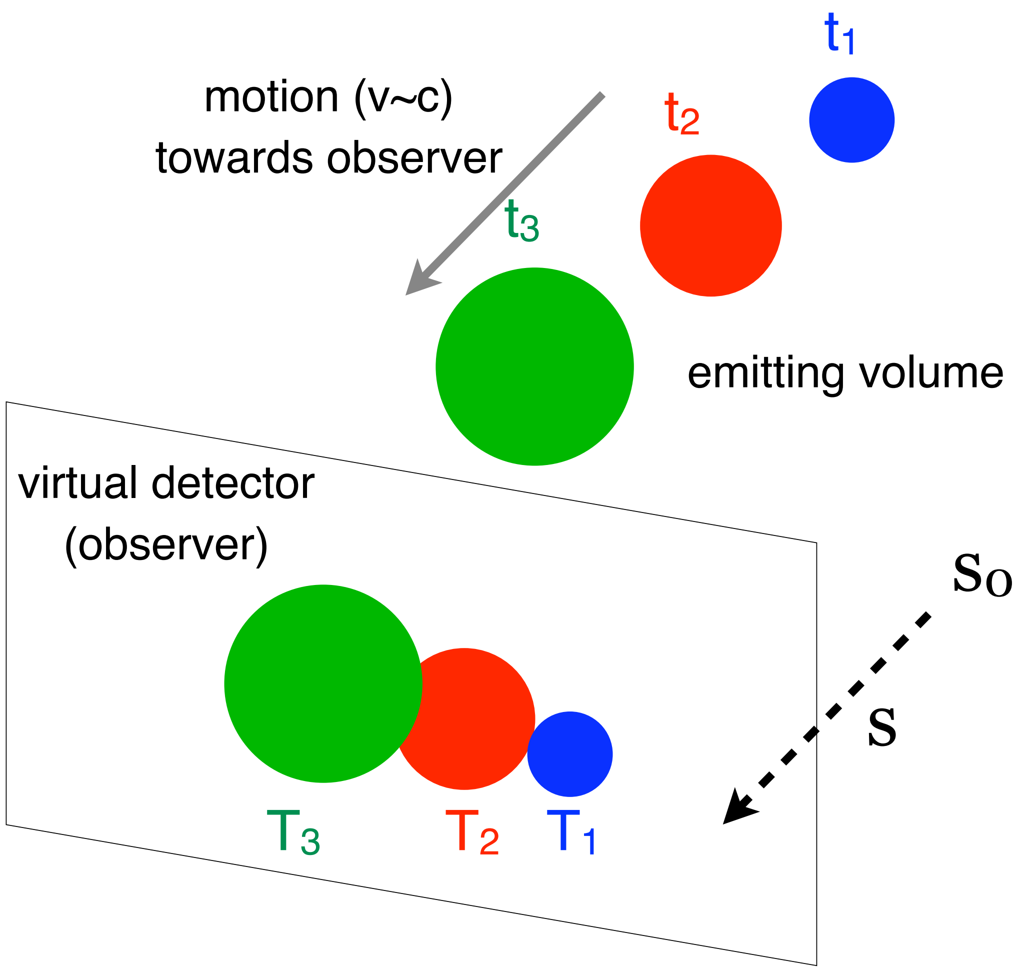

- for a fixed observer time T, need to process the **whole** spacetime evolution to compute a **single** virtual image
- tightly coupled, highly non-local problem
- **5D problem**:
  - virtual detector image **(x, y)**
  - observation time **T**
  - observation frequency **ν**
  - contributions along the line of sight **s**

synchrotron, inverse-Compton

synchrotron self-absorption

I_ν : intensity j_ν α_ν : emission, absorption

T : observer time t : jet evolution time

s : path towards the detector

radiation transfer equation:

$$\frac{\mathrm{d}I_\nu}{\mathrm{d}s} = j_\nu + \alpha_\nu I_\nu$$

$$s = c(t - T) + s_0$$

for a fixed T, equation gives an isochrone *(s, t)* along each line of sight

- SPEV (Mimica et al., Astrophysical J. **696** (2009) 1142) :
  - non-thermal electron transport and evolution equations
  - time- and frequency-dependent radiative transfer in a dynamically changing background
  - parallelization: OpenMP (needs lot of shared memory)

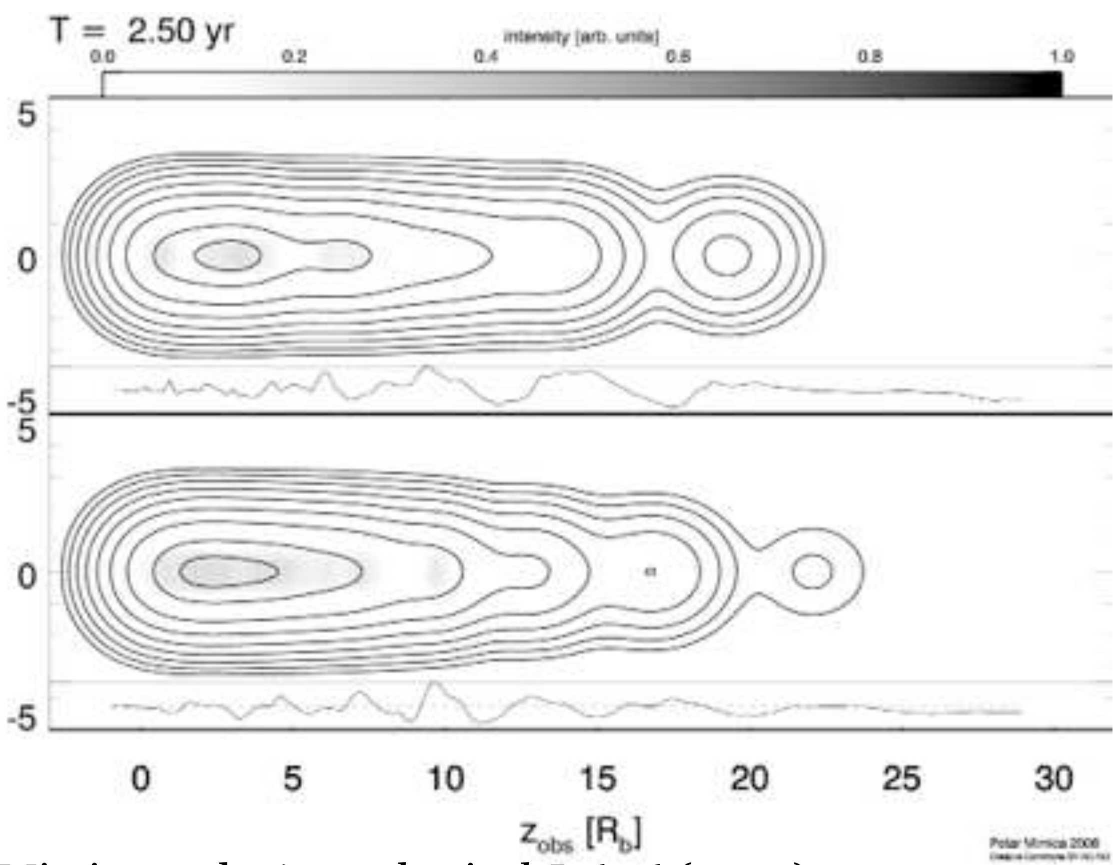

Mimica et al., *Astrophysical J.* **696** (2009) 1142

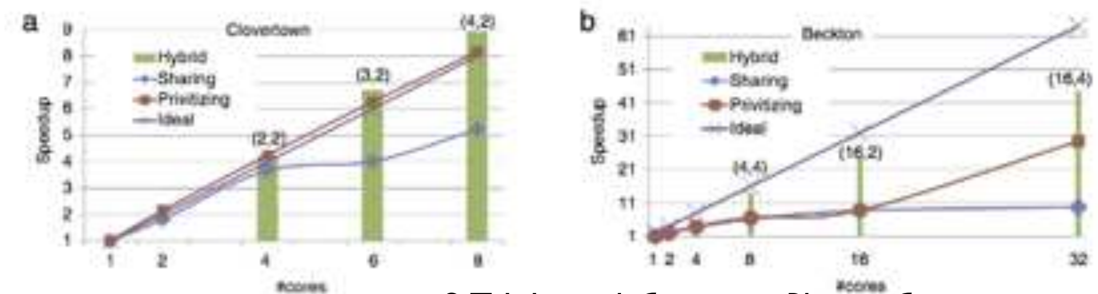

S. Tabik *et al. Computer Physics Communications* ***183*** *(2012) 1937*

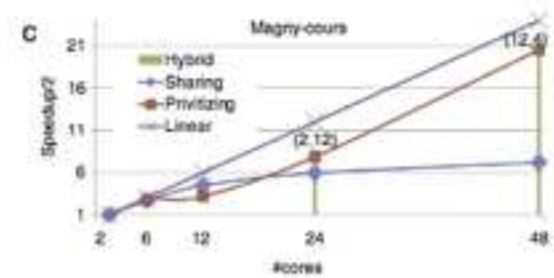

SPectral ***EV***olution Code

- SPEV (Mimica et al., Astrophysical J. **696** (2009) 1142) :
  - non-thermal electron transport and evolution equations
  - time- and frequency-dependent radiative transfer in a dynamically changing background
  - parallelization: OpenMP (needs lot of shared memory)

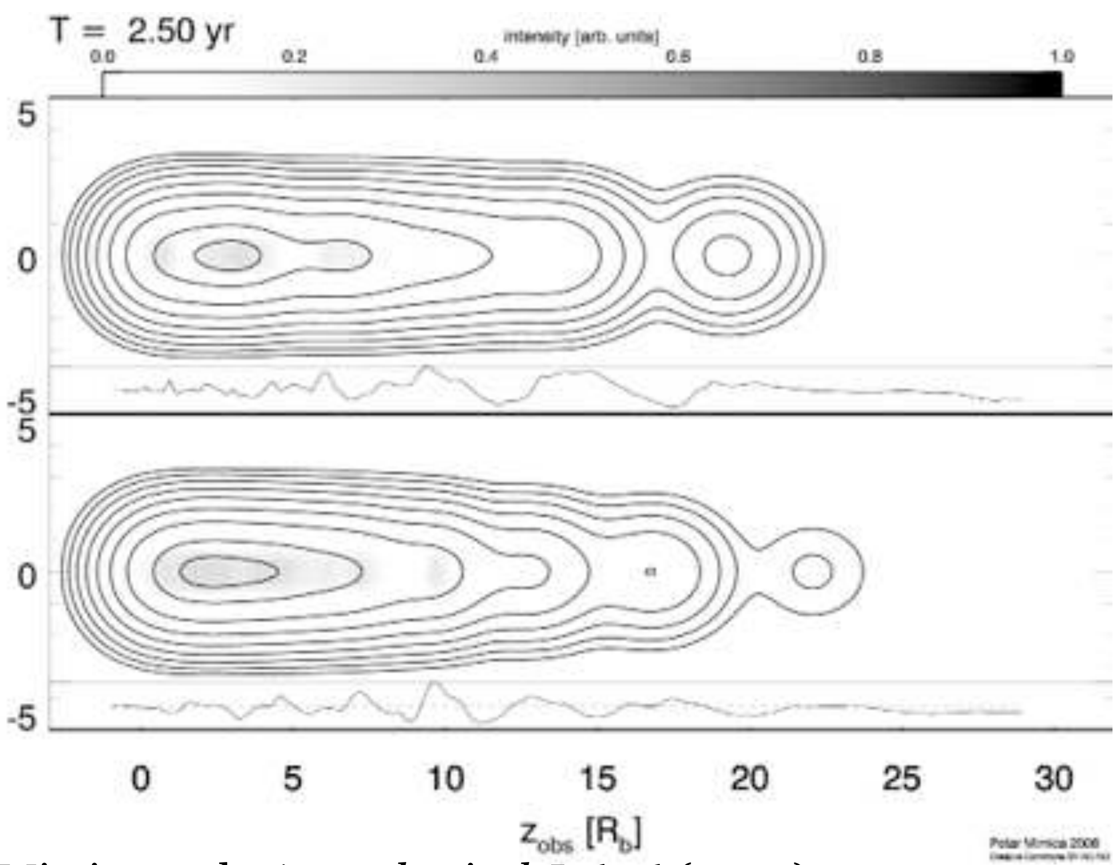

Mimica et al., *Astrophysical J*. **696** (2009) 1142

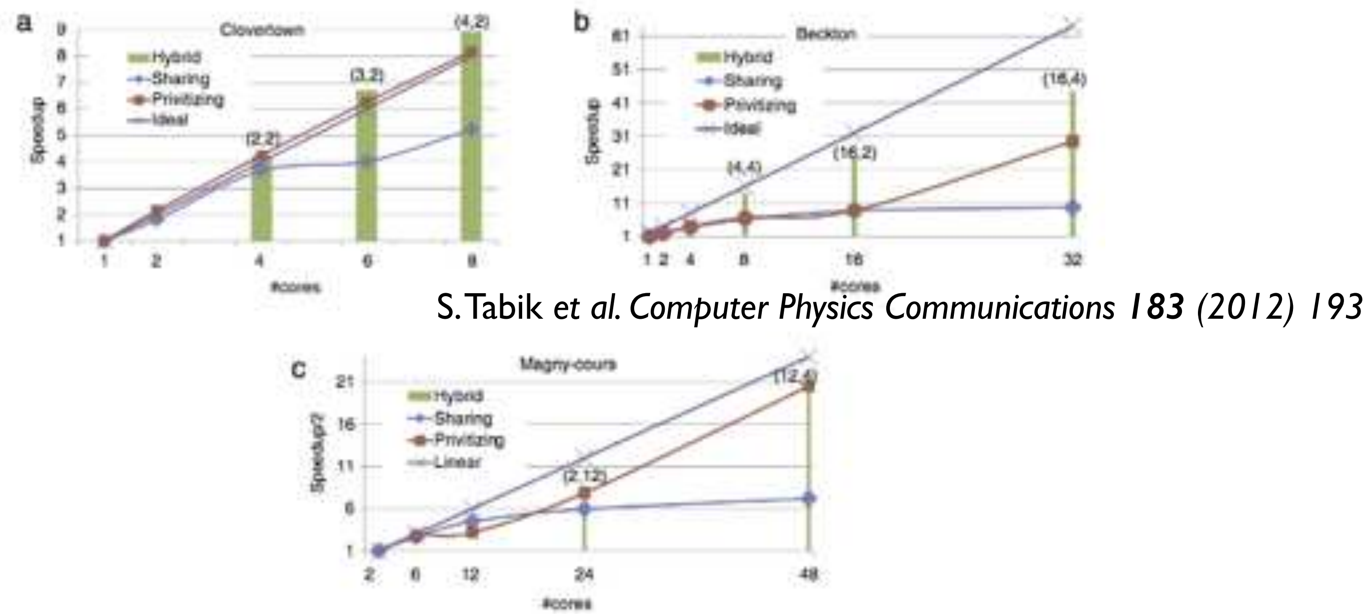

S.Tabik *et al. Computer Physics Communications* ***183*** *(2012) 1937*

SPectral ***EV***olution Code

- SPEV (Mimica et al., Astrophysical J. **696** (2009) 1142) :
  - non-thermal electron transport and evolution equations
  - time- and frequency-dependent radiative transfer in a dynamically changing background
  - parallelization: OpenMP (needs lot of sha

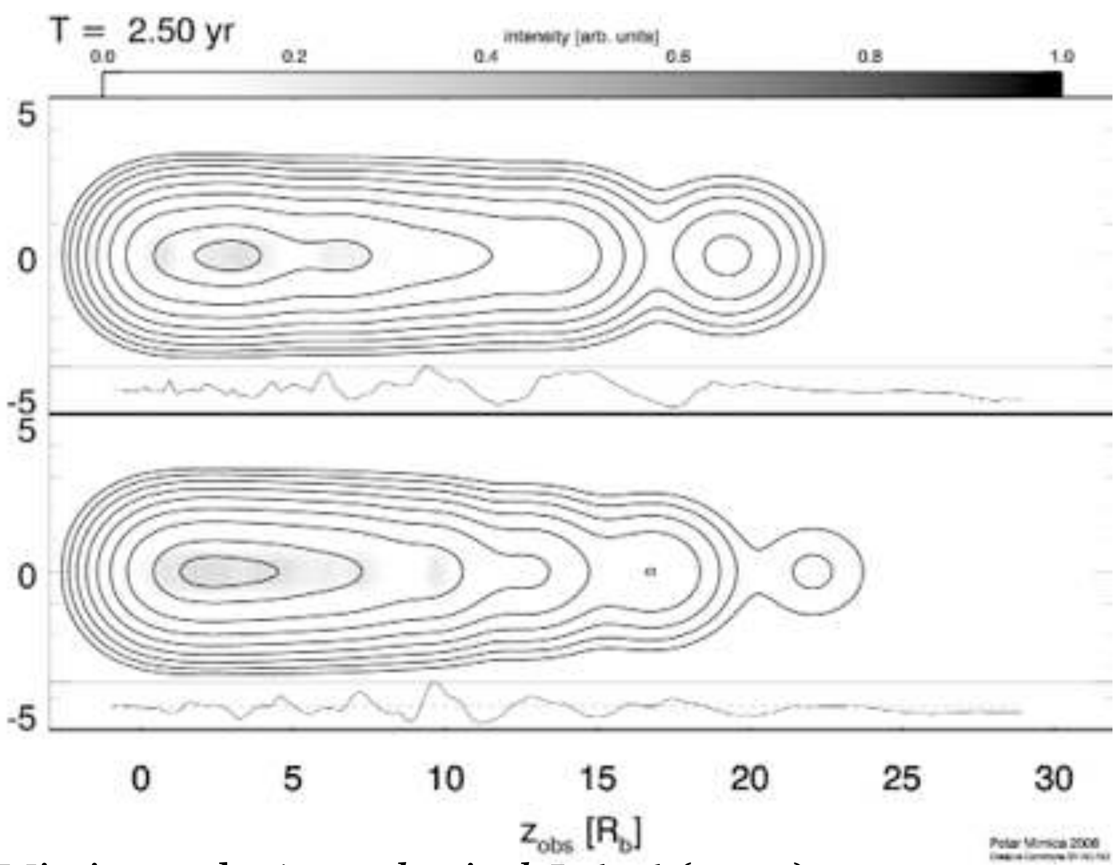

Mimica et al., *Astrophysical J.* **696** (2009) 1142

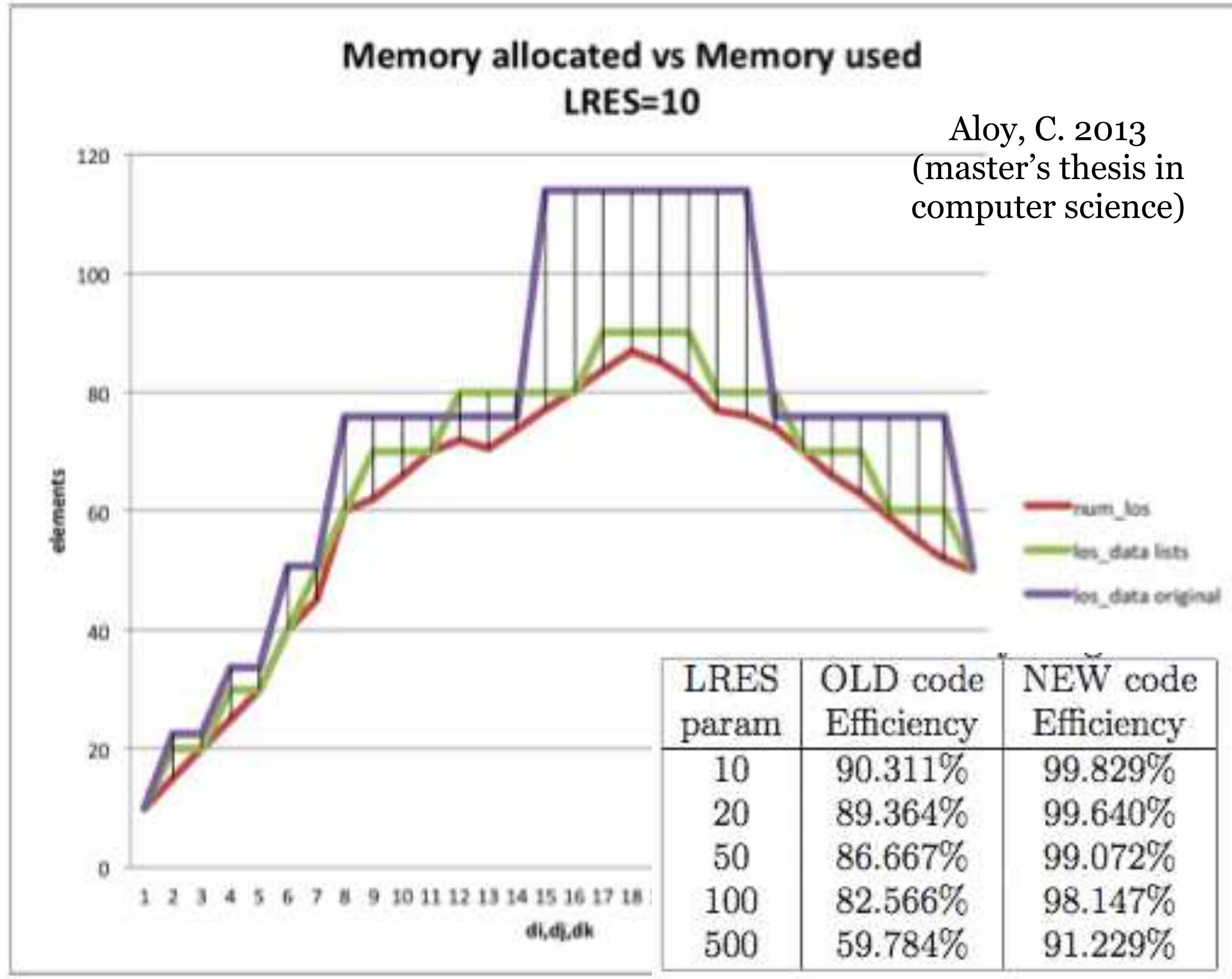

Aloy, C. 2013 (master's thesis in computer science)

LRES param	OLD code Efficiency	NEW code Efficiency
10	90.311%	99.829%
20	89.364%	99.640%
50	86.667%	99.072%
100	82.566%	98.147%
500	59.784%	91.229%

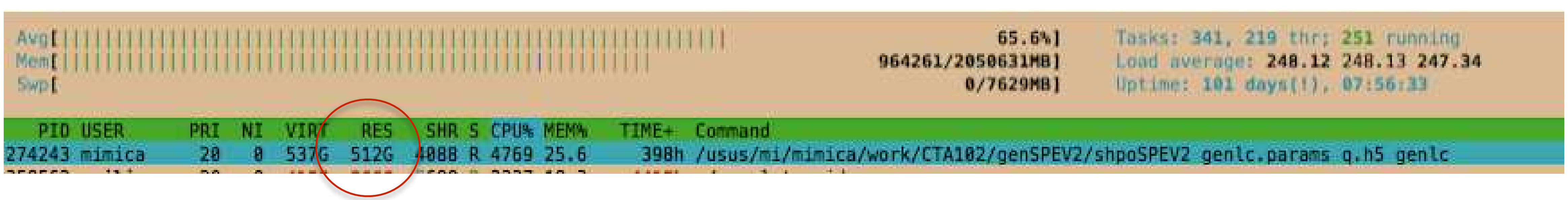

Jet Simulations Building Blocks

easy — difficult — very difficult

treatment of hydrodynamic evolution

Riemann solver
(blazar, GRB internal shocks)

RHD
(AGN jets, TDE jets)

RMHD
(GRBs, blazars)

RRMHD
(non-ideal dissipative processes in blazars)

treatment of non-thermal particles

1D transport
(blazar/GRB internal shocks, on-axis GRB blast wave)

2D transport
(radio maps, off-axis light curves)

3D transport
(?)

treatment of radiative processes

Synchrotron + EC
(radio maps, blazar X light curves, GRB afterglows, TDE radio transients)

Syn. + EC + SSC
(blazar radio-to-γ-ray light curves and spectra)

additional
(blazar leptonic-hadronic models?)

GRB 101225A - Observations

Why study it?

- γ-ray emission exceptionally long-lived (T$_{90}$ ~ 7.000 s, Levan+ ’14).
- no classical afterglow: the X-ray and UVOIR emission following the GRB is best fitted with BB (+ PL).
- member of new (sub-)class of GRBs??

Black-body dominated GRBs (BBD-GRBs):

  - BB component in optical/X-ray spectrum (GRB 090618, Page+ 2011; GRB 060218 Campana+ 2006)
  - classical afterglow suppressed

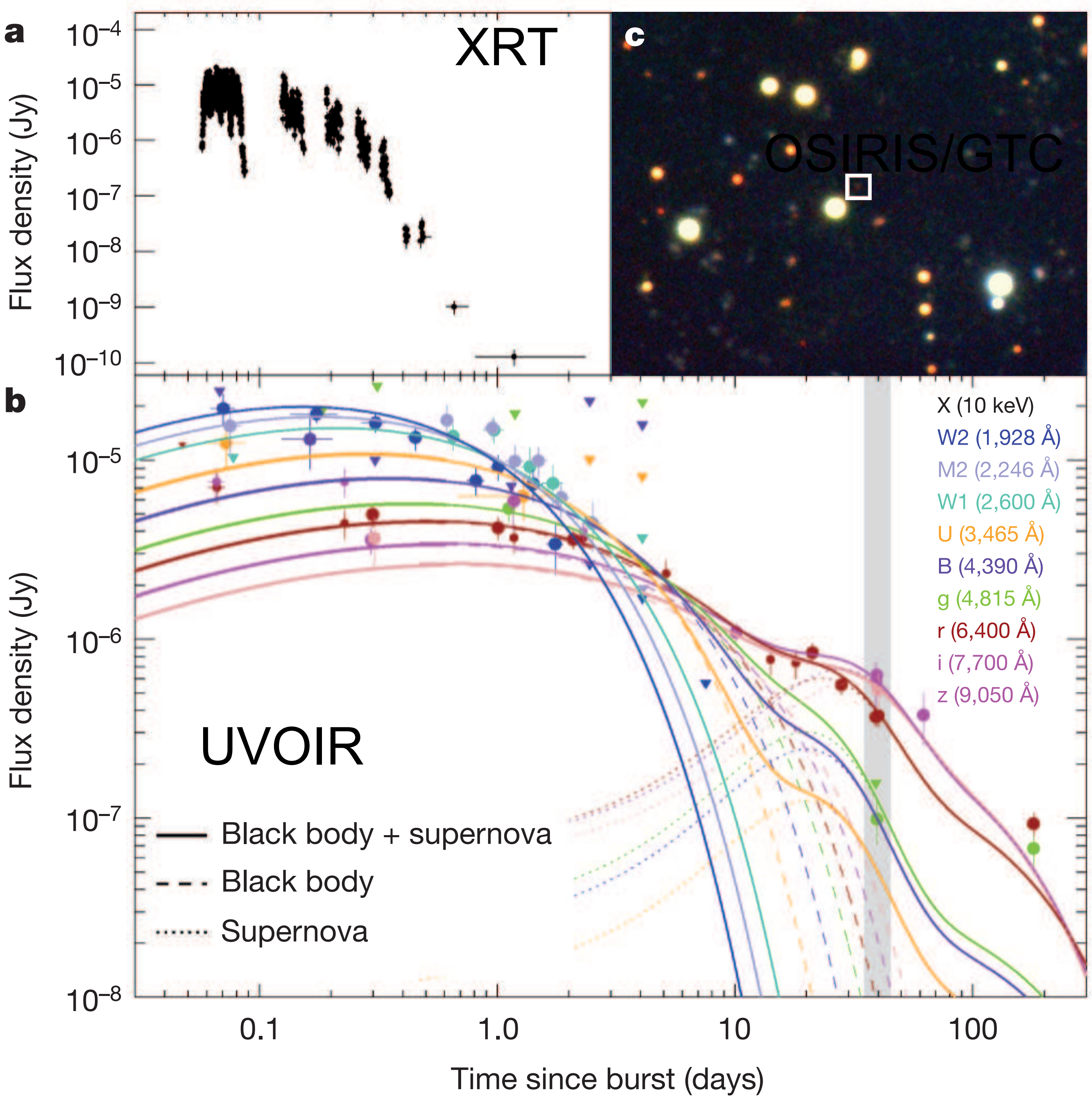

(Thöne et al. 2011)

GRB 101225A - Progenitor System

- **Thöne et al., 2011**: progenitor system is a **He-star / NS merger**. (Fryer&Woosley, ’98, Zhang & Fryer ’01; Barkov & Komissarov ’10, ‘11)
- model properties:
  - long-duration central engine
  - structured, high-density circumburst environment
  - tidally ejected hydrogen shell (CE-shell): located at ~ 10^{14} cm, non-uniform

Plane perpendicular to the orbital motion

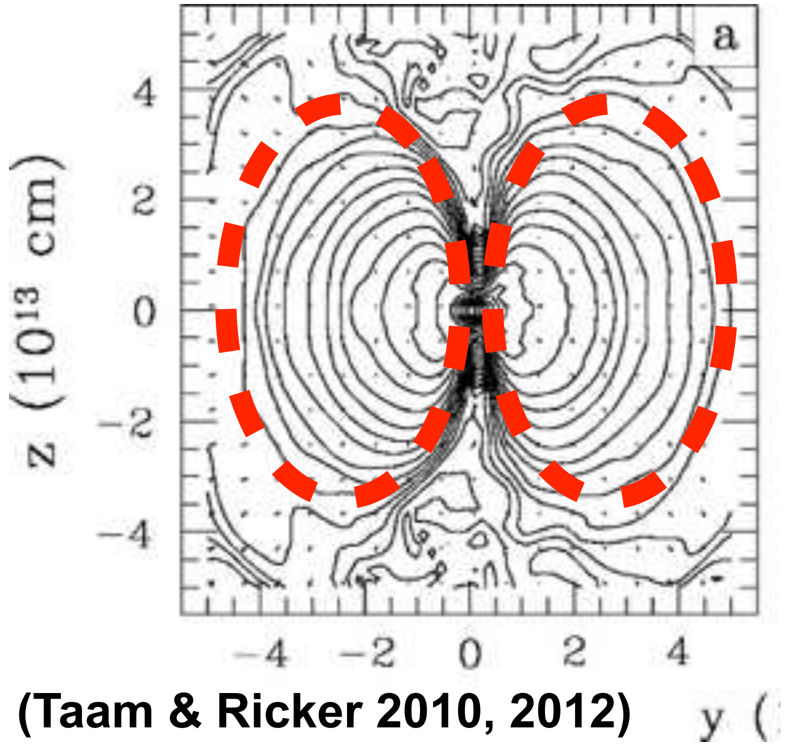

(Taam & Ricker 2010, 2012)

GRB 101225A - Progenitor System

- **Thöne et al., 2011**: progenitor system is a **He-star / NS merger**. (Fryer&Woosley, '98, Zhang & Fryer '01; Barkov & Komissarov '10, '11)
- model properties:
  - long-duration central engine
  - structured, high-density circumburst environment
  - tidally ejected hydrogen shell (CE-shell): located at ~ 10^{14} cm, non-uniform

Plane perpendicular to the orbital motion

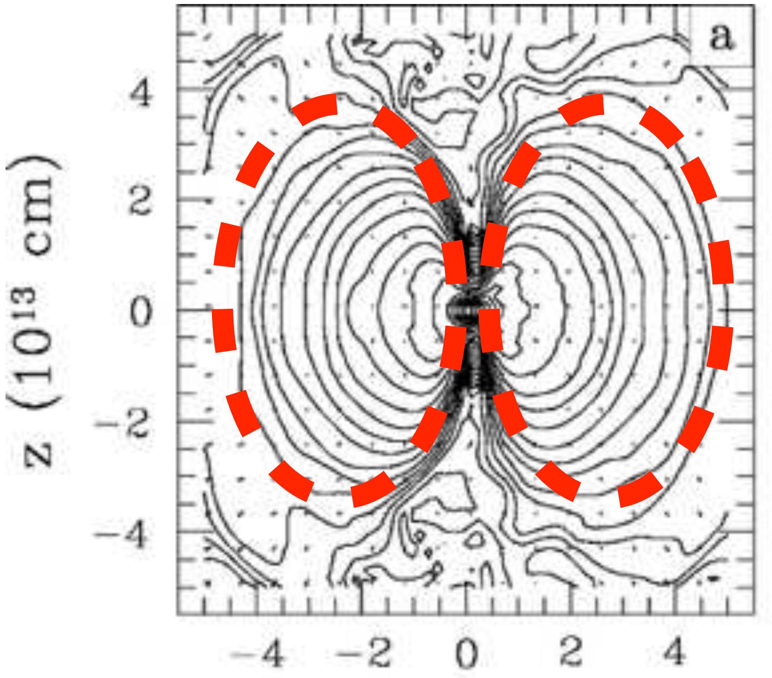

(Taam & Ricker 2010, 2012)

GRB 101225A - Progenitor System

- **Thöne et al., 2011**: progenitor system is a **He-star / NS merger**. (Fryer&Woosley, ’98, Zhang & Fryer ’01; Barkov & Komissarov ’10, ‘11)
- model properties:
  - long-duration central engine
  - structured, high-density circumburst environment
  - tidally ejected hydrogen shell (CE-shell): located at ~ 10^{14} cm, non-uniform

Plane perpendicular to the orbital motion

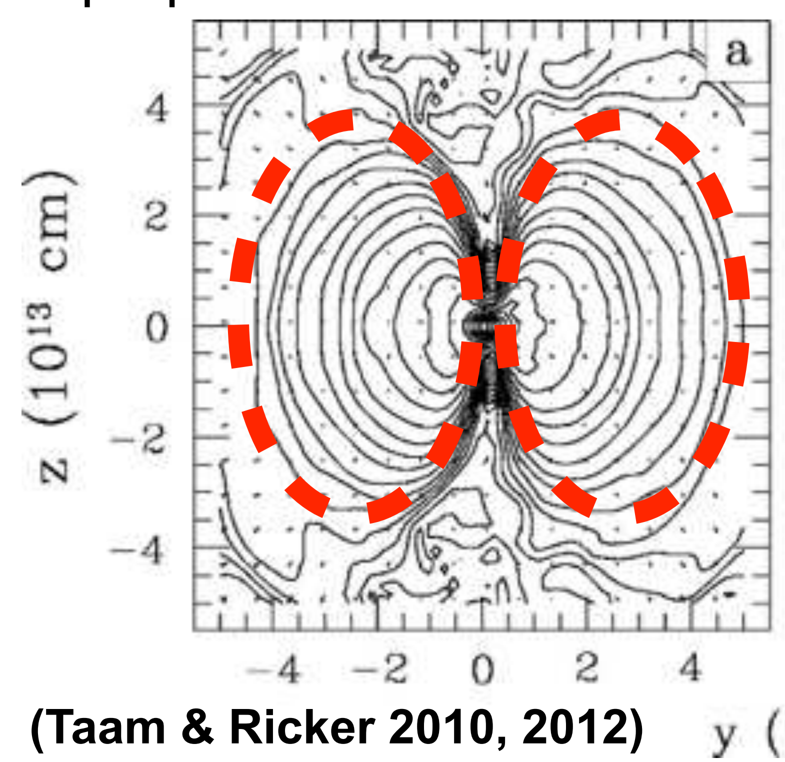

(Taam & Ricker 2010, 2012)

Jet and Shell Model

- redshift z = 0.847 (Levan et al. 2013)
- we perform a number of simulations covering a range of parameters

JET:

- **Isotropic energy** of the jet, $\mathbf{E_{iso} = 4x10^{53}}$ **erg**
- **Opening angle**: θ_j = 14º,17º
- True jet energy, $E_{jet} \sim 10^{51} - 10^{52}$ erg
- Injection radius, $\mathbf{R_0}$ = $3x10^{13}$ cm
- Γ_i = 80, Γ_{inf} = 400, T_1 = 1100s, T_2 = 3800s

Density of the jet,

$\rho_j \propto E_{iso} T_{inj}^{-1} \Gamma_i^{-1} \Gamma_{inf}^{-1} R_0^{-2}$

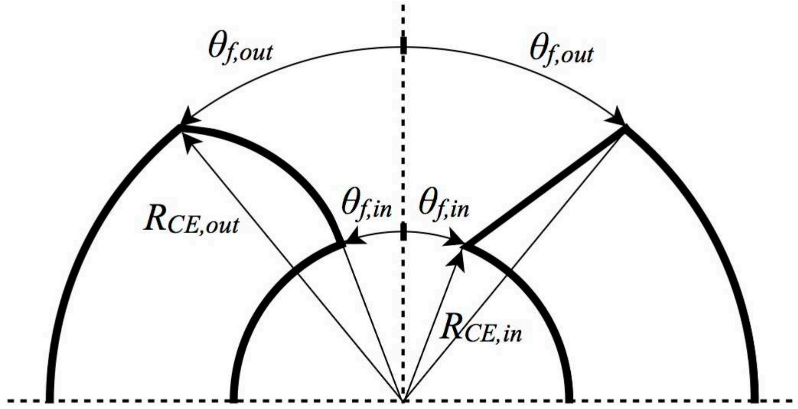

In agreement with simulations by Ricker & Taam (2012)

SHELL:

- **Toroidal-like shape.**
- **Common-enevelope (CE) shell,** $\boldsymbol{M_{sh}}$ = 0.14, $\mathbf{0.26\ M_{sun}}$
- Internal/external radius of the shell, $\mathbf{R_{CE,in}}$ = $4.5x10^{13}$ cm, $\mathbf{R_{CE,out}}$ = $1.05x10^{14}$ cm
- Internal/external opening angle of the funnel, $\theta_{f,in}$ = 1º, $\theta_{f,in}$ = 30º
- Medium density, ρ_{ext} = $8x10^{-14}$ g cm^{-3}, $\boldsymbol{\rho_{sh} / \rho_{ext}}$ **= 1500 (if** $\mathbf{M_{sh} = 0.26\ M_{sun}}$**)**

Hydrodynamic Evolution

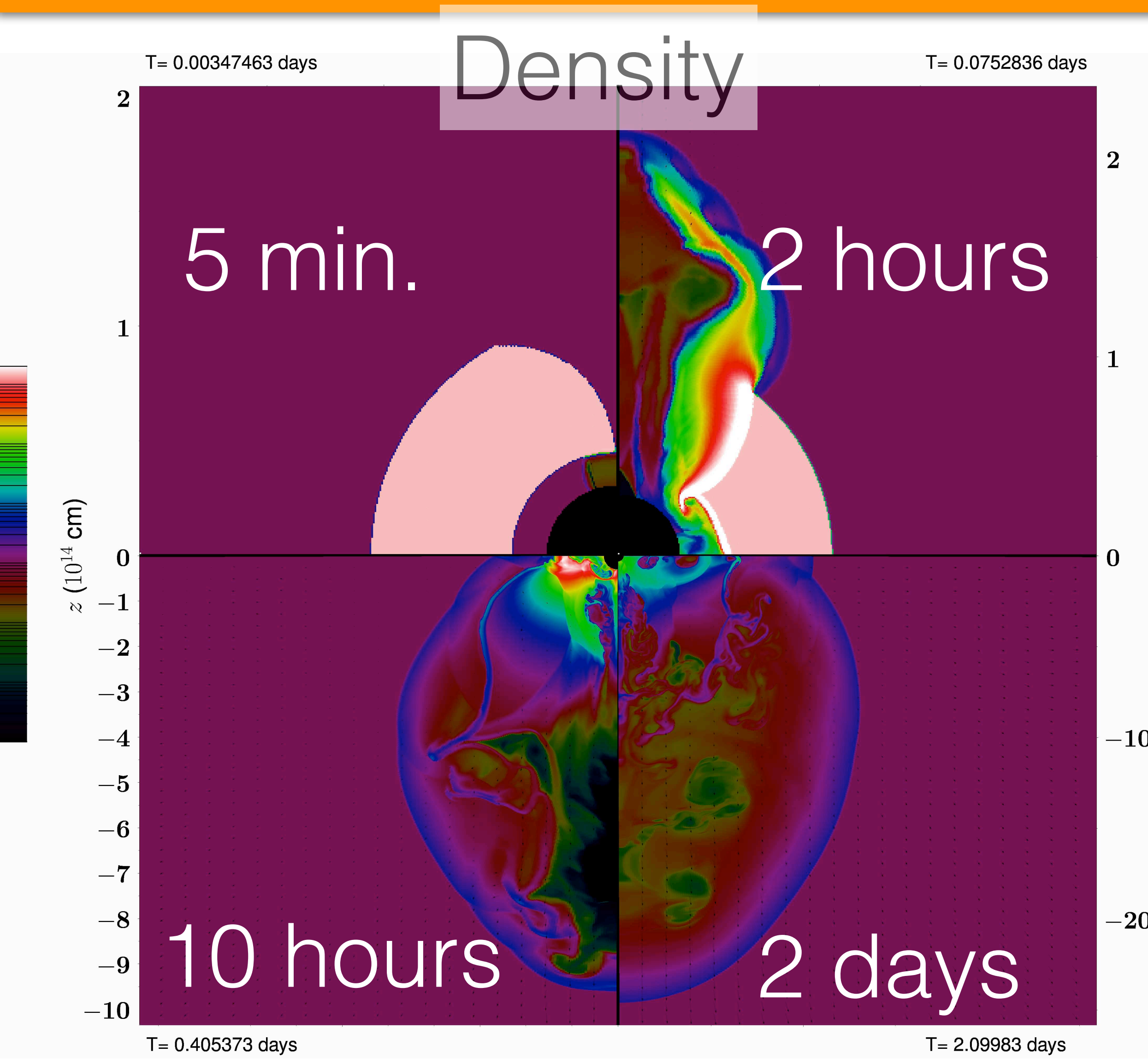

- jet injected with constant luminosity up to 1100 s
- luminosity decreasing as $t^{-5/3}$ until 3800 s
- jet hits inner shell boundary after ~ minutes
- 2 shocks form (not typical GRB afterglow shocks):
  - propagate from funnel walls towards jet axis
  - heate jet fluid to few x 10^6 K
  - penetrate CE shell and propagate sideways
- jet-shell interaction decelerates jet to subrel. vel.
- long-term: cavity in CE and ext. medium blown, containing 1 - 2 M_{sun}

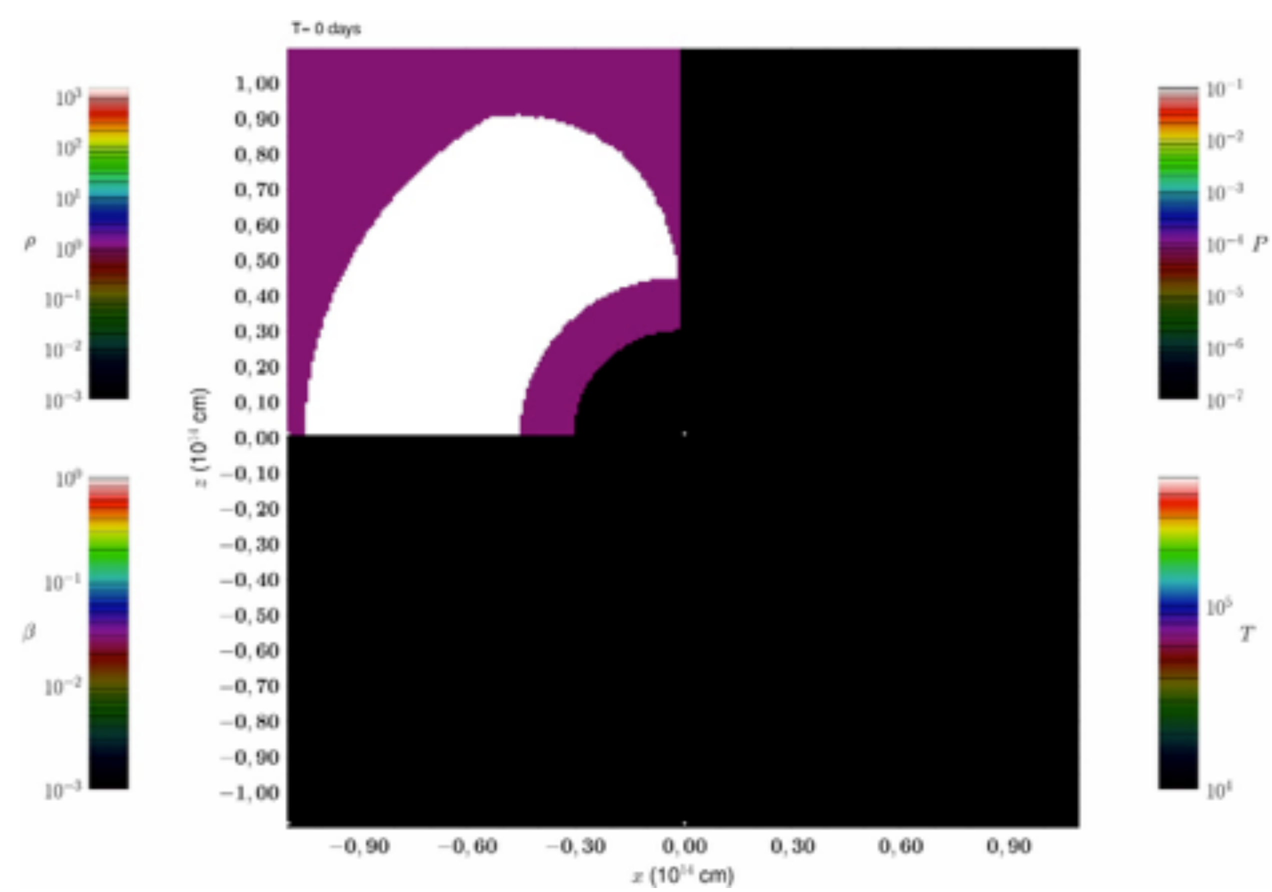

Reference model parameters:

$E_{\rm ISO} = 4 \times 10^{53}$ erg $\theta_j = 17°$ $\rho_{\rm CE}/\rho_{\rm ext} = 1500$

$R_{\rm inj} = 3 \times 10^{13}$ cm $R_{\rm CE,in} = 4.5 \times 10^{13}$ cm $R_{\rm CE,out} = 1.05 \times 10^{14}$ cm

$\theta_{\rm f,in} = 1°$ $\theta_{\rm f,out} = 30°$ $\rho_{\rm ext} = 8 \times 10^{-14}$ g cm^{-3}

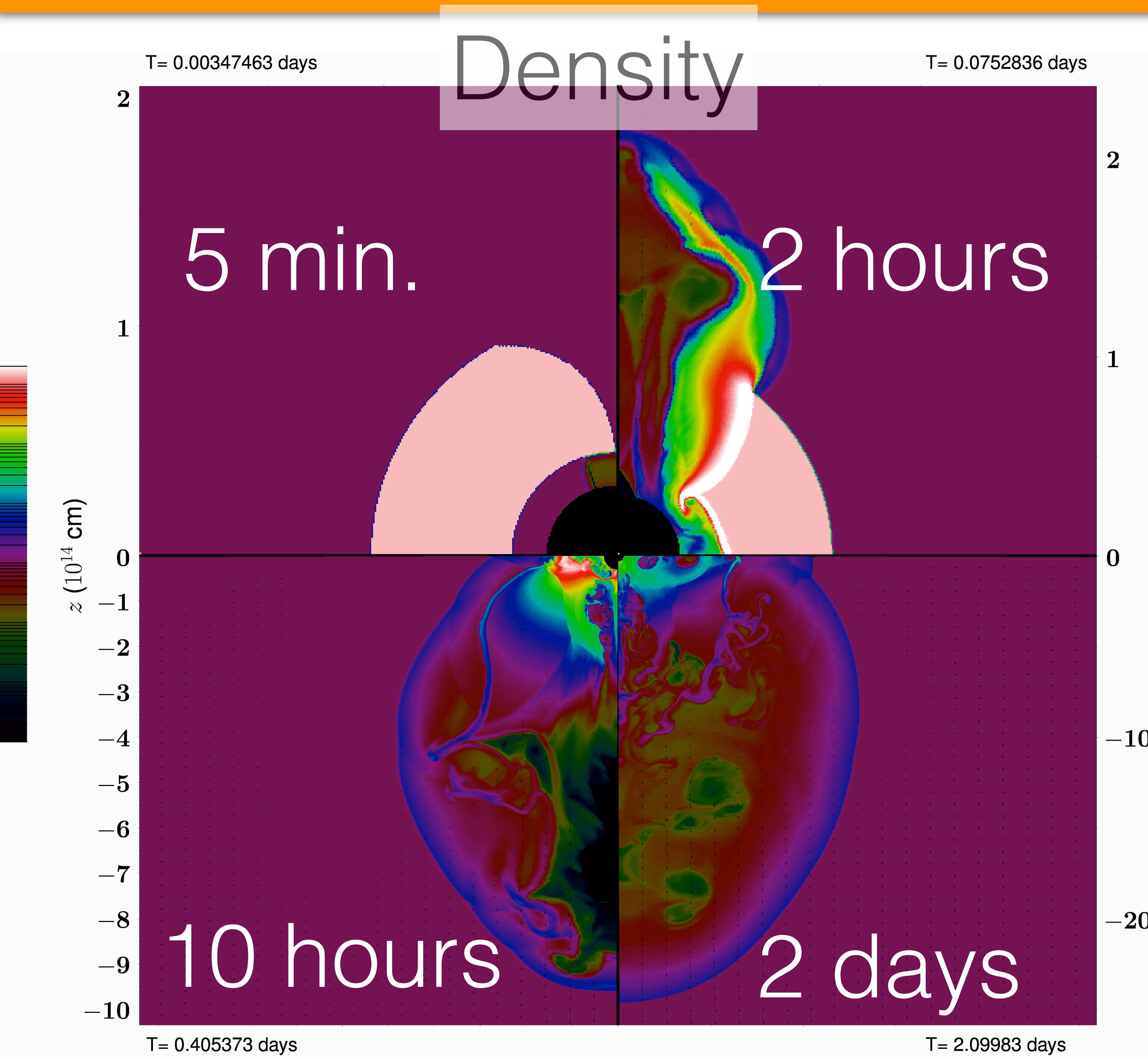

- jet injected with constant luminosity up to 1100 s
- luminosity decreasing as $t^{-5/3}$ until 3800 s
- jet hits inner shell boundary after ~ minutes
- 2 shocks form (<u>not</u> typical GRB afterglow shocks):
  - propagate from funnel walls towards jet axis
  - heate jet fluid to few x 10^6 K
  - penetrate CE shell and propagate sideways
- jet-shell interaction decelerates jet to subrel. vel.
- long-term: cavity in CE and ext. medium blown, containing 1 - 2 M_{sun}

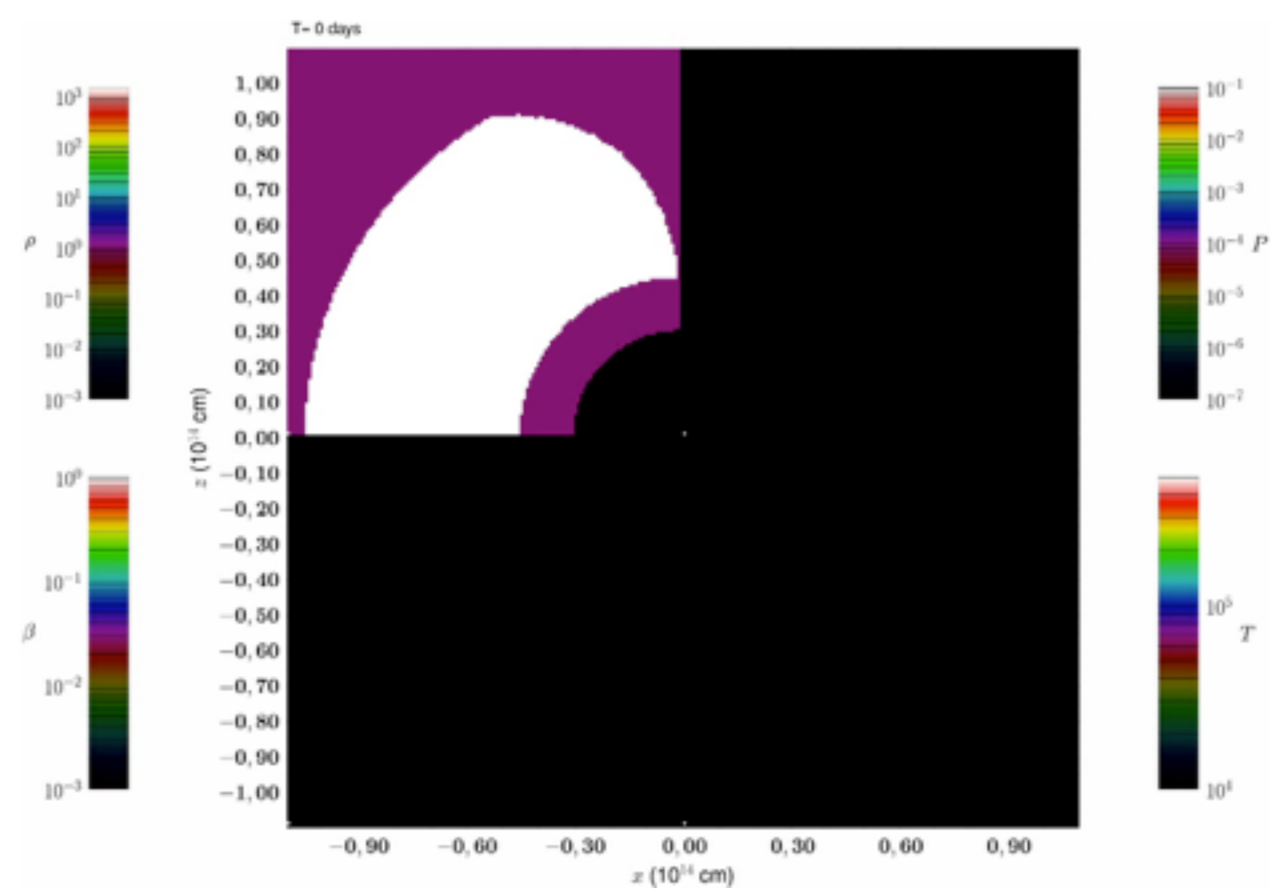

Reference model parameters:

$E_{\rm ISO} = 4 \times 10^{53}$ erg $\quad \theta_j = 17^\circ \quad \rho_{\rm CE}/\rho_{\rm ext} = 1500$

$R_{\rm inj} = 3 \times 10^{13}$ cm $\quad R_{\rm CE,in} = 4.5 \times 10^{13}$ cm $\quad R_{\rm CE,out} = 1.05 \times 10^{14}$ cm

$\theta_{\rm f,in} = 1^\circ \quad \theta_{\rm f,out} = 30^\circ \quad \rho_{\rm ext} = 8 \times 10^{-14}$ g cm^{-3}

Parametric Scan

Density

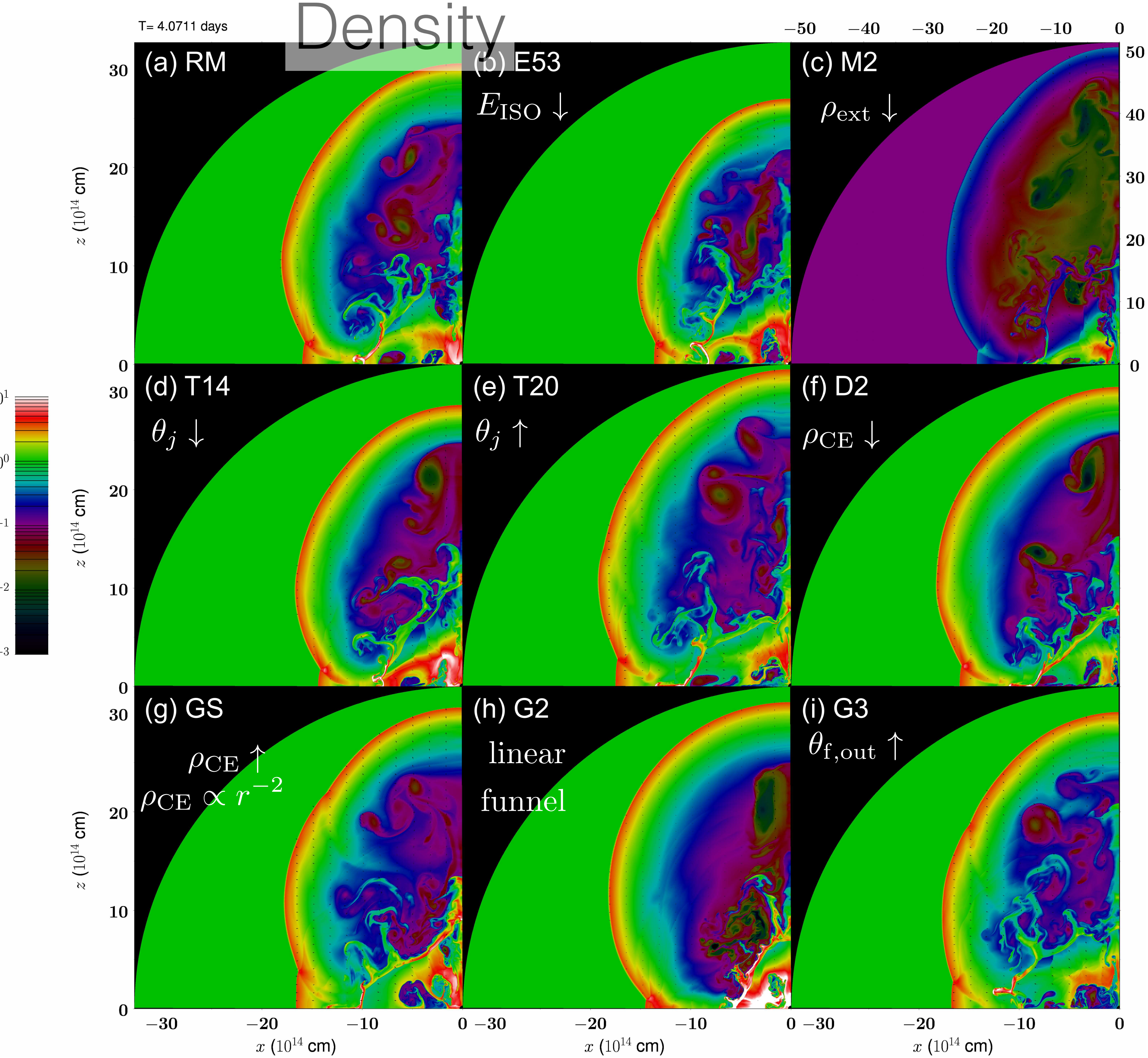

Rest-mass in the bubble

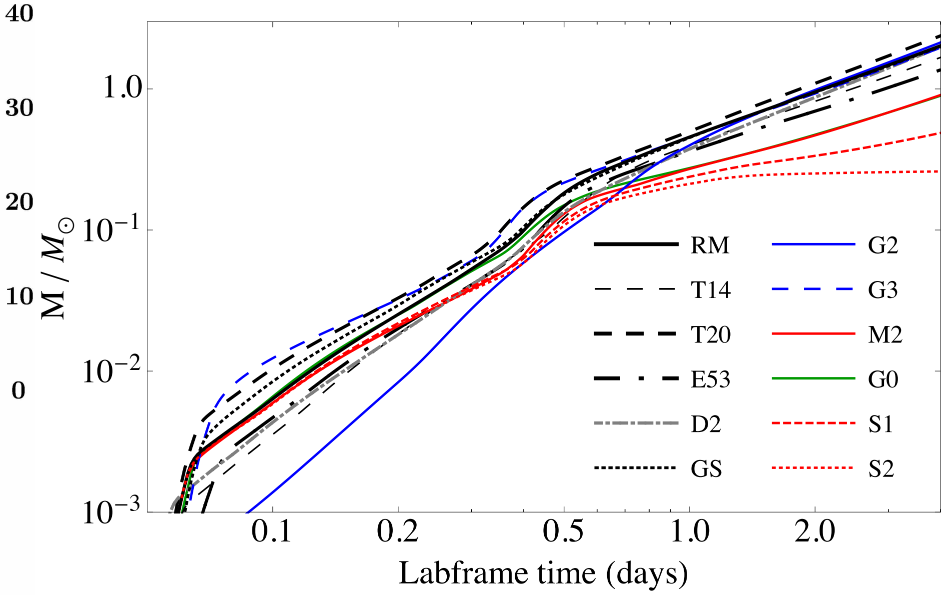

Transversal radius

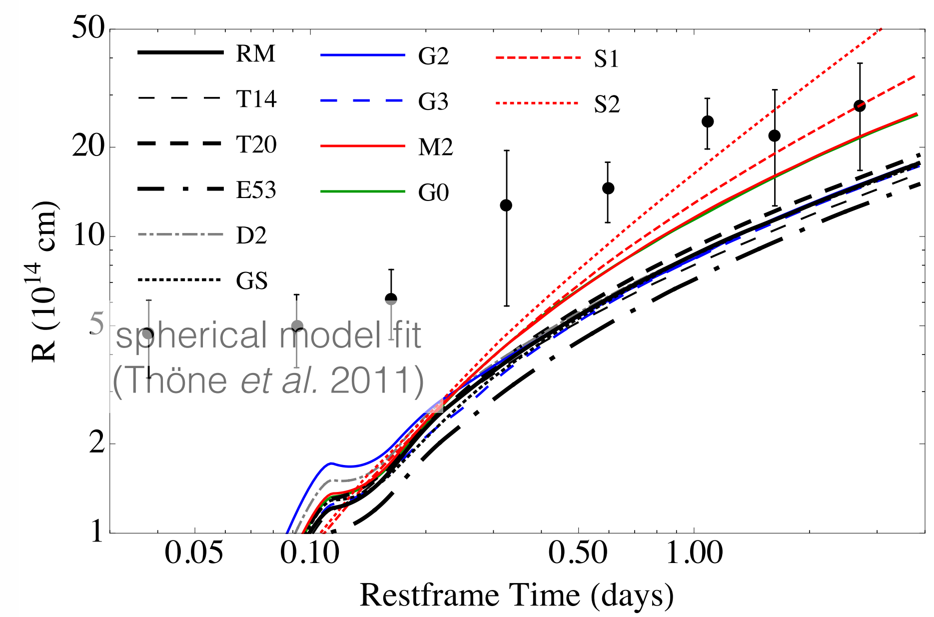

Thermal and Non-thermal Emissivity and Absorption

- using the radiative transport code ***SPEV*** (Mimica et al. 2009) we compute **synthetic LCs & Spectra** and compare the synthetic emission from our model with observations
  - **Thermal-Bremsstrahlung** model

1. **Emission**: thermal-bremsstrahlung (free-free).

$$j_\nu = \frac{1}{4\pi} 6,8 \times 10^{-38} Z^2 \frac{\rho^2}{m_p^2} T^{-1/2} e^{-x} \bar{g}_{\rm ff}(\nu, T) \, \mathrm{erg\ s^{-1}\ cm^{-3}\ Hz^{-1}}. \qquad x = \frac{h\nu}{kT}$$

2. **Absorption**: following Kramers law.

$$\alpha_\nu \simeq 4.1 \times 10^{-23} Z^2 \frac{\rho^2}{m_p^2} T^{-7/2} x^{-3} (1 - e^{-x}) \bar{g}_{\rm ff}(\nu, T) \, \mathrm{cm^{-1}}. \qquad B_\nu\ (T, \nu) = j_\nu / \alpha_\nu$$

3. Maxwellian temperature averaged (free-free) **Gaunt factor**, $\bar{g}_{ff}(\nu,T)$ (**Sutherland 1998**)

4. Temperature? P(T) = $P_e + P_{rad}\,(1 - e^{-\tau})$

   Iterative process because $\tau = \tau(T, \nu)$

(1) $\tau \ll 1$: $P = P_e$ $\qquad P_e = k\rho T/\mu m_p$

(2) $\tau \gg 1$: $P = P_e + P_{rad}$, $\qquad P_{rad} = a_R T^4/3$

+ Synchrotron (non-thermal particles): particles accelerated at shocks

Studying Thermal Emission

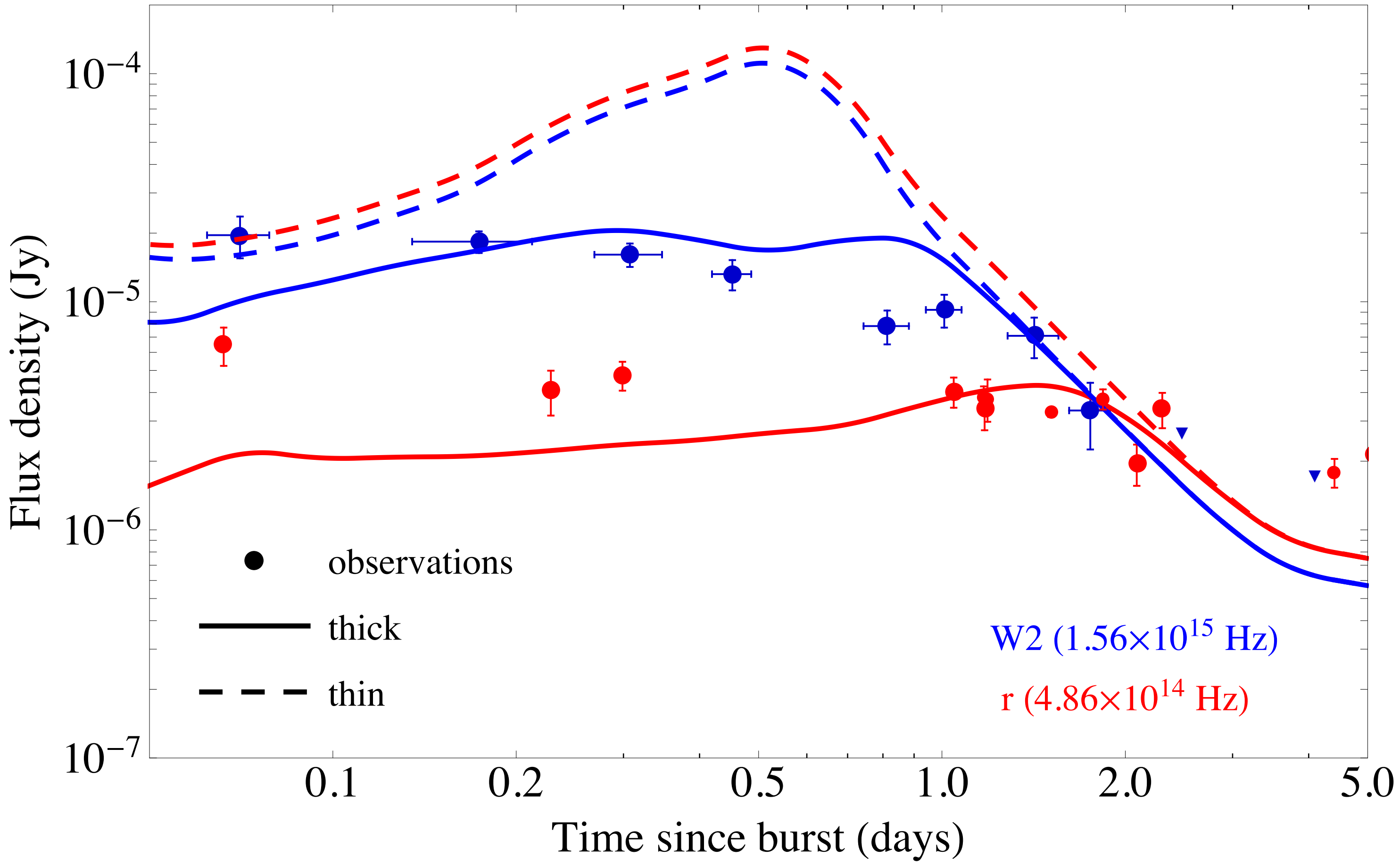

- *Temporal evolution up to 5 days*
- *Optical band: detections up to ~2 days (except r/i bands)*
- *We neglect the external medium emission*

Studying Thermal Emission

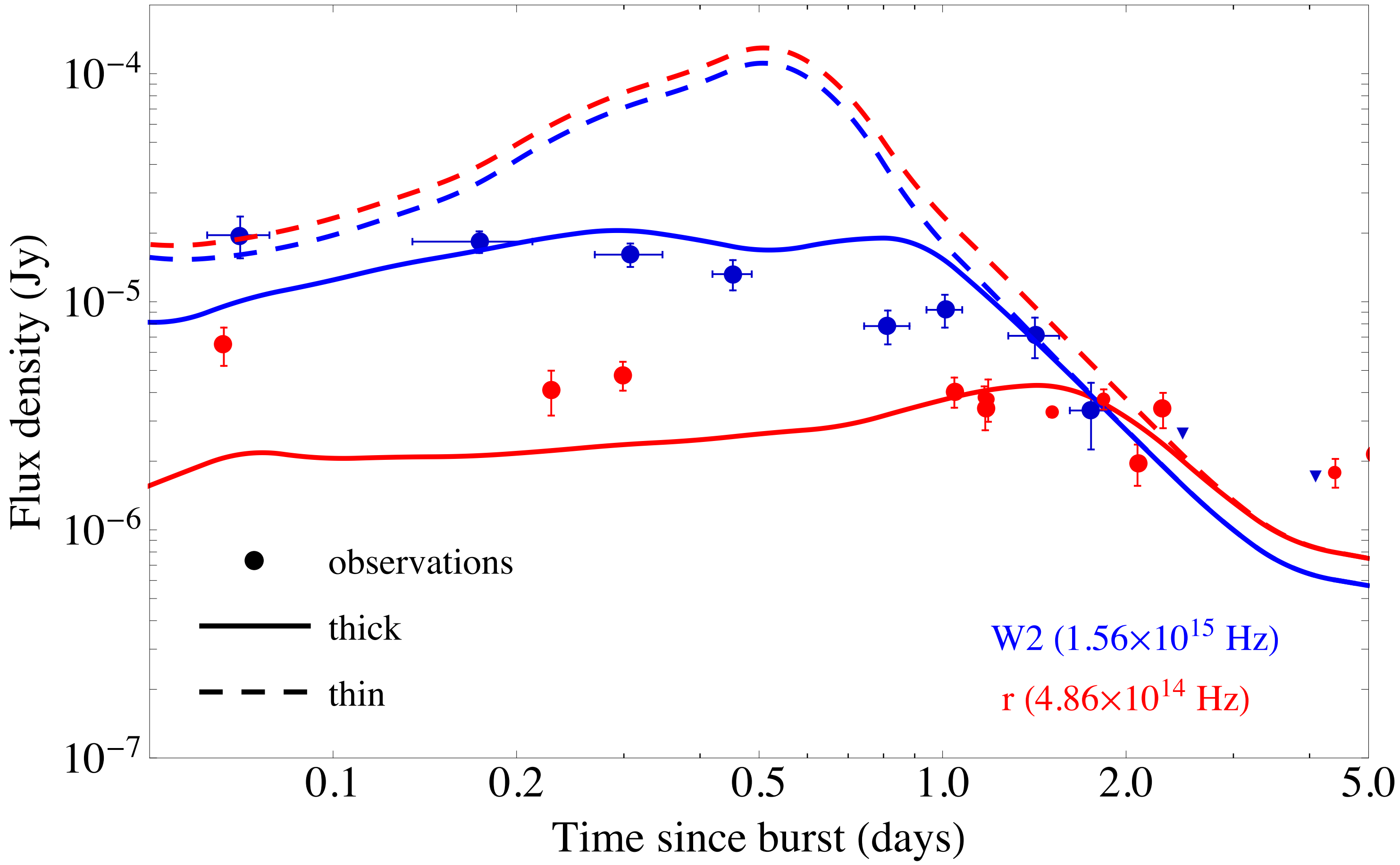

- *Temporal evolution up to 5 days*
- *Optical band: detections up to ~2 days (except r/i bands)*
- *We neglect the external medium emission*

(Line of sight, $\theta_{obs} = 0^o$)

Detector

Jet/shell interaction region

W2 band: 1.56 x 10^{15} Hz

Time obs.: 0.17d

$t_{obs} = T - z/c$

T: hydro. time (measured in the source rest frame)

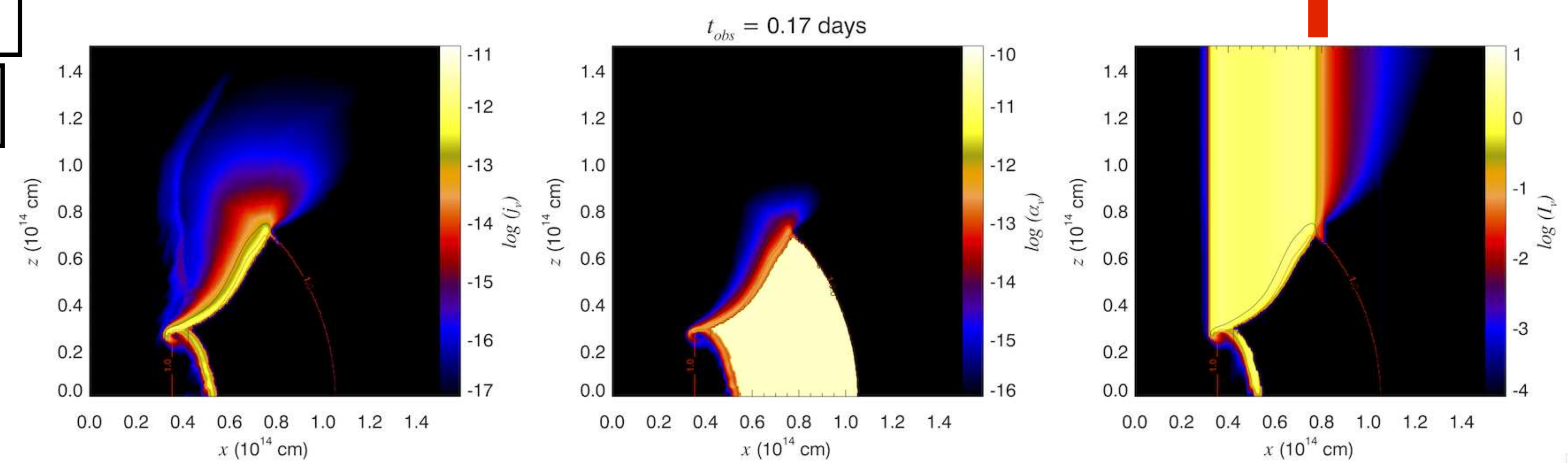

(1) emission

(2) absorption

Intensity

Origin of Thermal Emission

- in optical: system optically thick until ~ 1 day
  - spectral inversion at thick -> thin transition
- in X-rays: system optically thin
- origin of early-time thermal emission:
  - jet/CE-shell interaction region
  - X-rays emitted from closer to the CE shell than optical

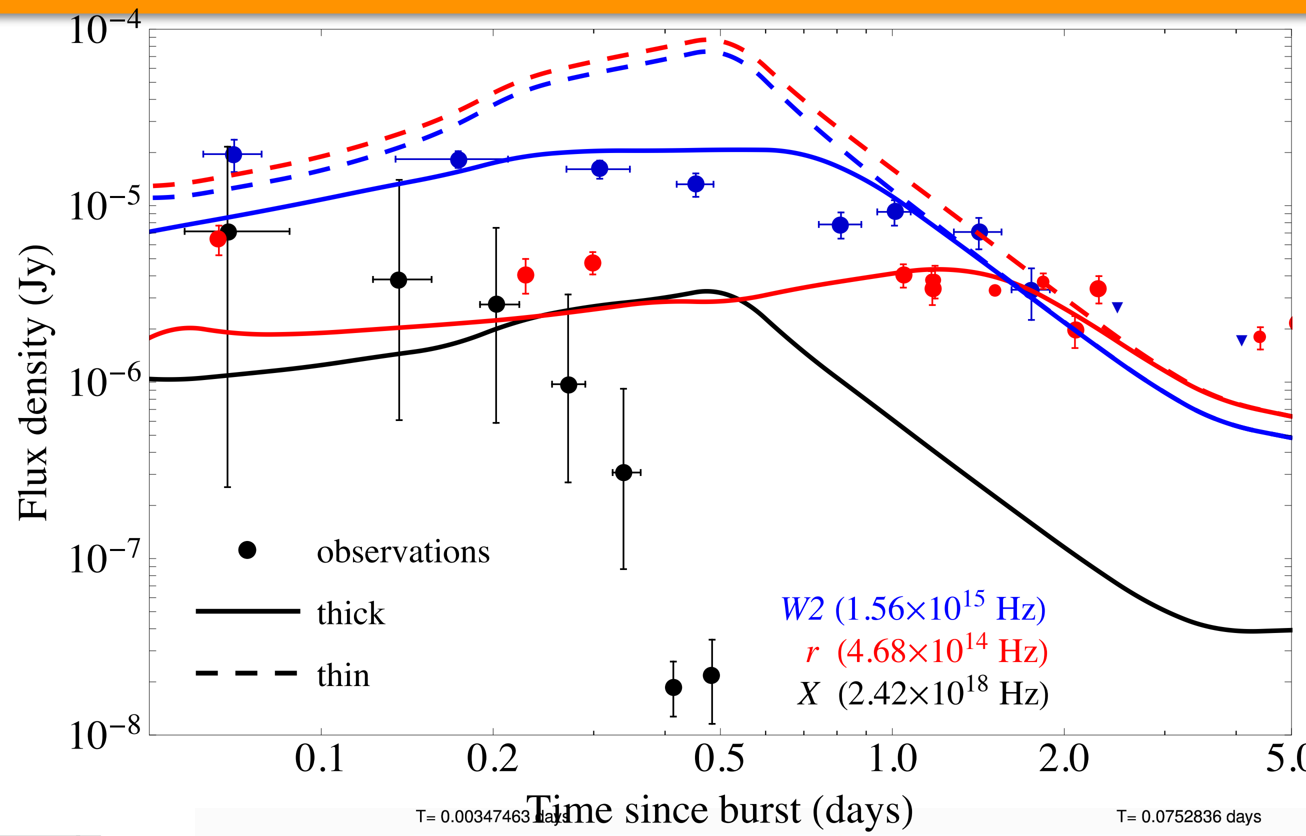

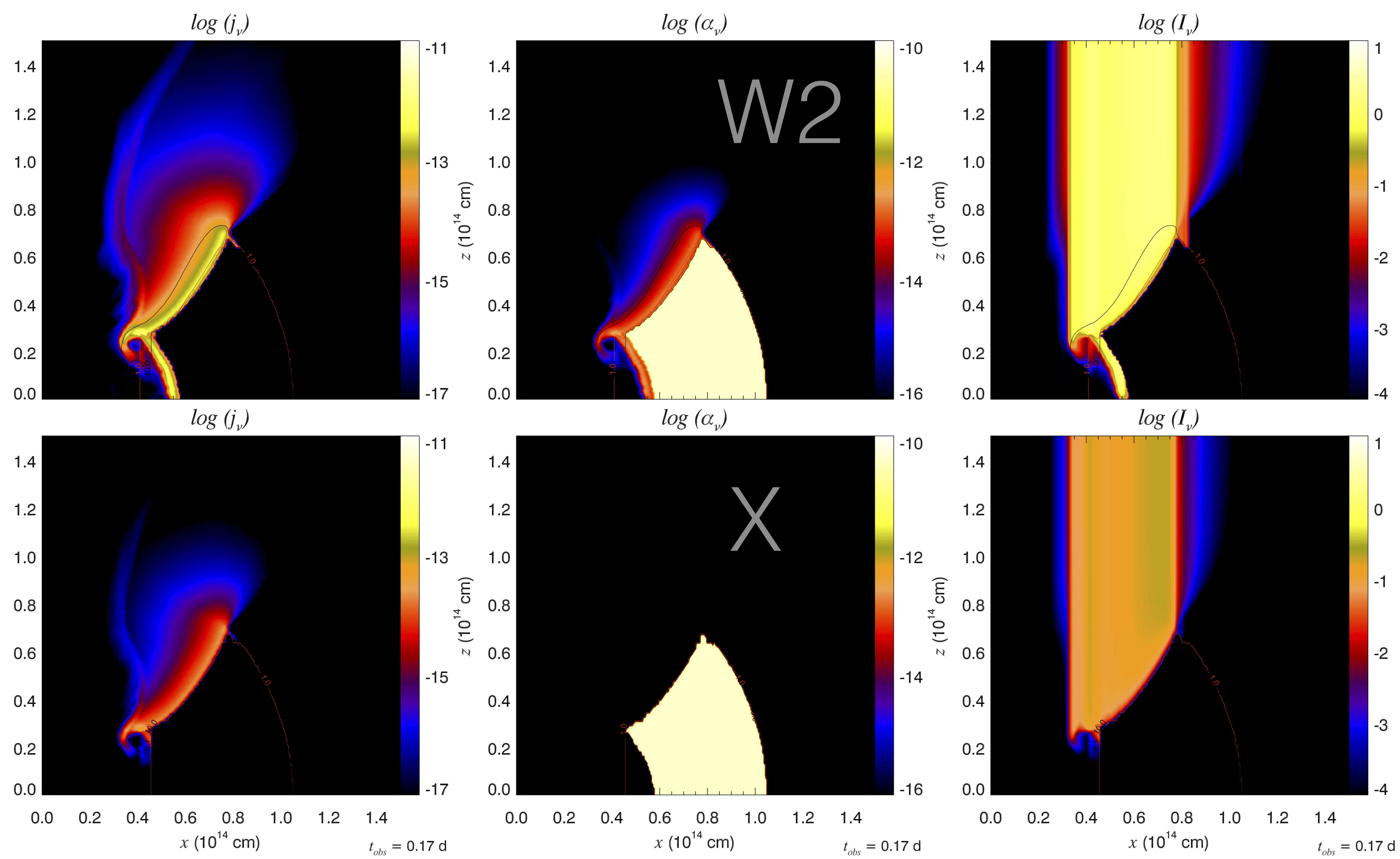

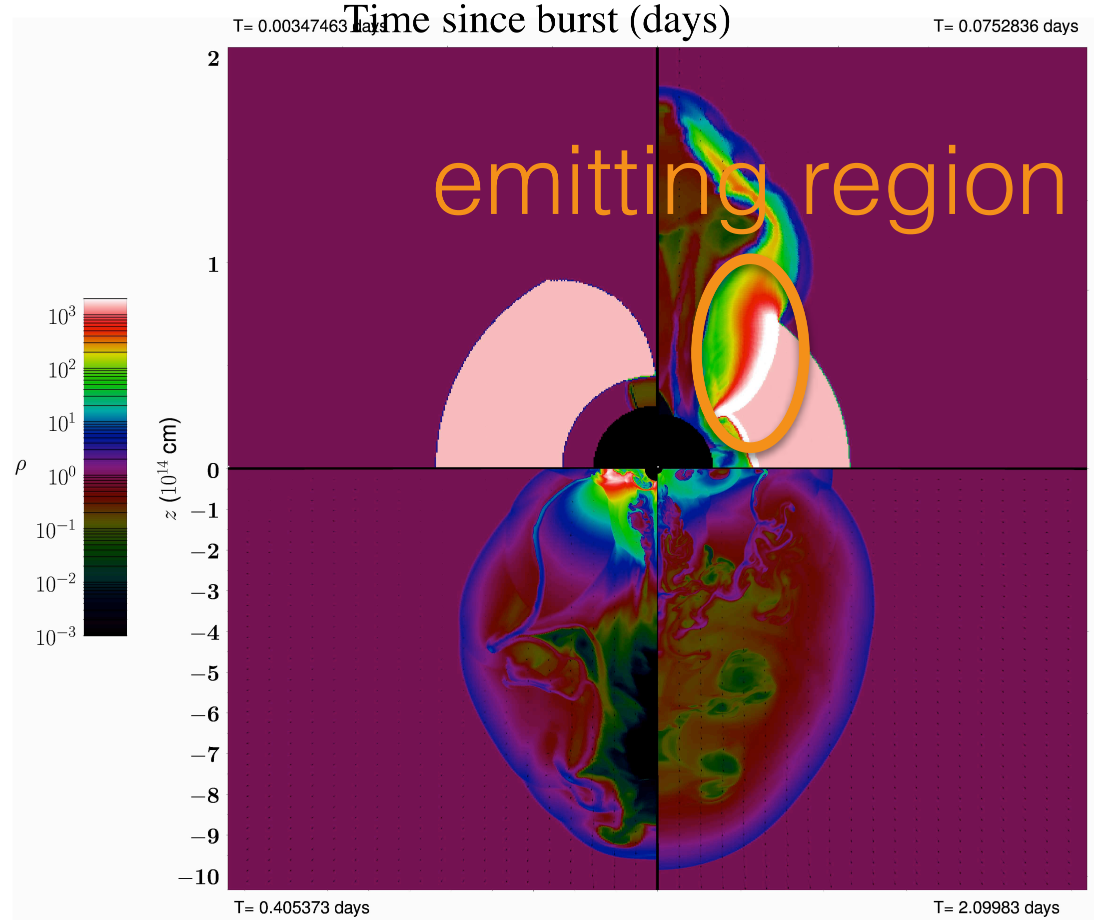

Evolution of Thermal Emission

- CE-shell: almost intact at 0.17 days, almost completely ablated at 0.6 days
- most thermal radiation emitted before 2 days
- minor, but long-lasting contribution from the bubble

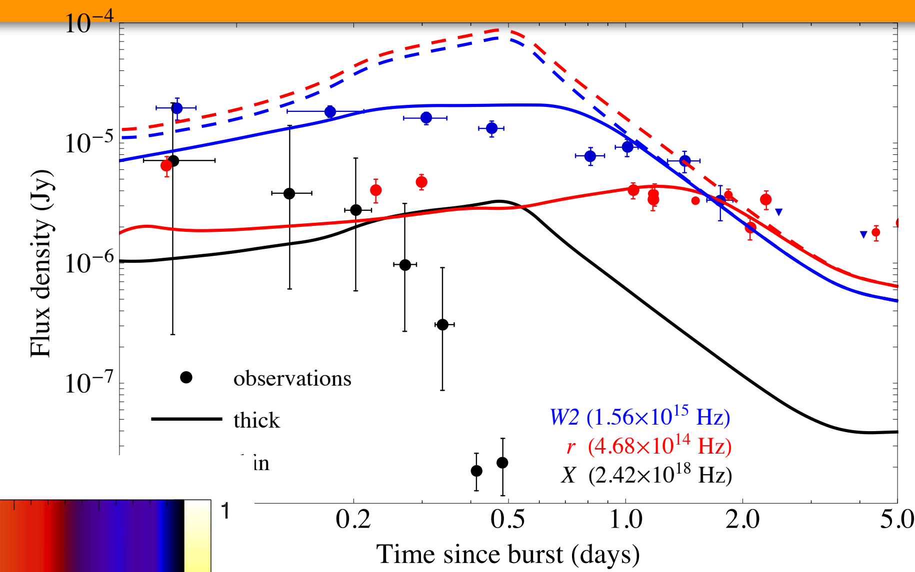

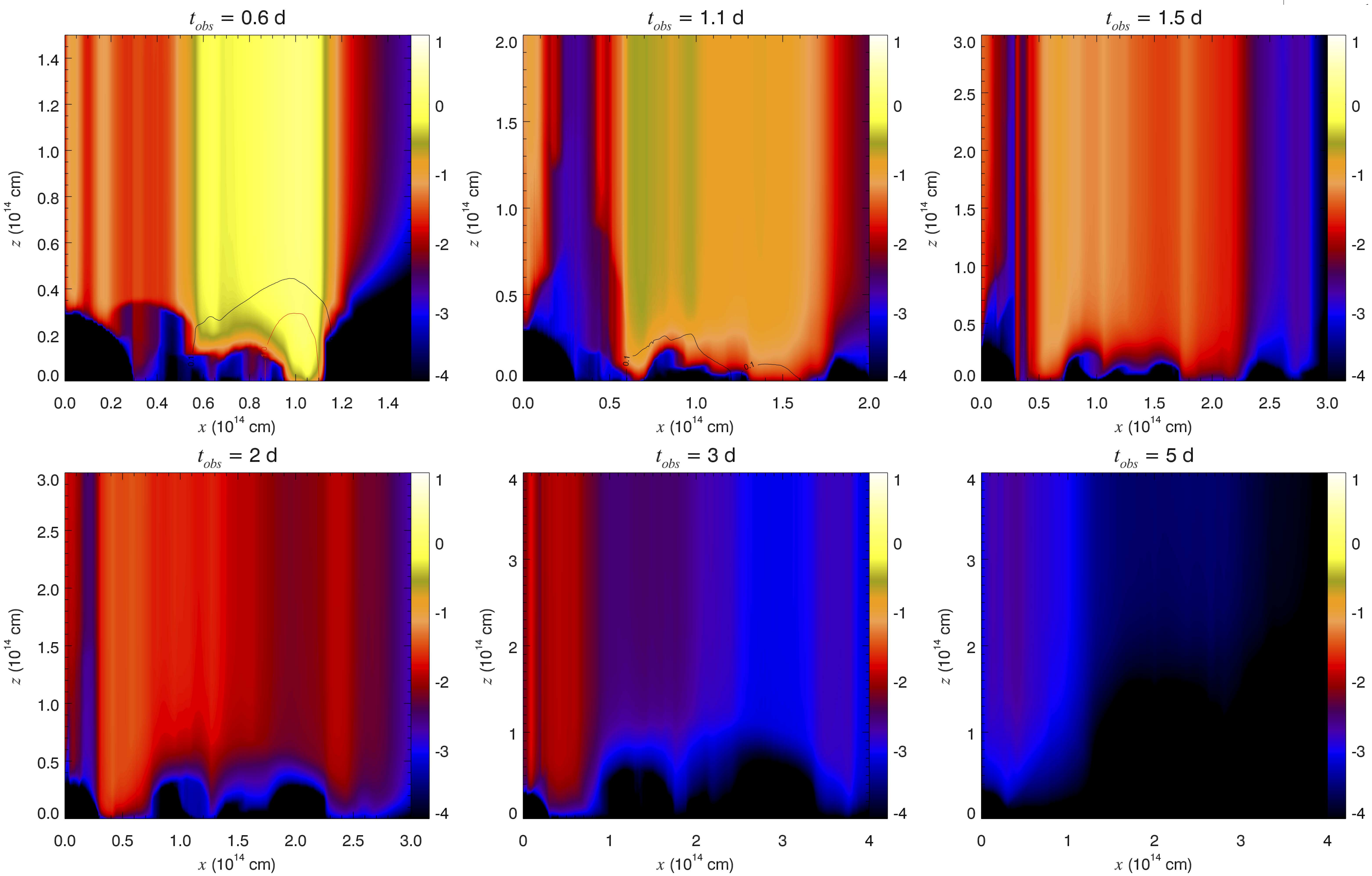

Importance of CE-Shell Mass

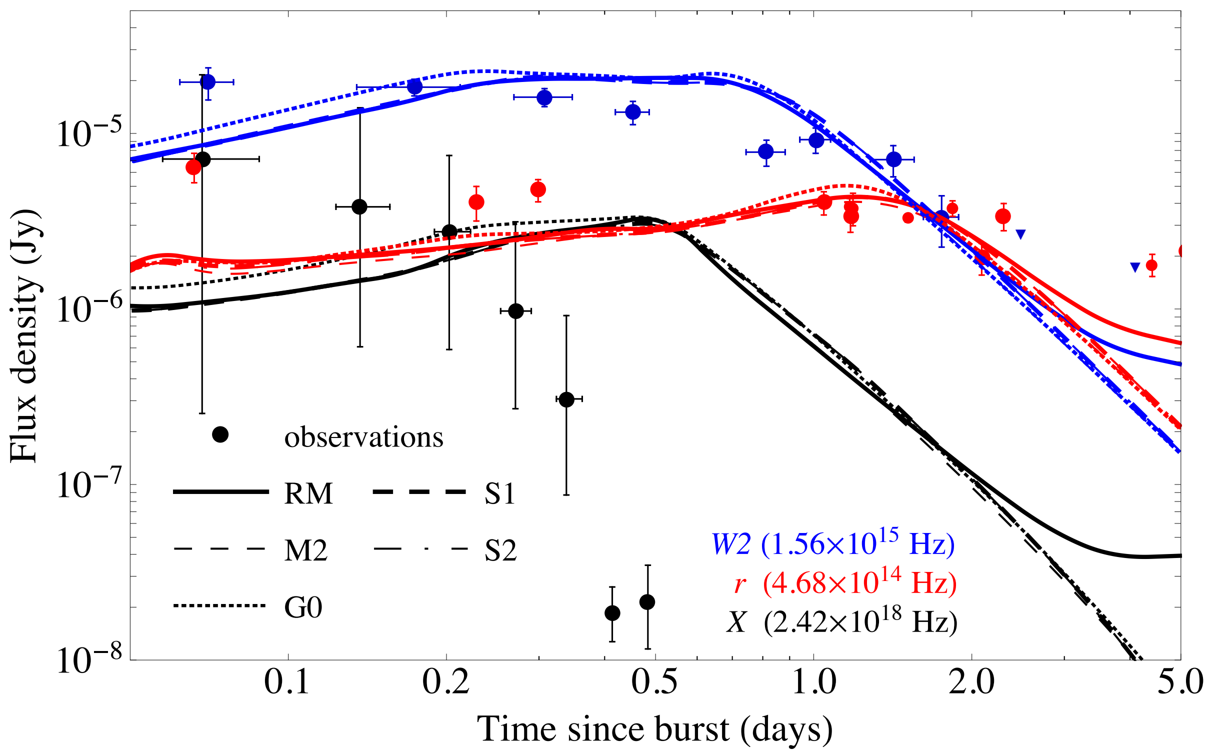

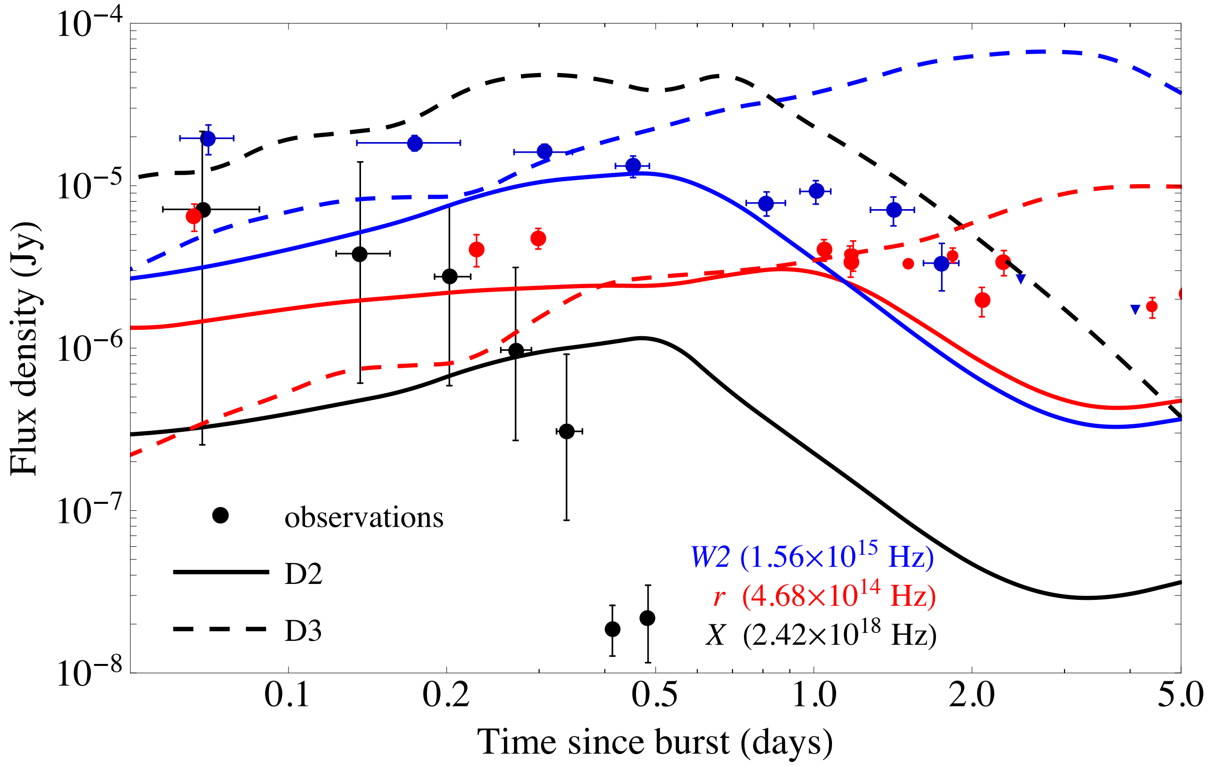

- RM - reference model
- G0, M2 - low density ext. medium
- S1, S2 - stratified ext. medium

- D2 - lower-mass CE-shell (0.5x)
- D3 - higher-mass CE-shell (10x)

- CE-shell mass much more important than ext. medium properties
- masses much lower(higher) than 0.26 $M_\odot$ cause light curve to peak and spectral inversion to happen too early(late)
- lower density external medium suppresses late-time flattening

Synchrotron Emission

Evolution of the **non-thermal particles**

- Injection of lagrangian particles
- **Forward shock**
- Params.: ϵ_e, ζ_e , ϵ_B, p, a_{acc}, $\gamma_{min,min}$
- Stochastic magn. field: $B'_{st} \propto (\epsilon_B u_s)^{1/2}$

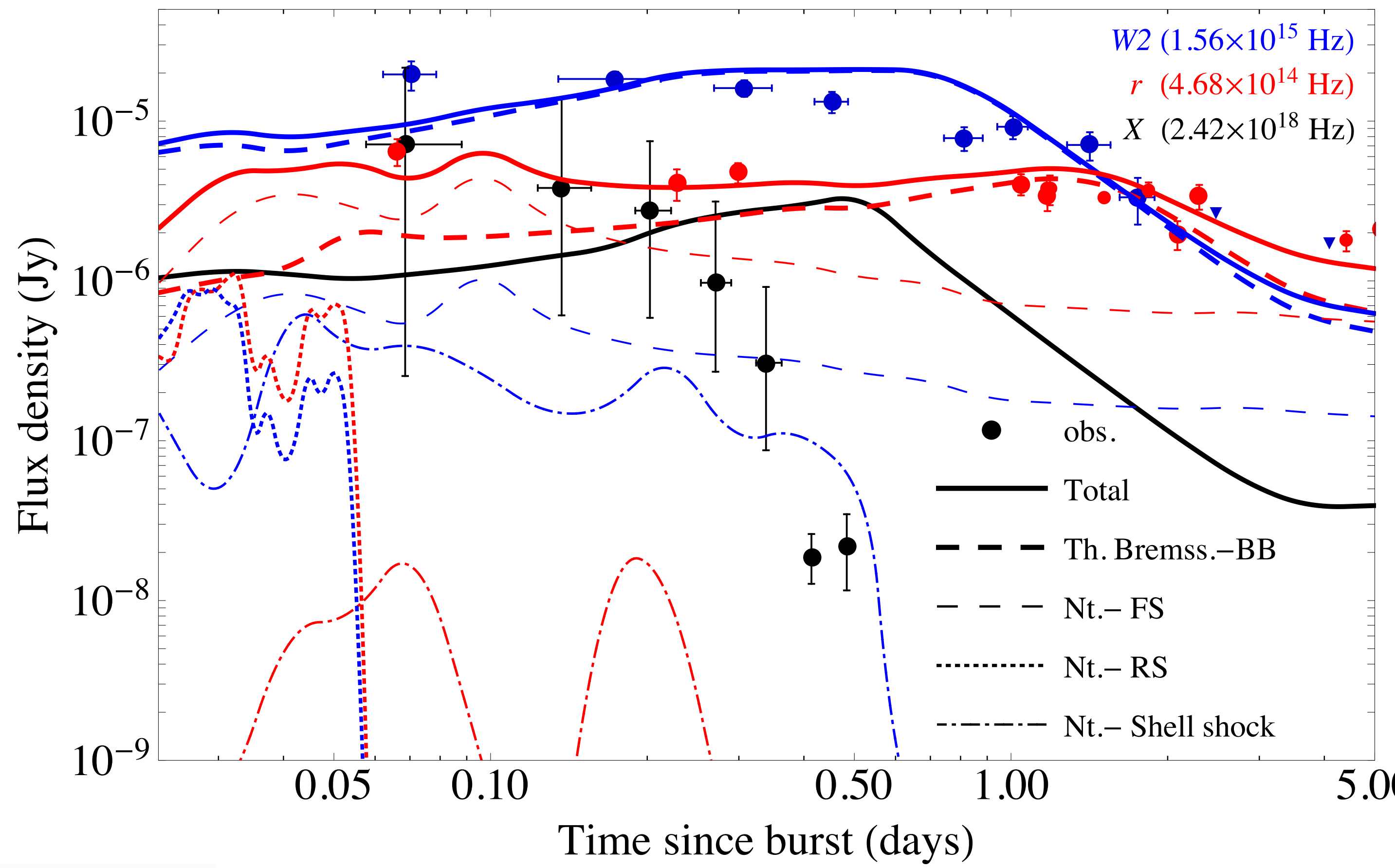

Cuesta-Martínez et al. 2014 arXiv:1408.1814

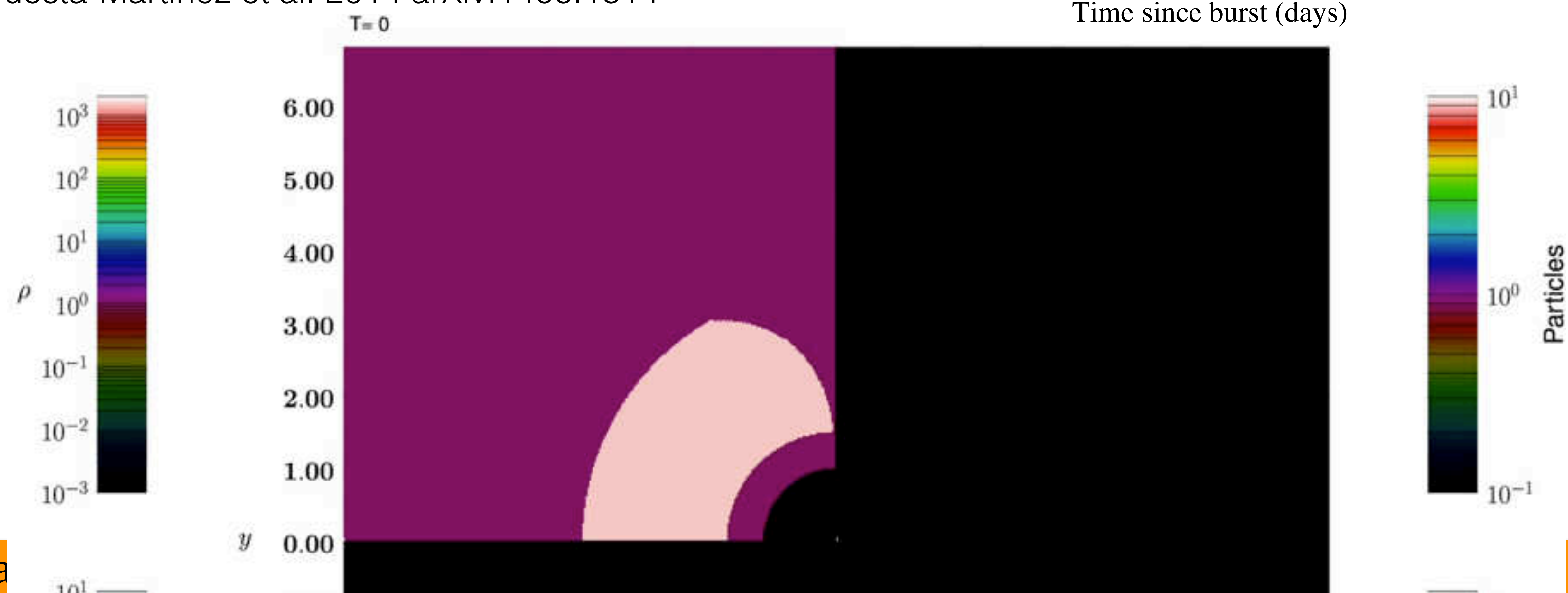

Synchrotron Emission

Evolution of the **non-thermal particles**

- Injection of lagrangian particles
- **Forward shock**
- Params.: ϵ_e, ζ_e, ϵ_B, p, a_{acc}, $\gamma_{min,min}$
- Stochastic magn. field: $B'_{st} \propto (\epsilon_B u_s)^{1/2}$

Cuesta-Martínez et al. 2014 arXiv:1408.1814

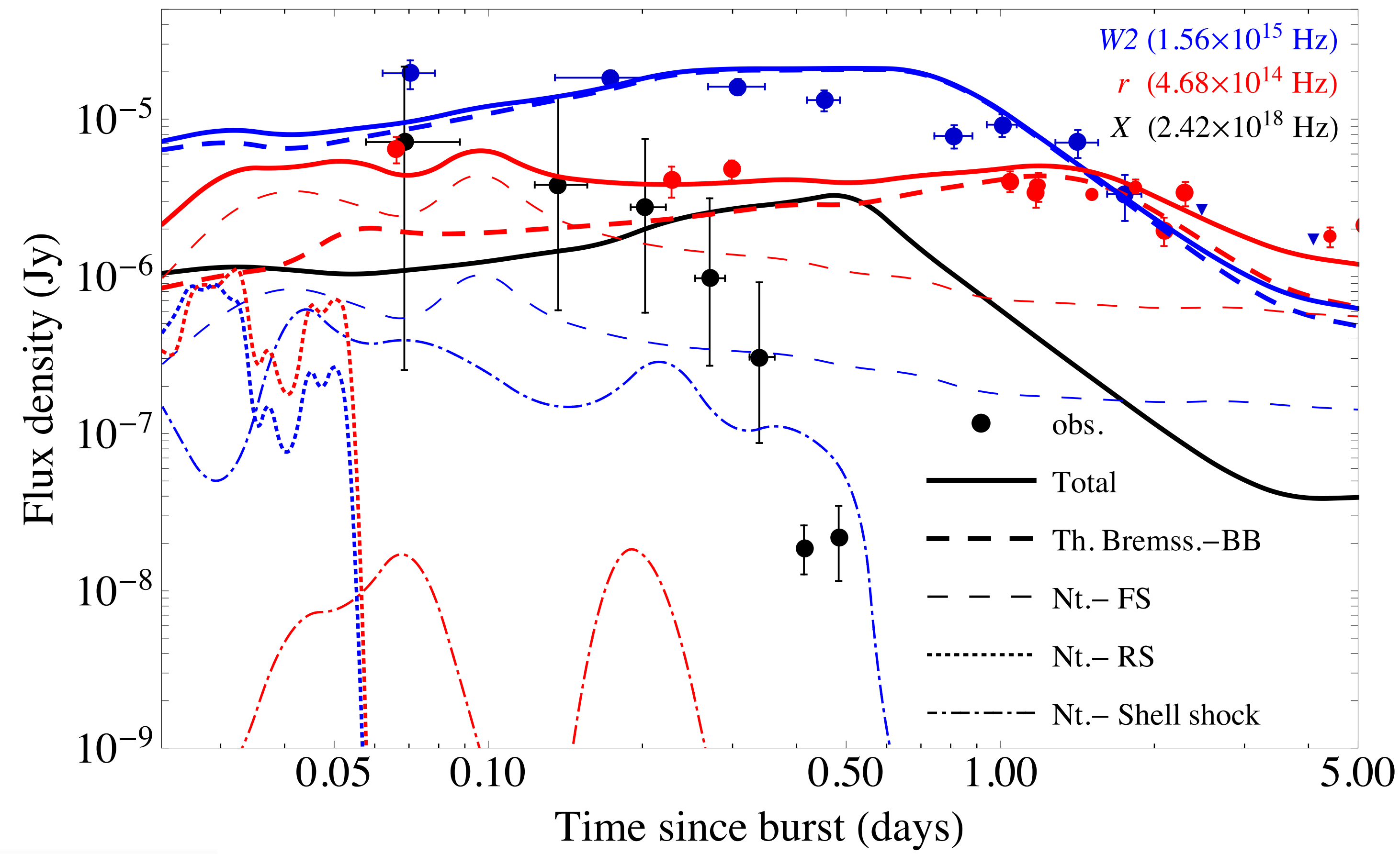

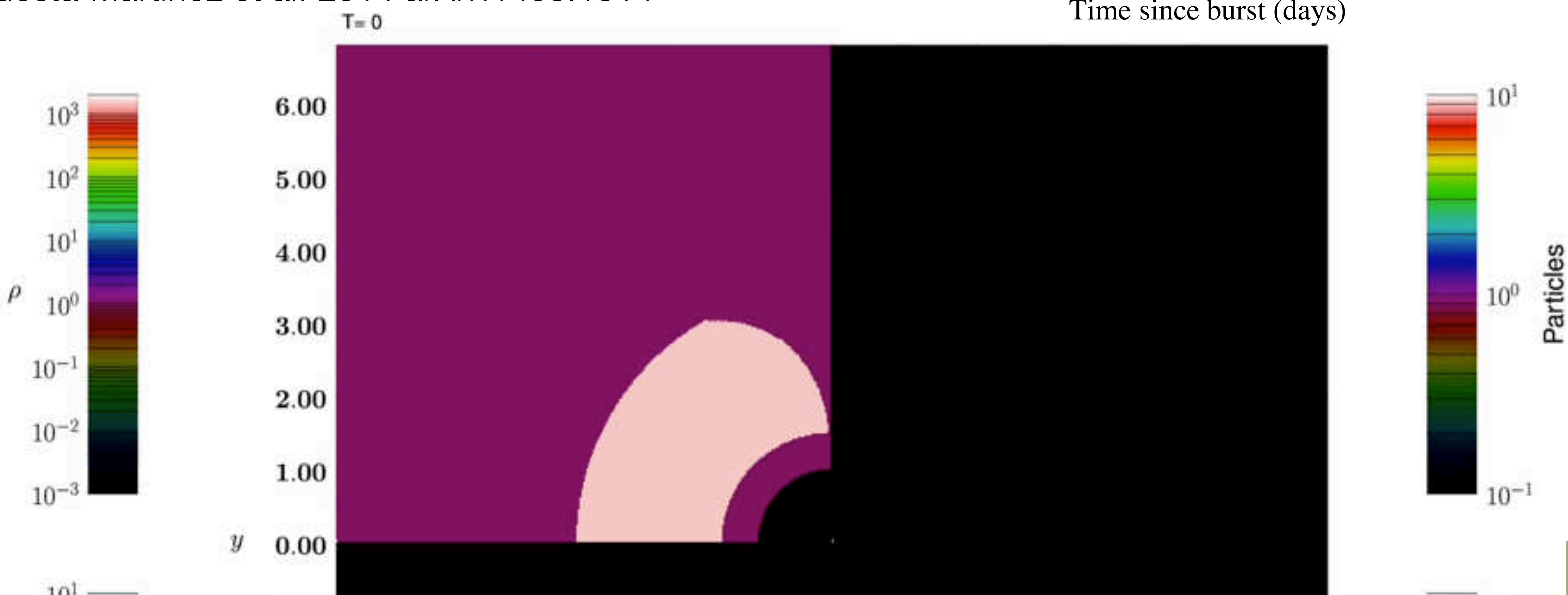

Origin of Non-Thermal Emission

t=0.17 days

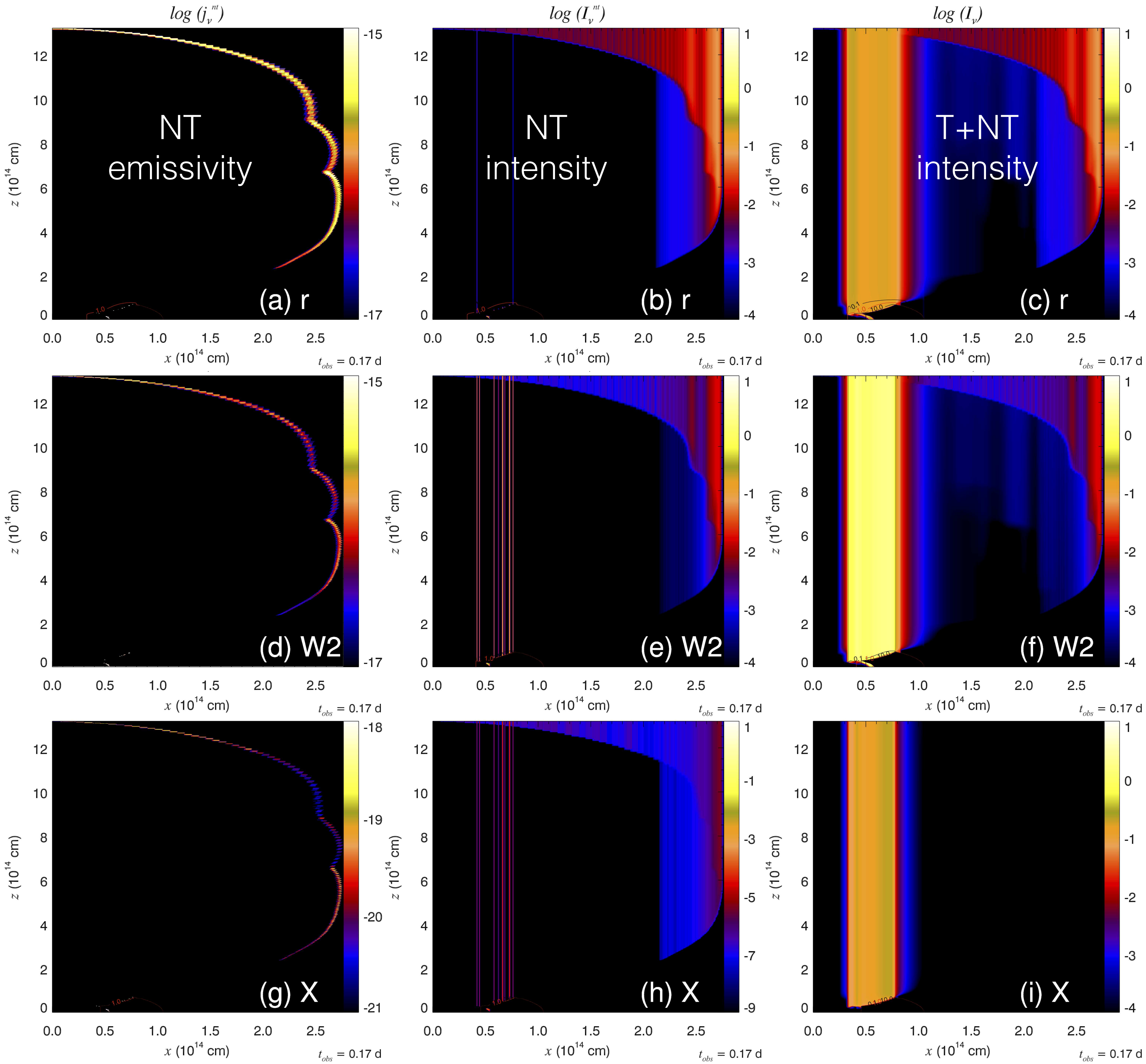

GRB 101225A Summary

- possible progenitor: NS + He core merger (Thöne *et al.* 2011)
- we model: jet propagation through secondary star outer layers and external medium:
  - phase 1: jet free expansion until hitting CE-shell
  - phase 2: jet (wider than the funnel) impacts against much denser CE-shell and heats and baryon-loads, ablating and disrupting the CE-shell in the process
  - phase 3: heated and baryon-loaded jet inflates a cavity, entering self-similar regime
- origin of thermal emission:
  - UVOIR observations can be explained as radiation from CE-shell/jet interaction region (~ 5×10^{13} c, much smaller than the surface of the expanding bubble ~ 10^{15} cm)
  - properties weakly dependent on external medium profile
  - X-rays: depend on the CE-shell funnel geometry => initially narrower and denser funnel would improve agreement with observations (increase of computational cost)
- non-thermal emission:
  - moderately relativistic forward shock dominates early evolution, emission compensates thermal deficit for t < 0.2 days
  - no classical afterglow signature due to quick deceleration
- submitted papers: arXiv:1408.1305, arXiv:1408.1814

Afterglow Model for Swift J1644 + 57

- Swift J164449.31+573451 (z = 0.354), initially GRB110328A
- longevity of its afterglow points to a different explanation: a blazar-like jet fed by a tidal disruption of a solar-mass star

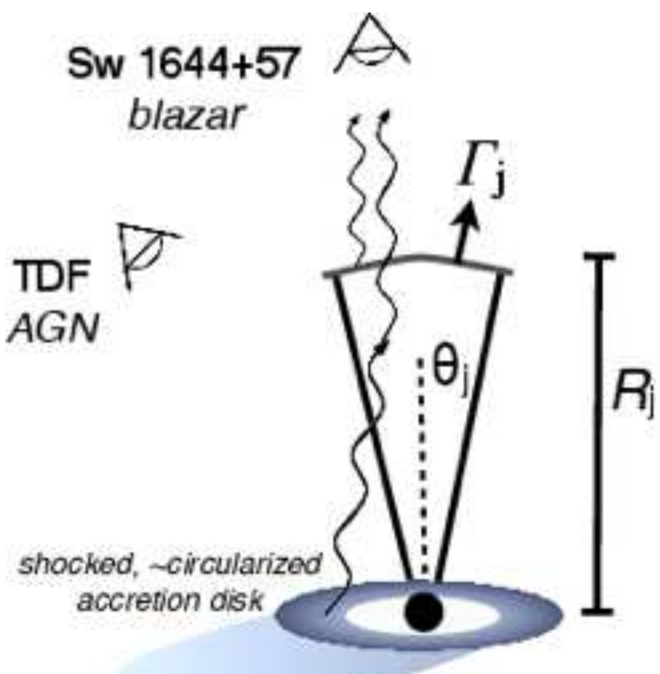

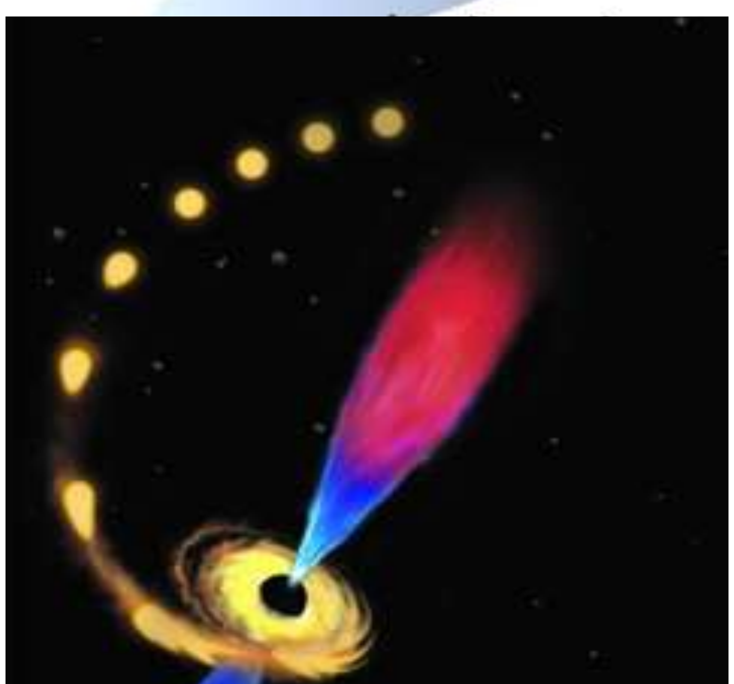

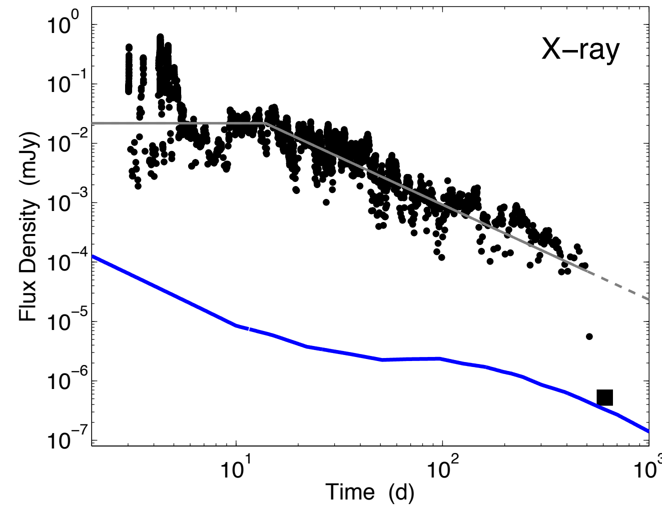

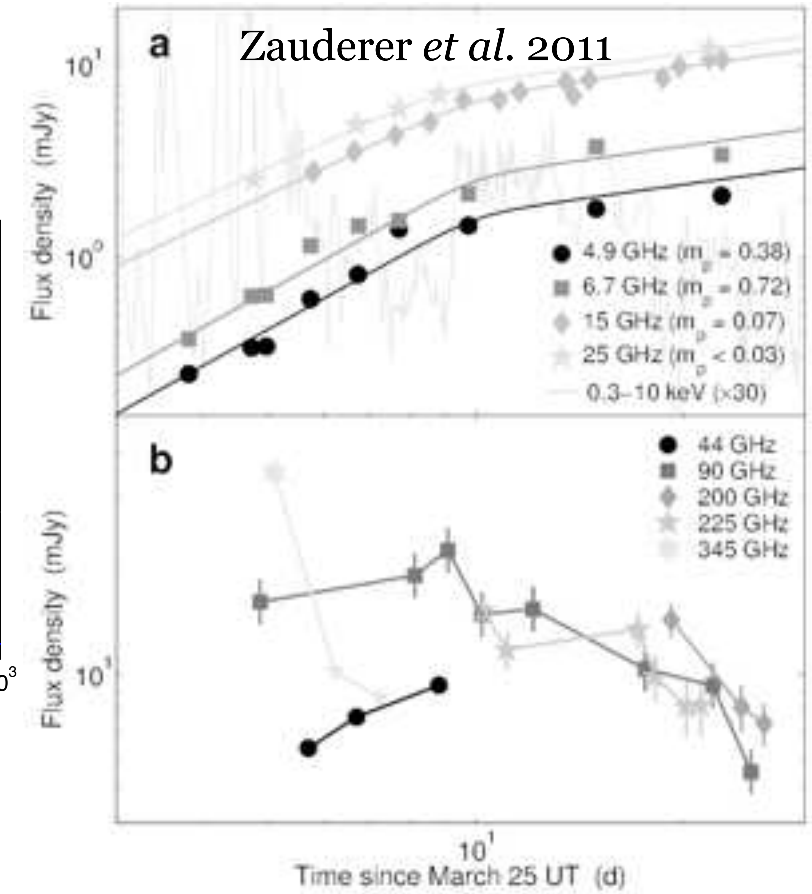

Afterglow Model for Swift J1644+57

- Swift J164449.31+573451 (z = 0.354), initially GRB110328A
- longevity of its afterglow points to a different explanation: a blazar-like jet fed by a tidal disruption of a solar-mass star

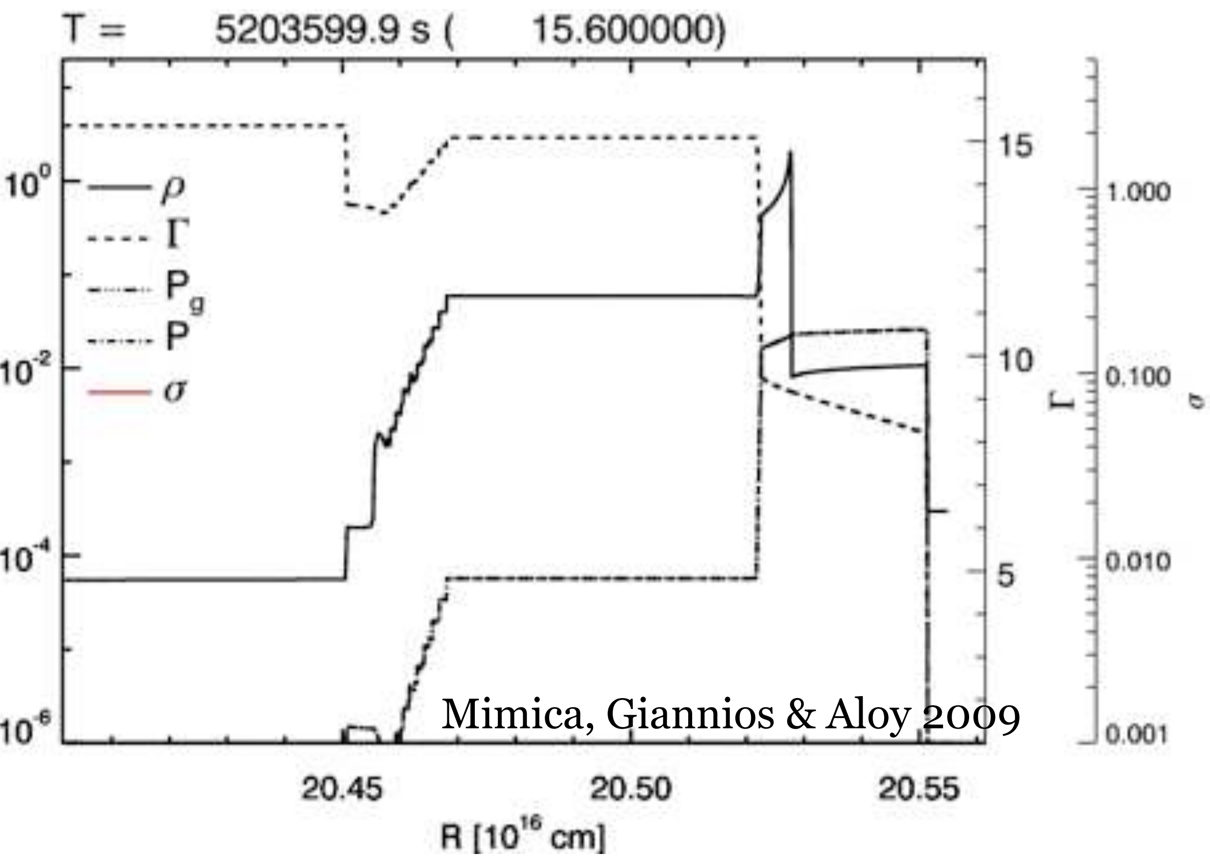

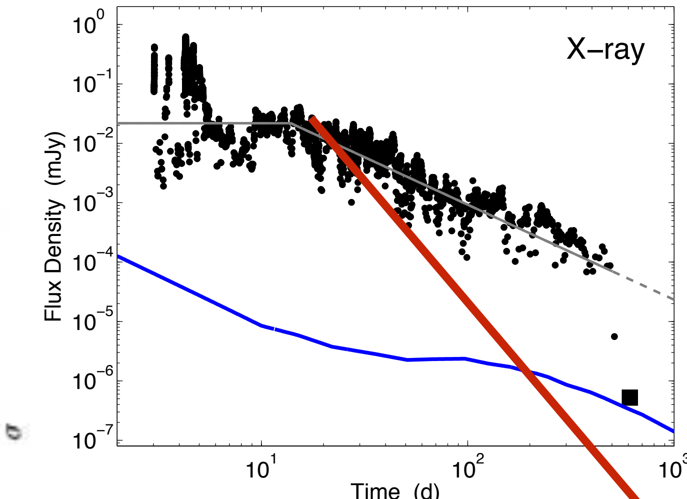

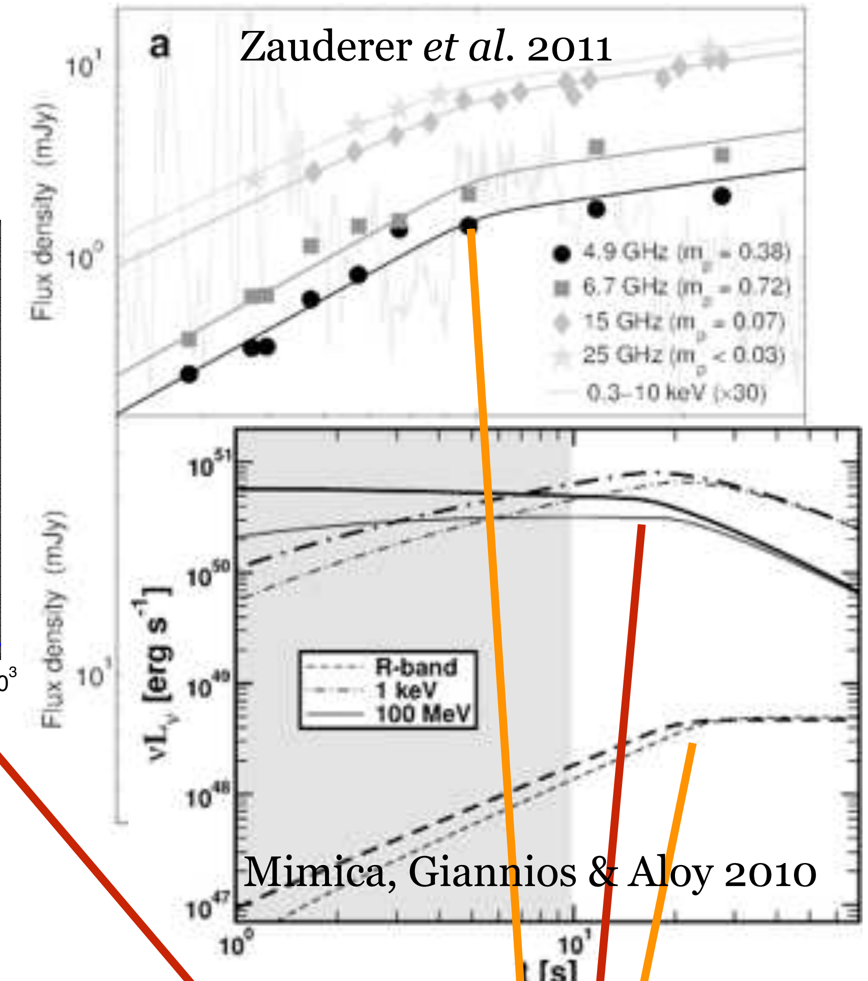

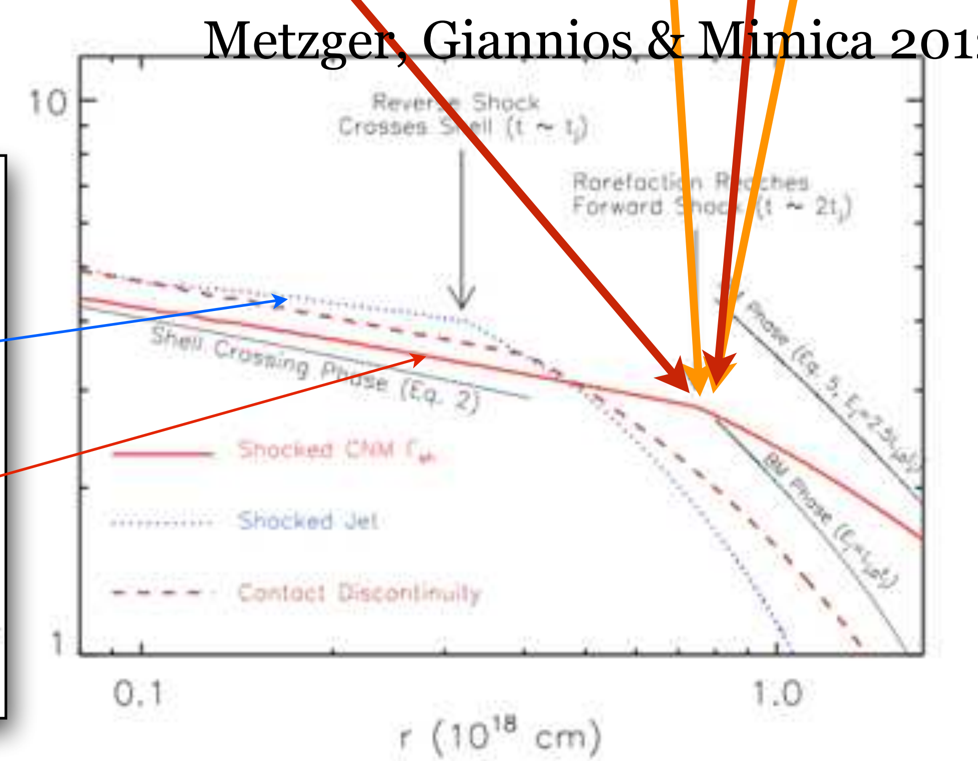

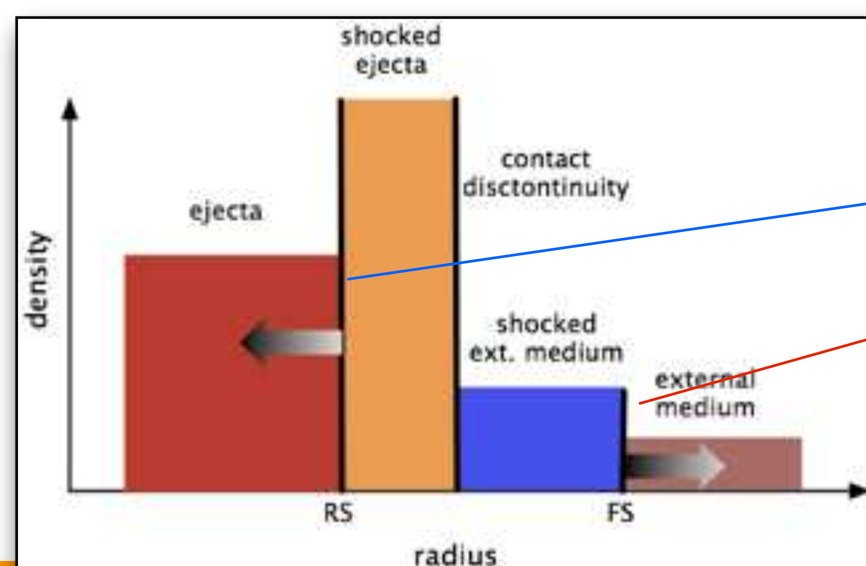

Long-term Evolution and Motivation for Simulations

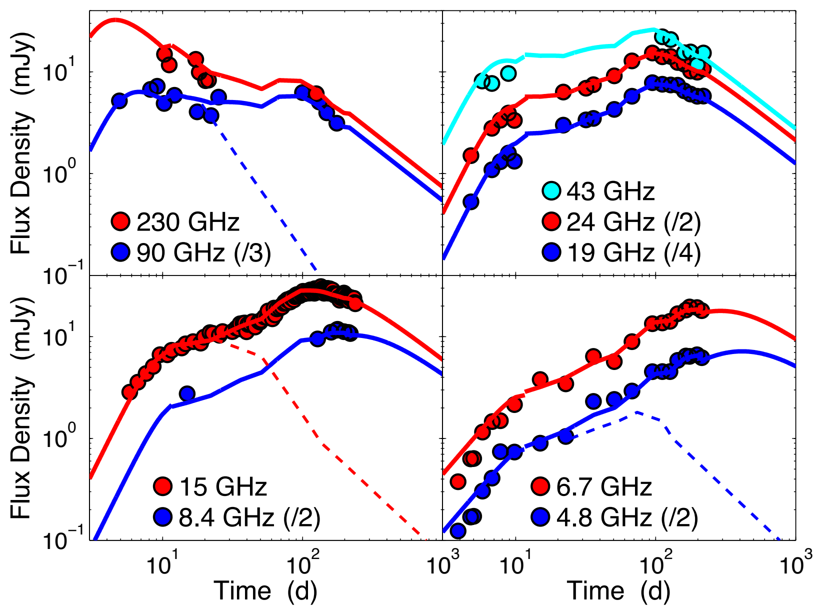

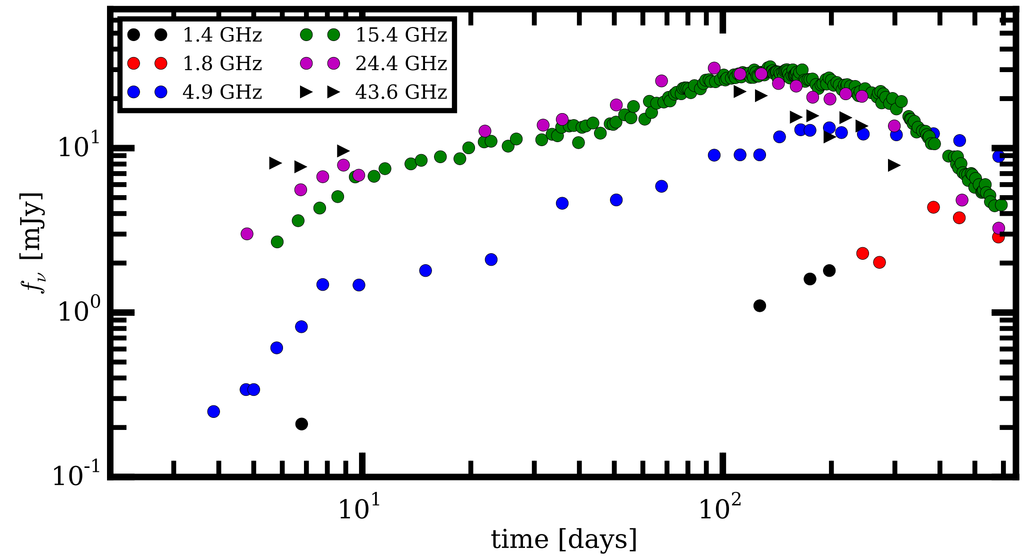

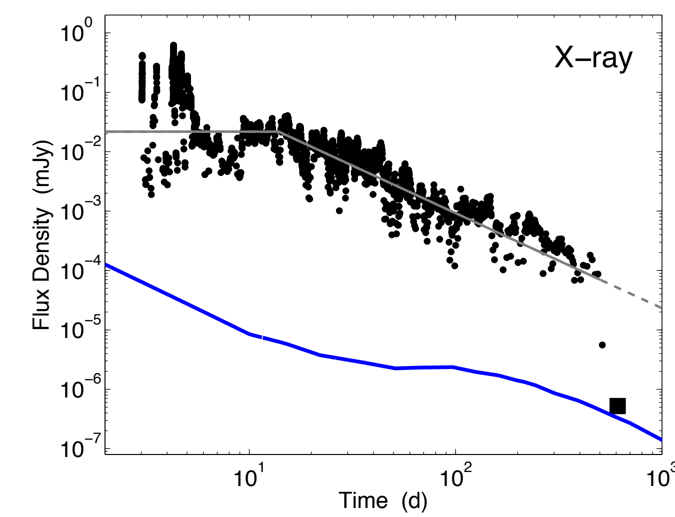

data from: Zauderer *et al.* 2013, Berger *et al.* 2012

- source unexpectedly brightens a few months after initial peak
- in contrast to predictions of a 1D blast wave model
- possibilities:
  - slower material ejected after fast jet, but containing 20x the energy (Berger *et al.* 2012)
  - complex environment: stellar debris and circumnuclear medium (de Colle *et al.* 2012)
  - abrupt change in CNM density profile (unlikely in GRB case; Mimica & Giannios 2011; Gat *et al.* 2013)
  - forward-shock accelerated electrons cooled by X-rays (Kumar *et al.* 2013)
  - jet has a complex angular structure (Tchekhovskoy *et al.* 2014;, Wang *et al.* 2014)
- our work: 1D- and 2D simulations exploring different possibilities

Example: 1D RHD Simulations

Physical model

$$L_j(t) = L_{j,0}\left(\max\left[1, \left(\frac{t}{t_{j,0}}\right)\right]\right)^{-5/3}$$

$$L_{j,0} = 5 \times 10^{47}\ \mathrm{erg\ s^{-1}}$$

$$t_{j,0} = 5 \times 10^{5}\ \mathrm{s}$$

$$\Gamma_{j,0} = 5 \qquad \theta_{j,0} = 0.3\ \mathrm{rad}$$

$$\Theta_0 := \frac{P_0}{\rho_0 c^2} = 10^{-2}$$

$$\mathrm{TM\ EOS}: h(\Theta) = \frac{5}{2}\Theta + \sqrt{\frac{9}{4}\Theta^2 + 1}$$

(Mignone *et al.* 05)

$$R_{j,0} = 5 \times 10^{16}\ \mathrm{cm}$$

$$n_{\mathrm{ext}}(R) = 3.33 \times 10^{1}\ \mathrm{cm^{-3}}\left(\frac{R}{R_{j,0}}\right)^{-1}$$

$$T_{\max} \approx 15\ \mathrm{years}$$

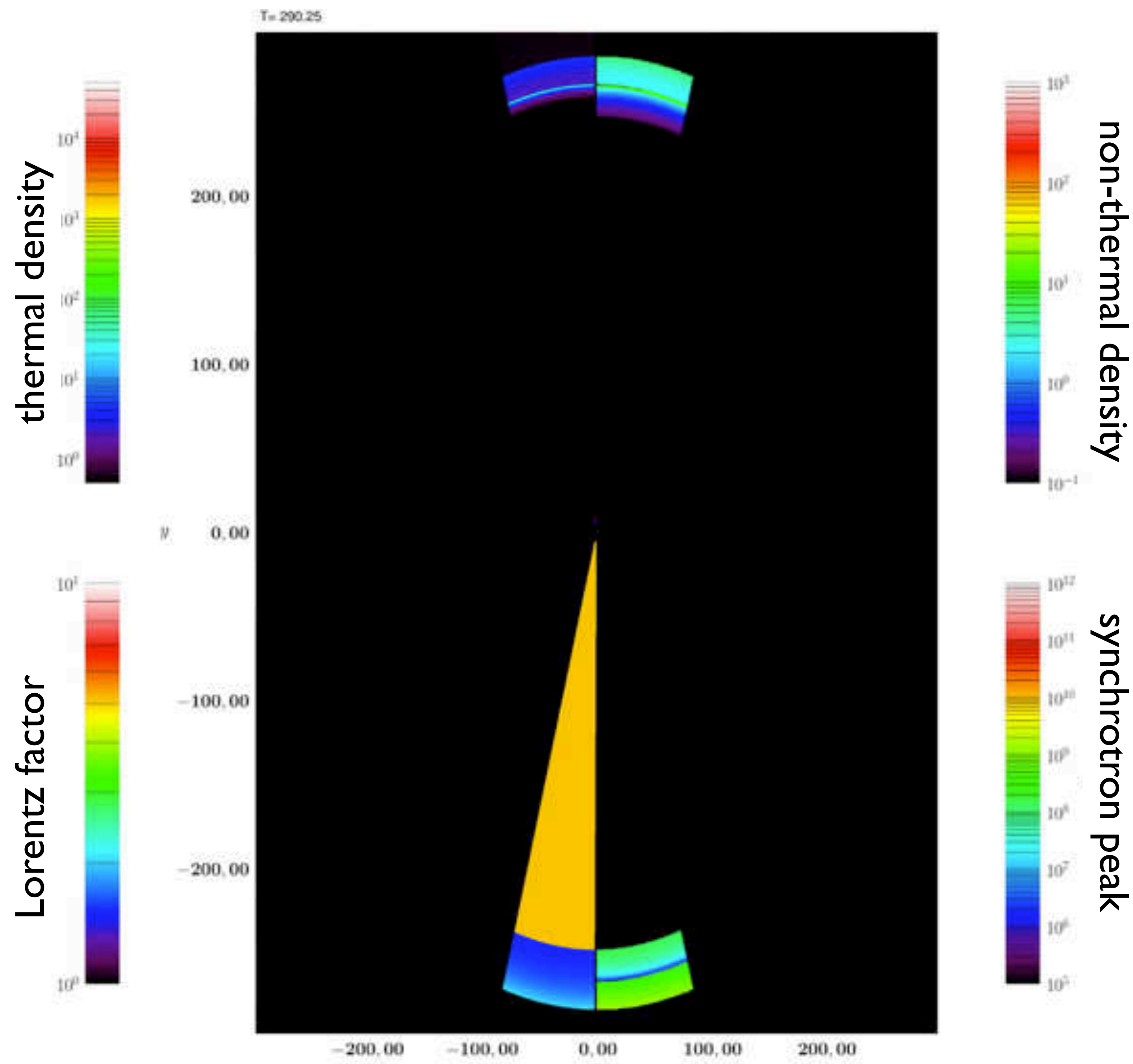

Mimica, Giannios, Metzger & Aloy, in prep.

Example: 1D RHD Simulations

Physical model

$$L_j(t) = L_{j,0}\left(\max\left[1, \left(\frac{t}{t_{j,0}}\right)\right]\right)^{-5/3}$$

$$L_{j,0} = 5 \times 10^{47}\ \mathrm{erg\ s^{-1}}$$

$$t_{j,0} = 5 \times 10^5\ \mathrm{s}$$

$$\Gamma_{j,0} = 5 \qquad \theta_{j,0} = 0.3\ \mathrm{rad}$$

$$\Theta_0 := \frac{P_0}{\rho_0 c^2} = 10^{-2}$$

$$\mathrm{TM\ EOS}: h(\Theta) = \frac{5}{2}\Theta + \sqrt{\frac{9}{4}\Theta^2 + 1}$$

(Mignone *et al.* 05)

$$R_{j,0} = 5 \times 10^{16}\ \mathrm{cm}$$

$$n_{\mathrm{ext}}(R) = 3.33 \times 10^1\ \mathrm{cm^{-3}}\left(\frac{R}{R_{j,0}}\right)^{-1}$$

$$T_{\max} \approx 15\ \mathrm{years}$$

Mimica, Giannios, Metzger & Aloy, in prep.

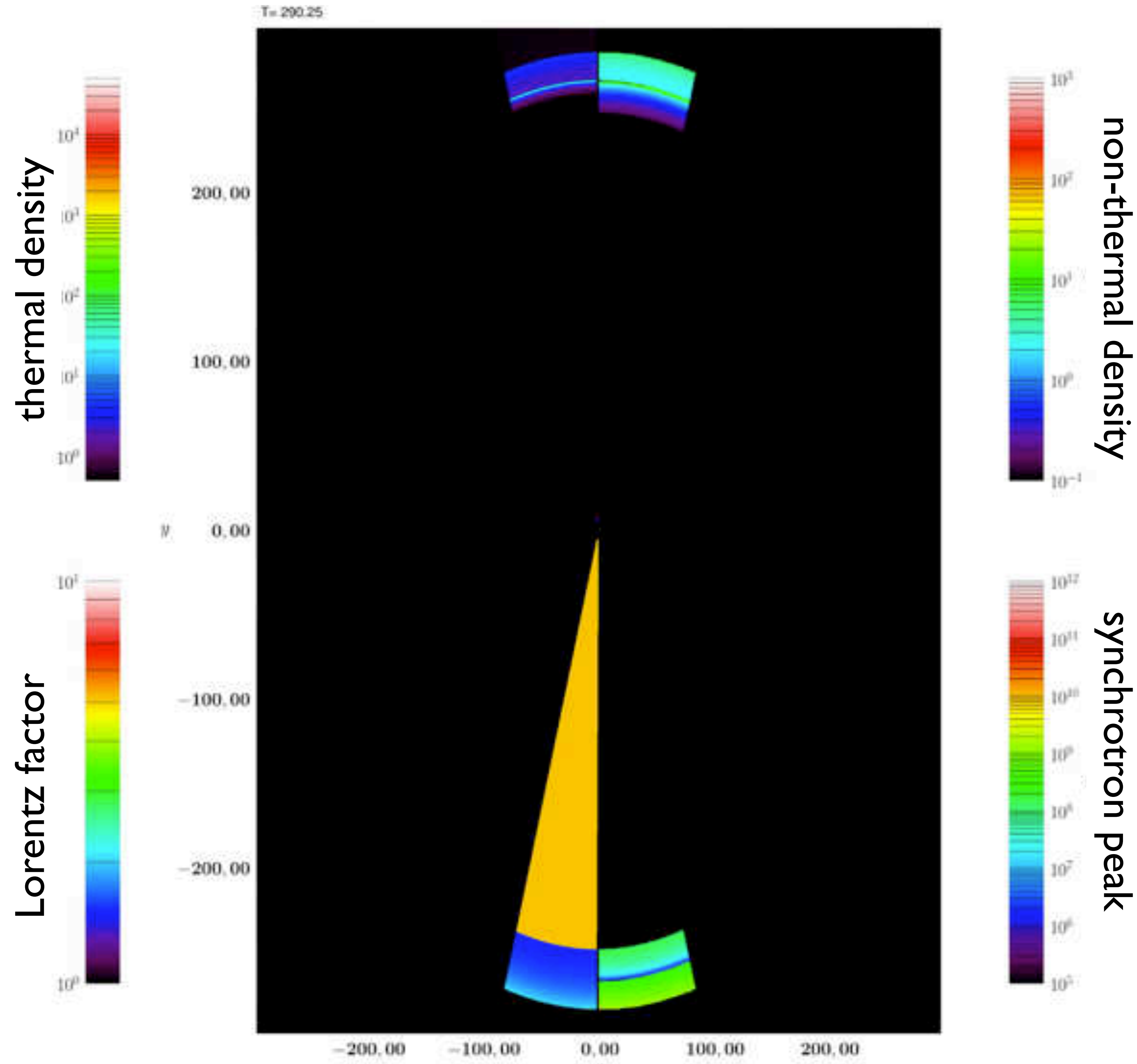

On-axis 1D Simulation Light Curves

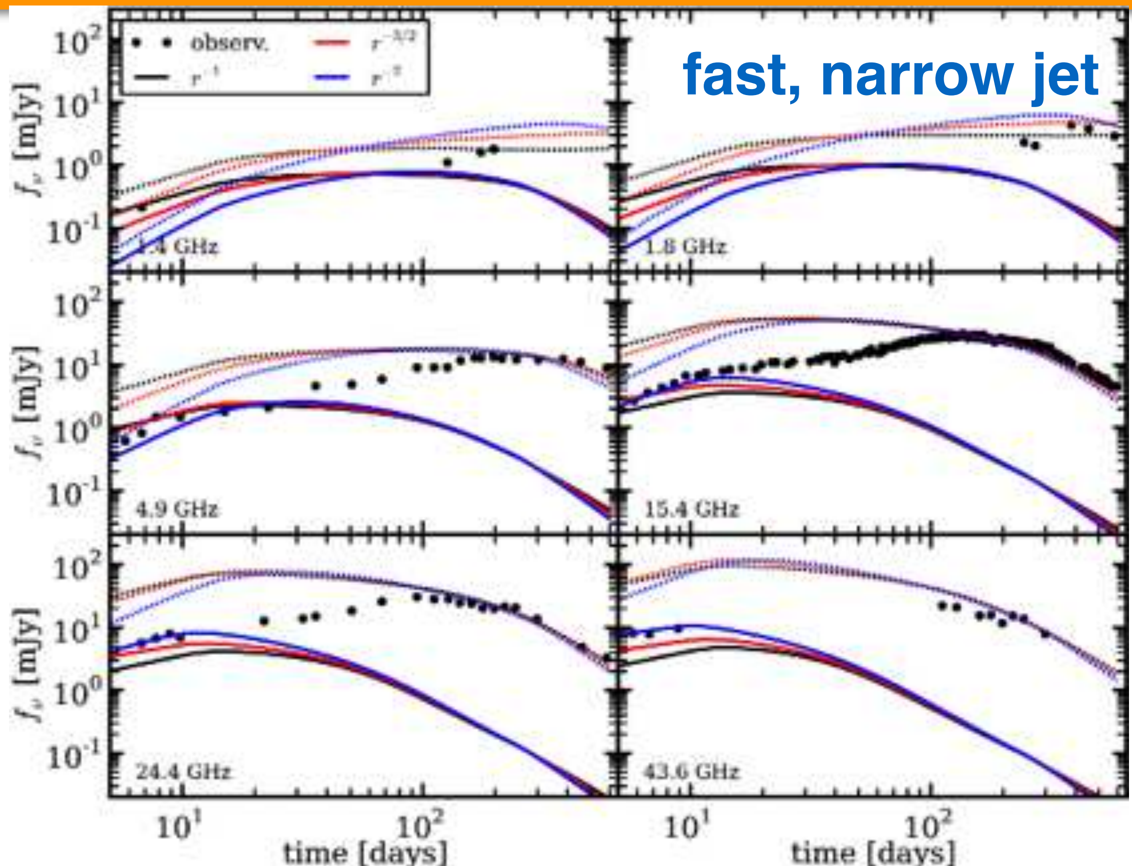

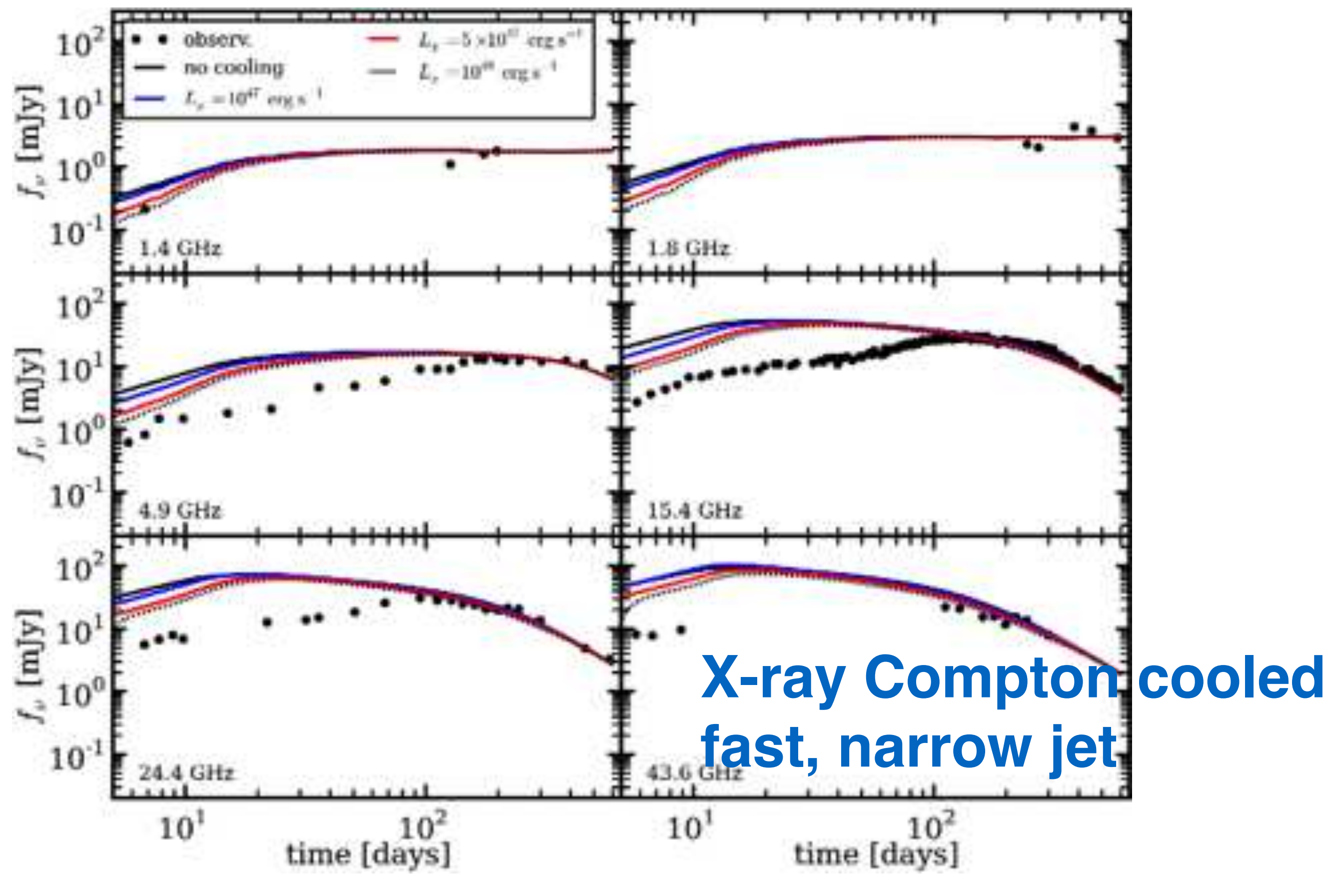

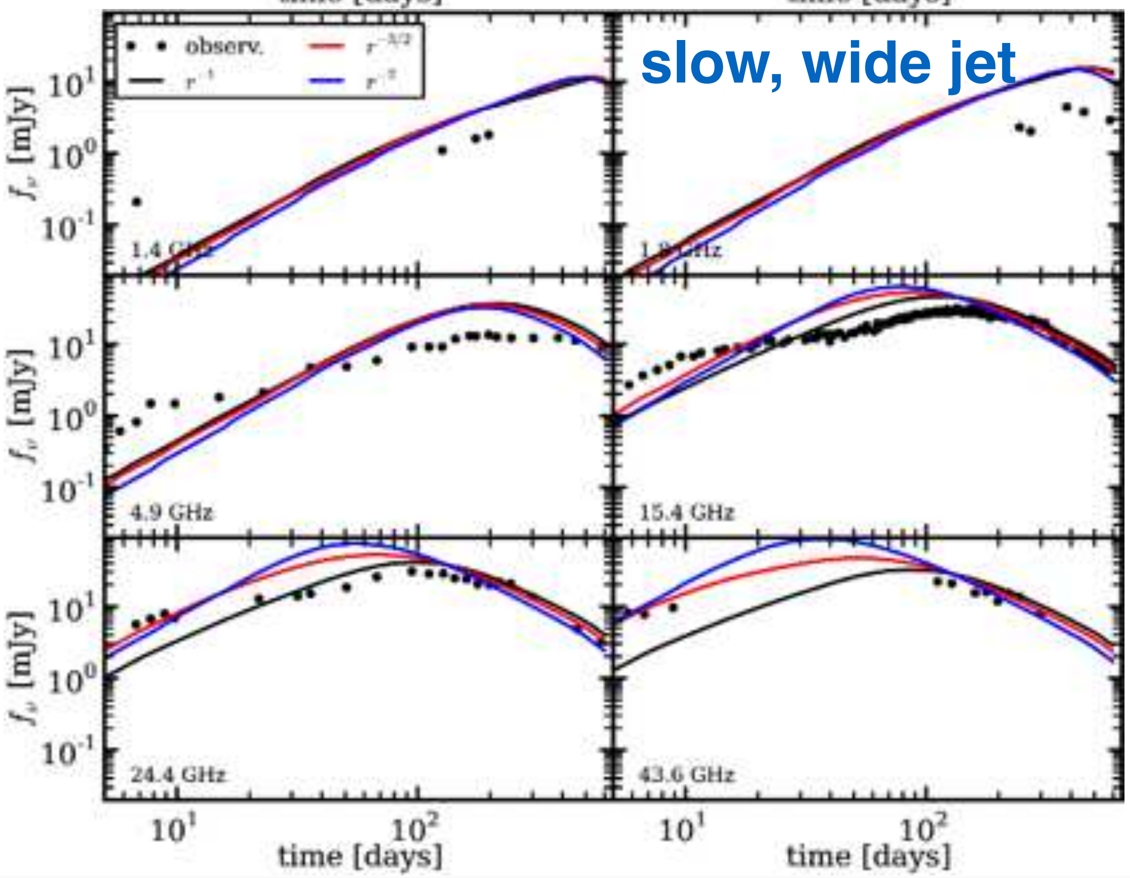

- 1D simulation parameter scan:
  - fixed L_j/n_{18}, t_j, θ_j, Γ_j
  - variable n_{18}, ϵ_e, ϵ_B, ζ_e
- single-component jet models cannot explain early- and late-time observations simultaneously
  - fast, narrow jet: early times
  - slow, wide jet: late times
- X-ray cooling does not produce sufficient radio-emission early-time deficit

1D Two-component Jets: Light Curves

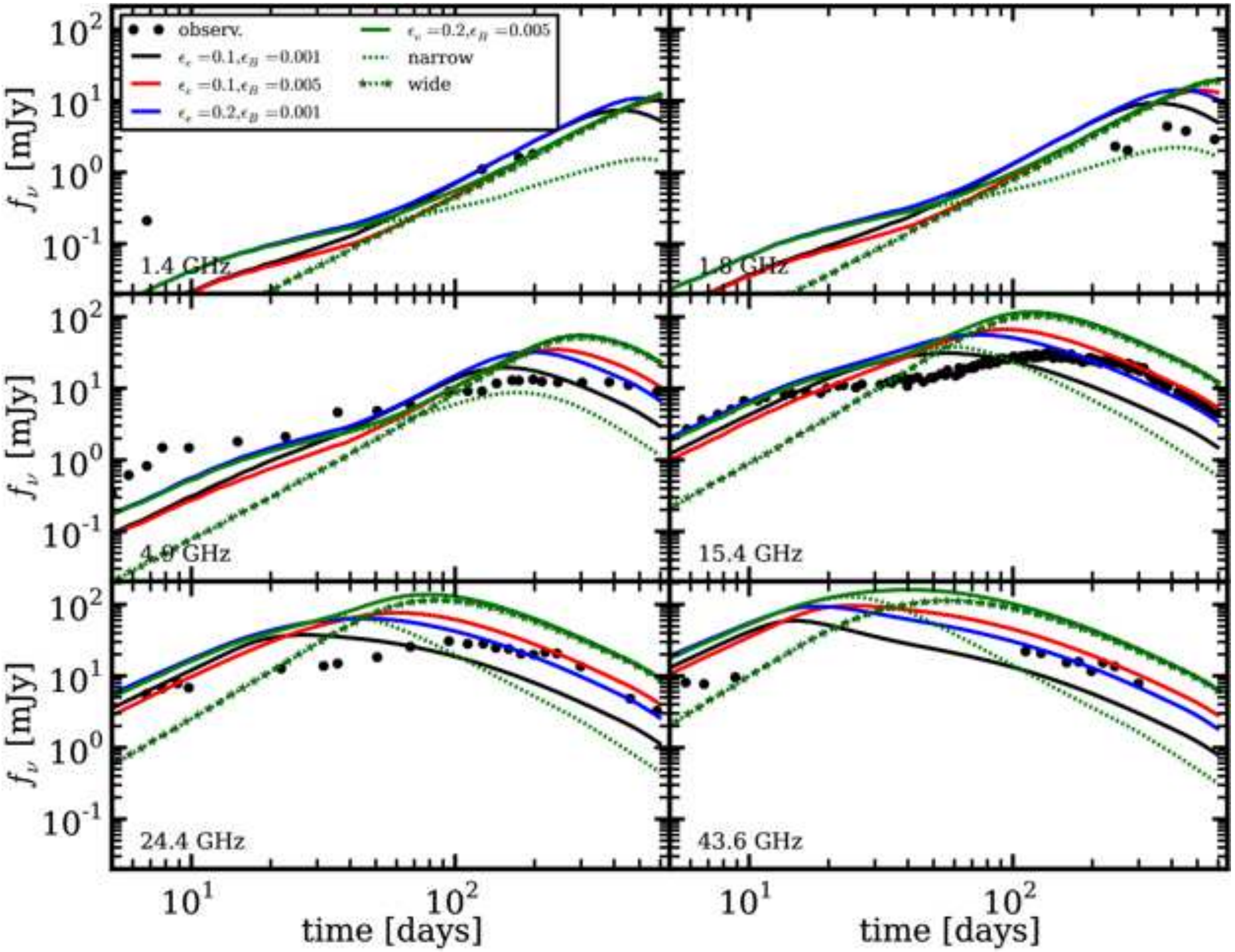

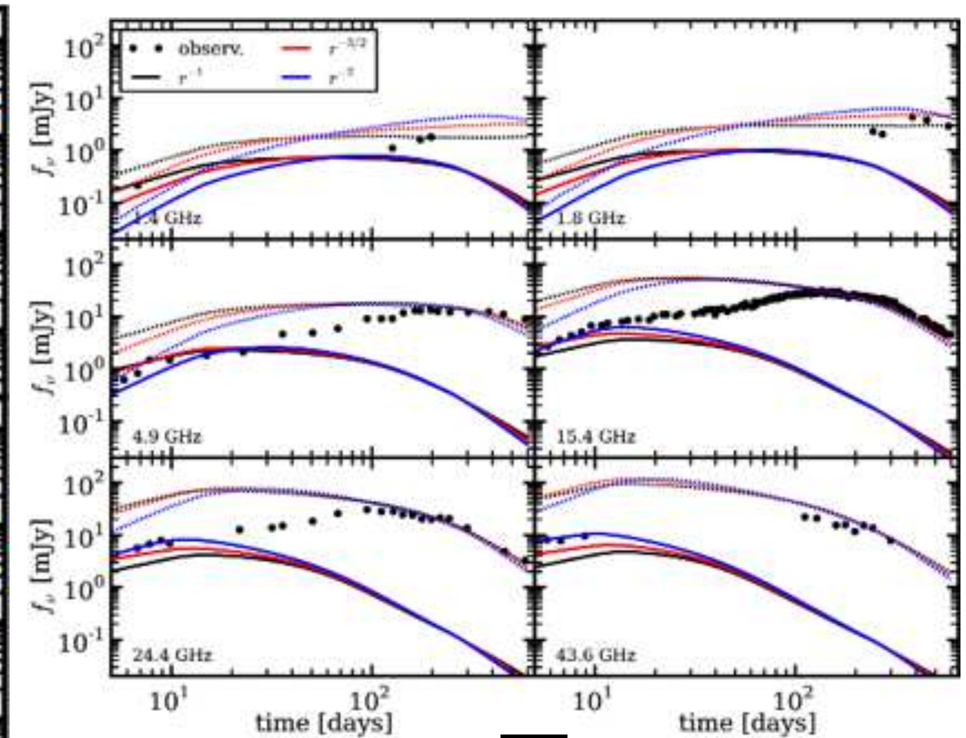

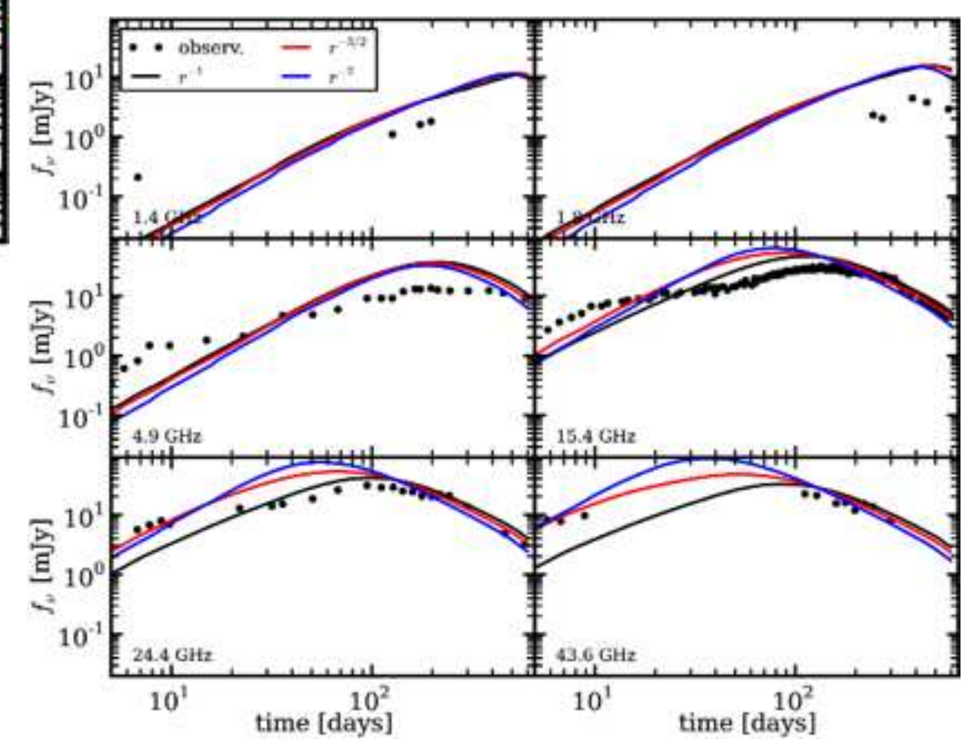

- two-component jet:
  - fast core $\Gamma_f=10$, $\theta_f=0.1$ rad
  - slow sheath $\Gamma_s=2$, $\theta_s=0.5$ rad
- strong dependence on ε_B, ε_E

1D Two-Component Jet: On-axis Radio Maps

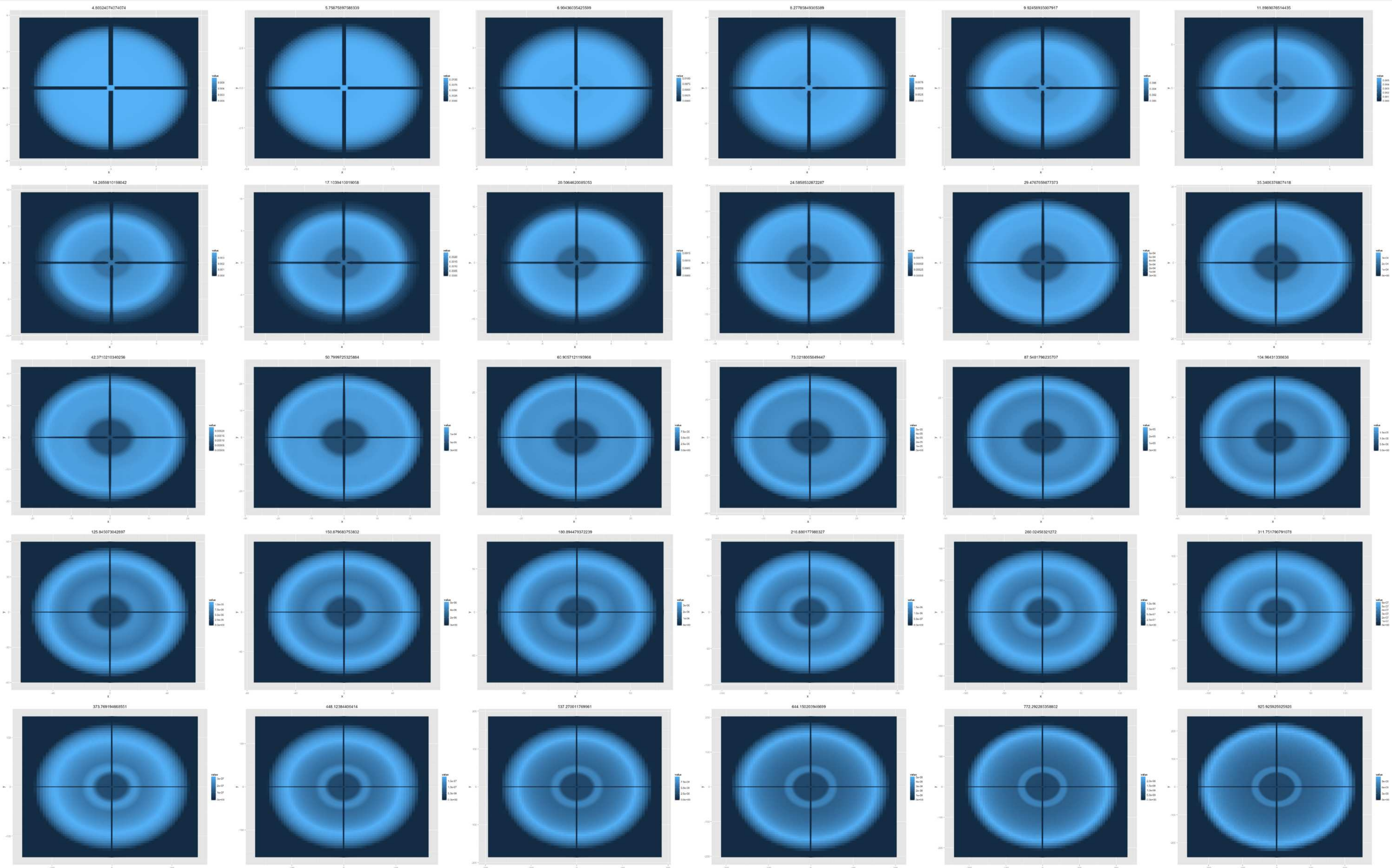

1D Two-Component Jet: On-axis Radio Maps

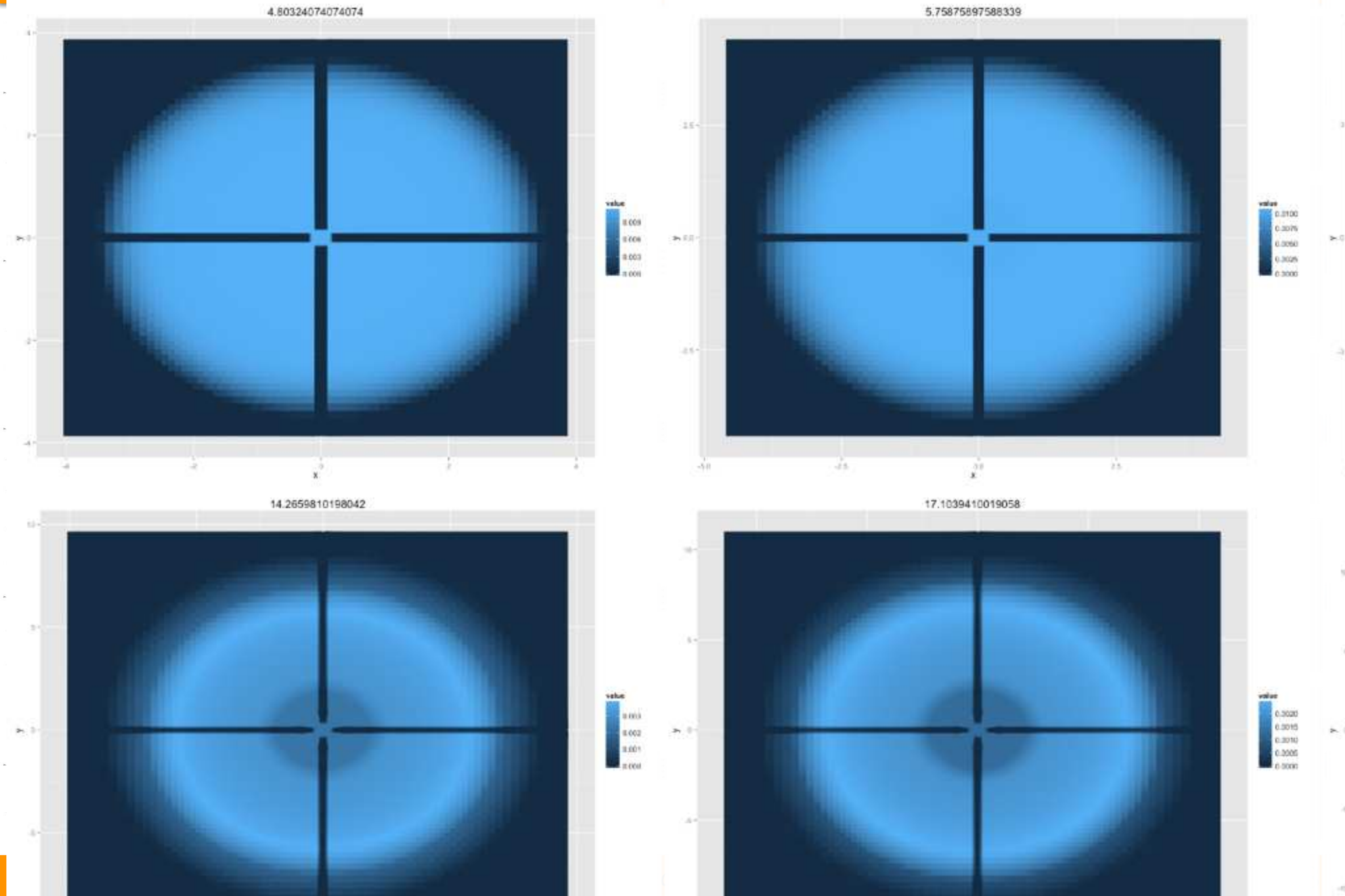

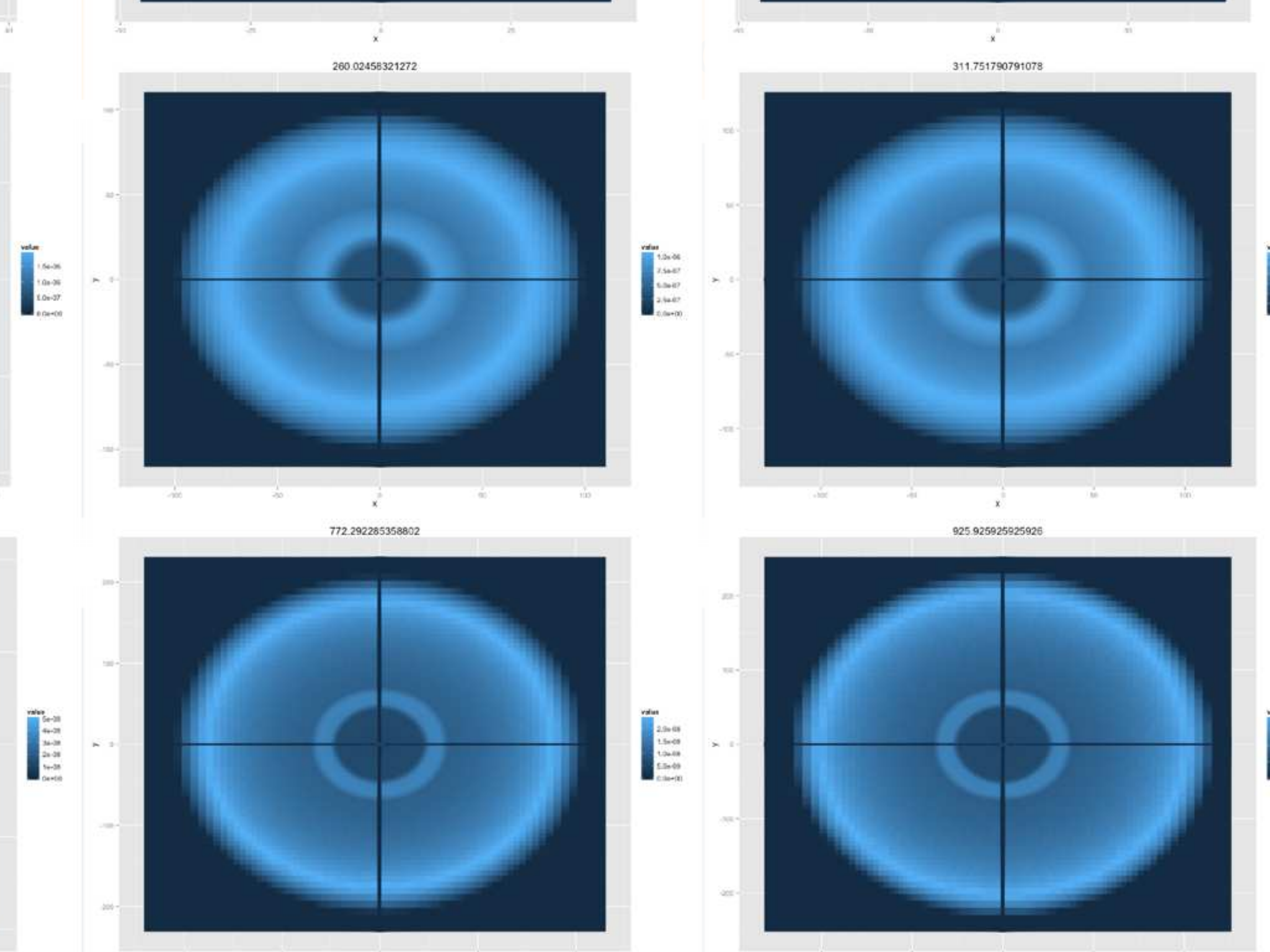
260.02458321272
311.751790791078
772.292285358802
925.925925925926
value
x
y

1D Two-Component Jet: Off-axis Radio Maps

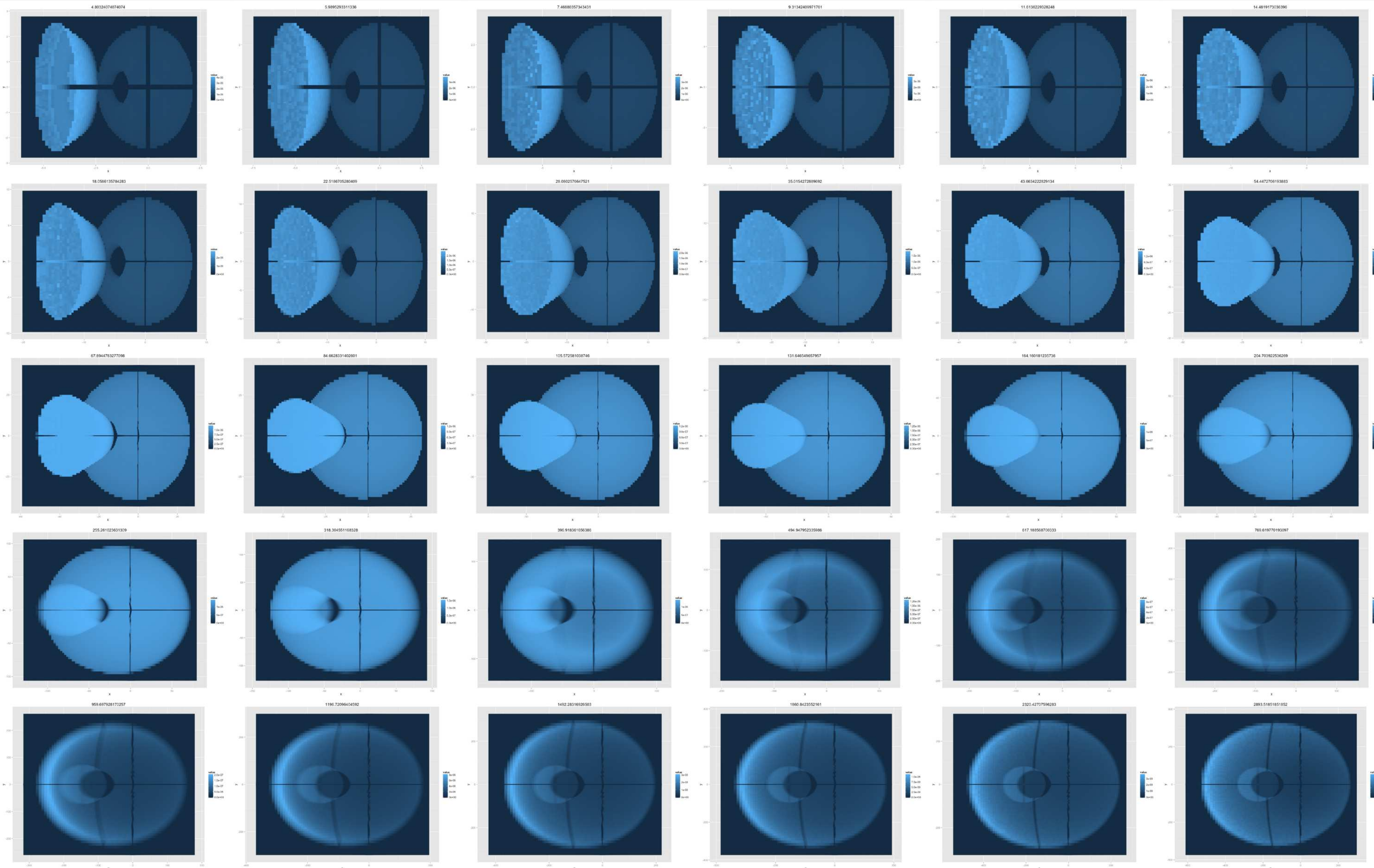

9.31342409971761

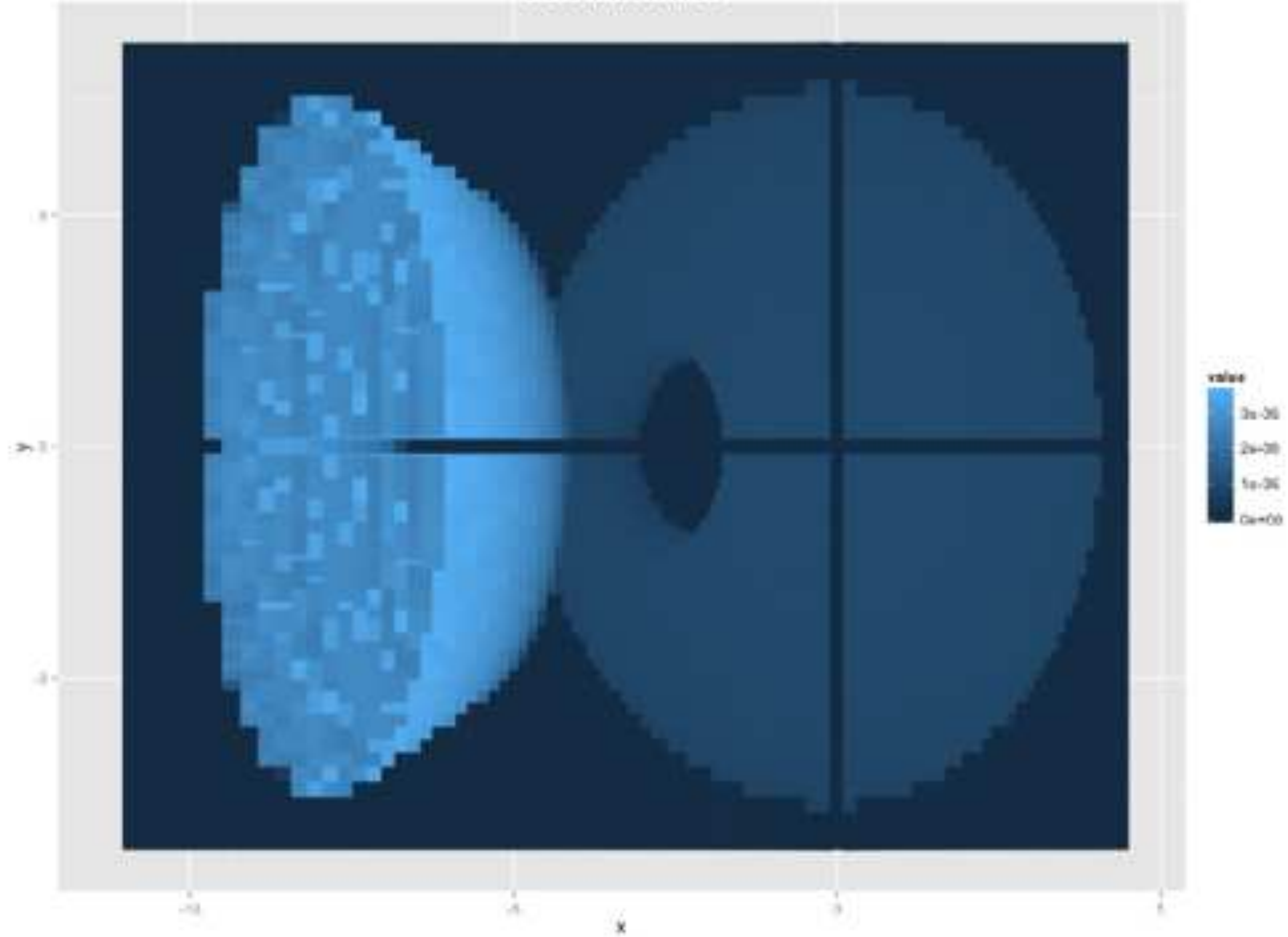

11.6136229328248

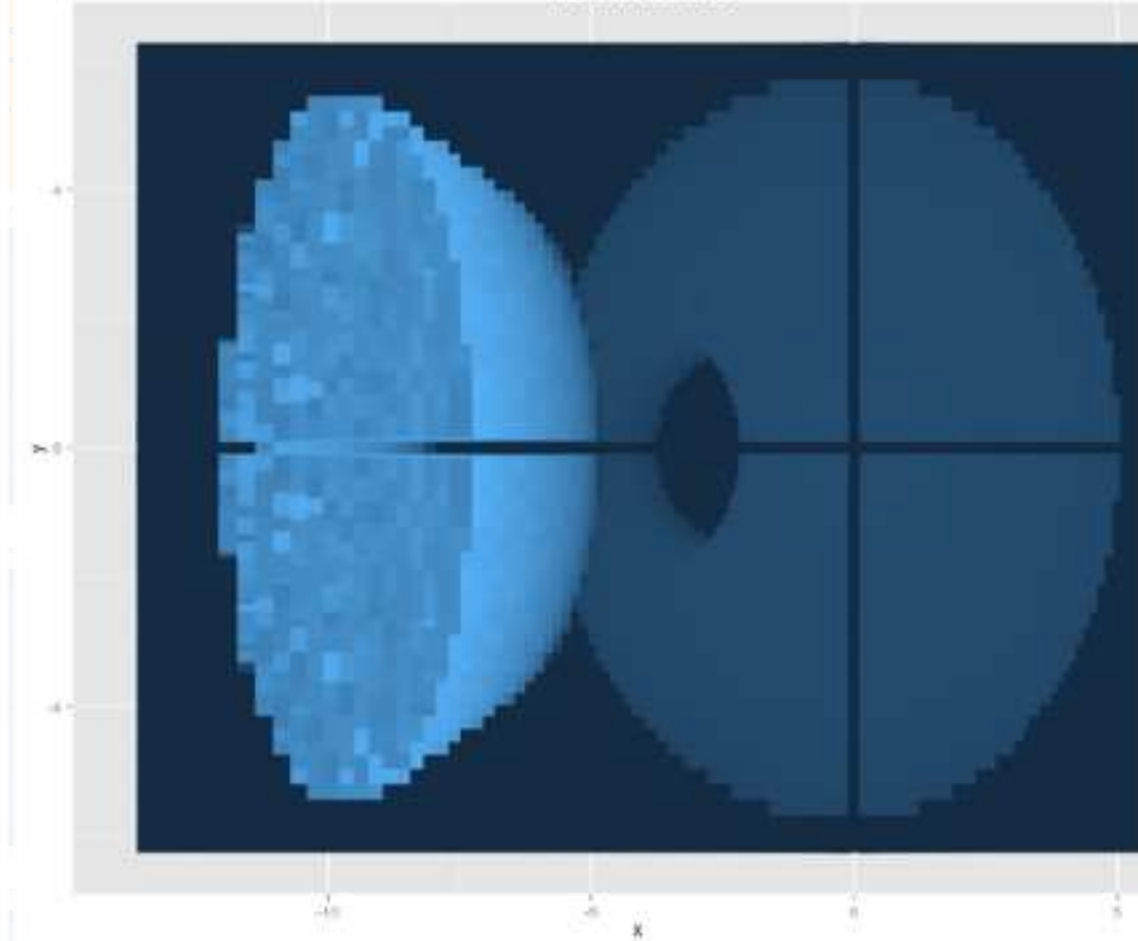

35.0154272889692

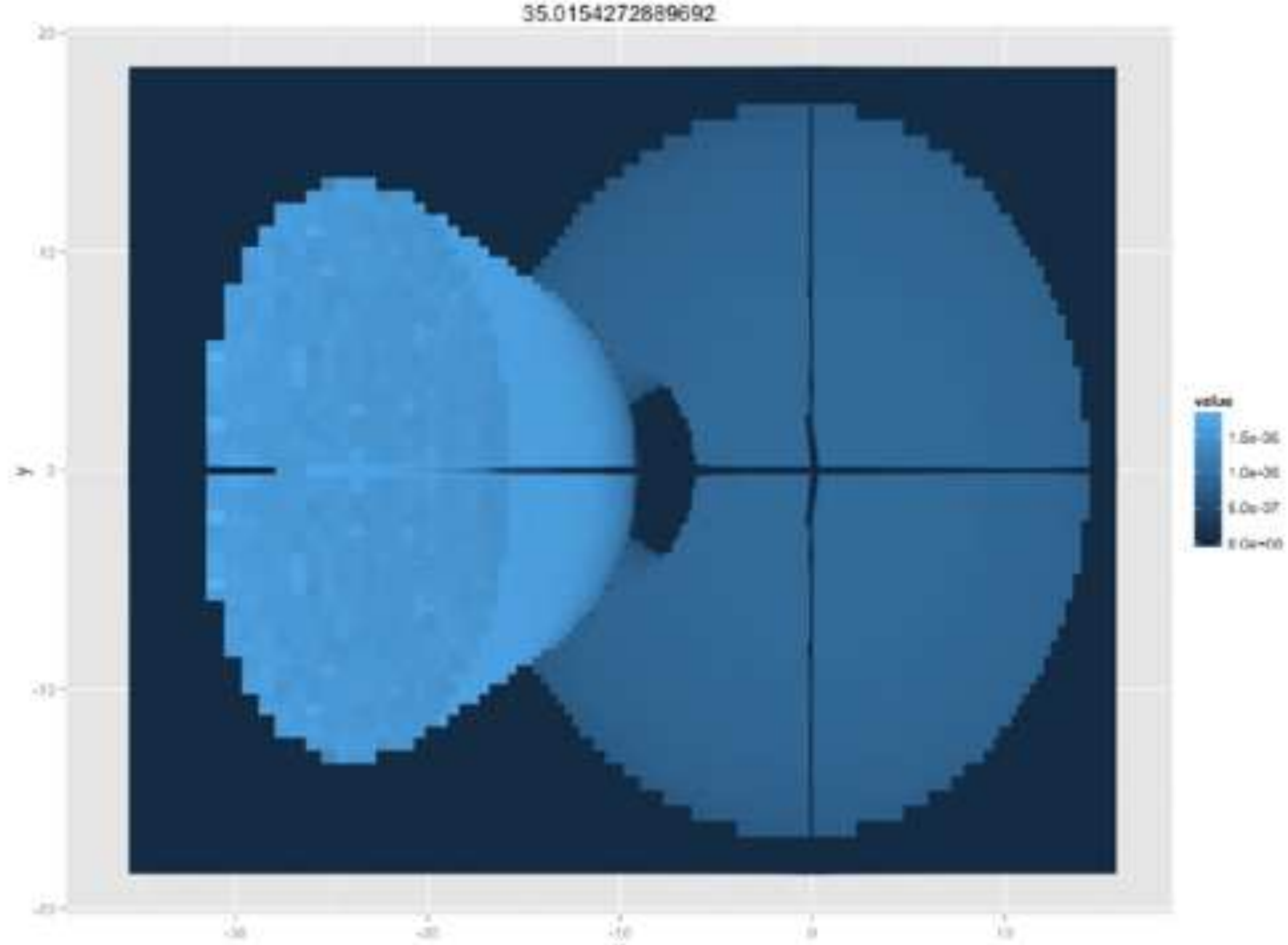

43.6634222829134

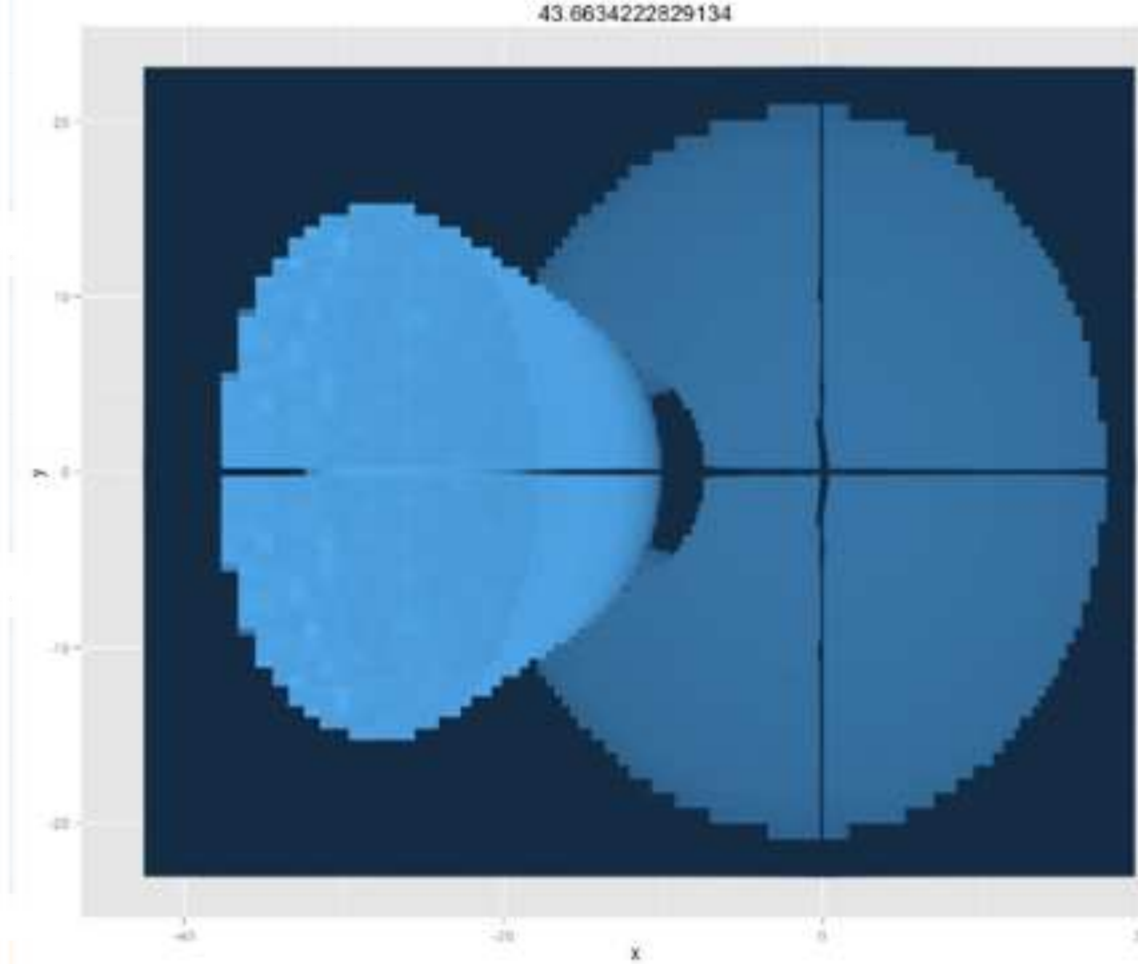

131.646549657957

164.160181235736

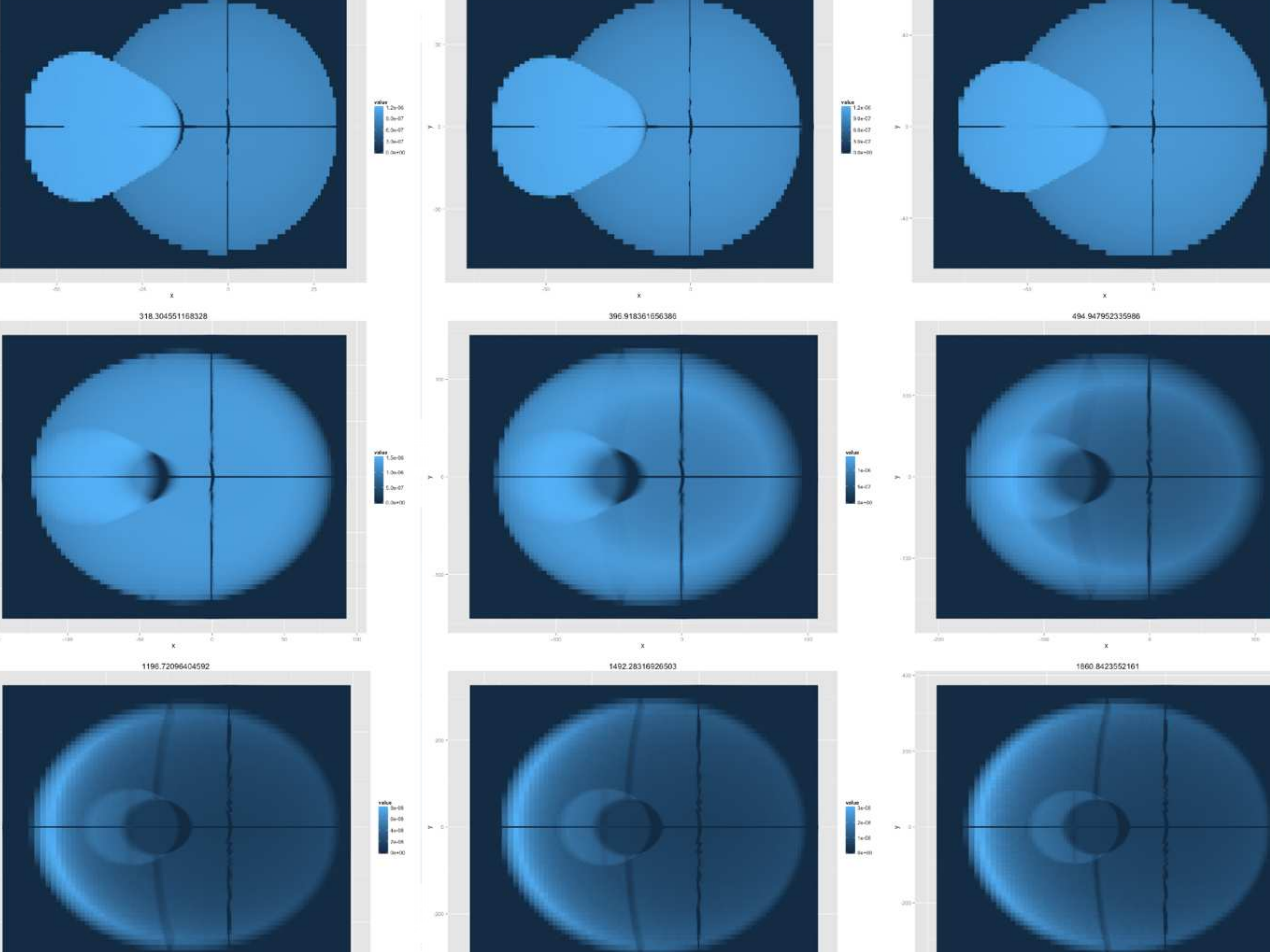

value
x
318.304551168328
396.918361656386
494.947952335986
1196.72096404592
1492.28316926503
1860.8423552161
y

2D Simulations *(preliminary)*

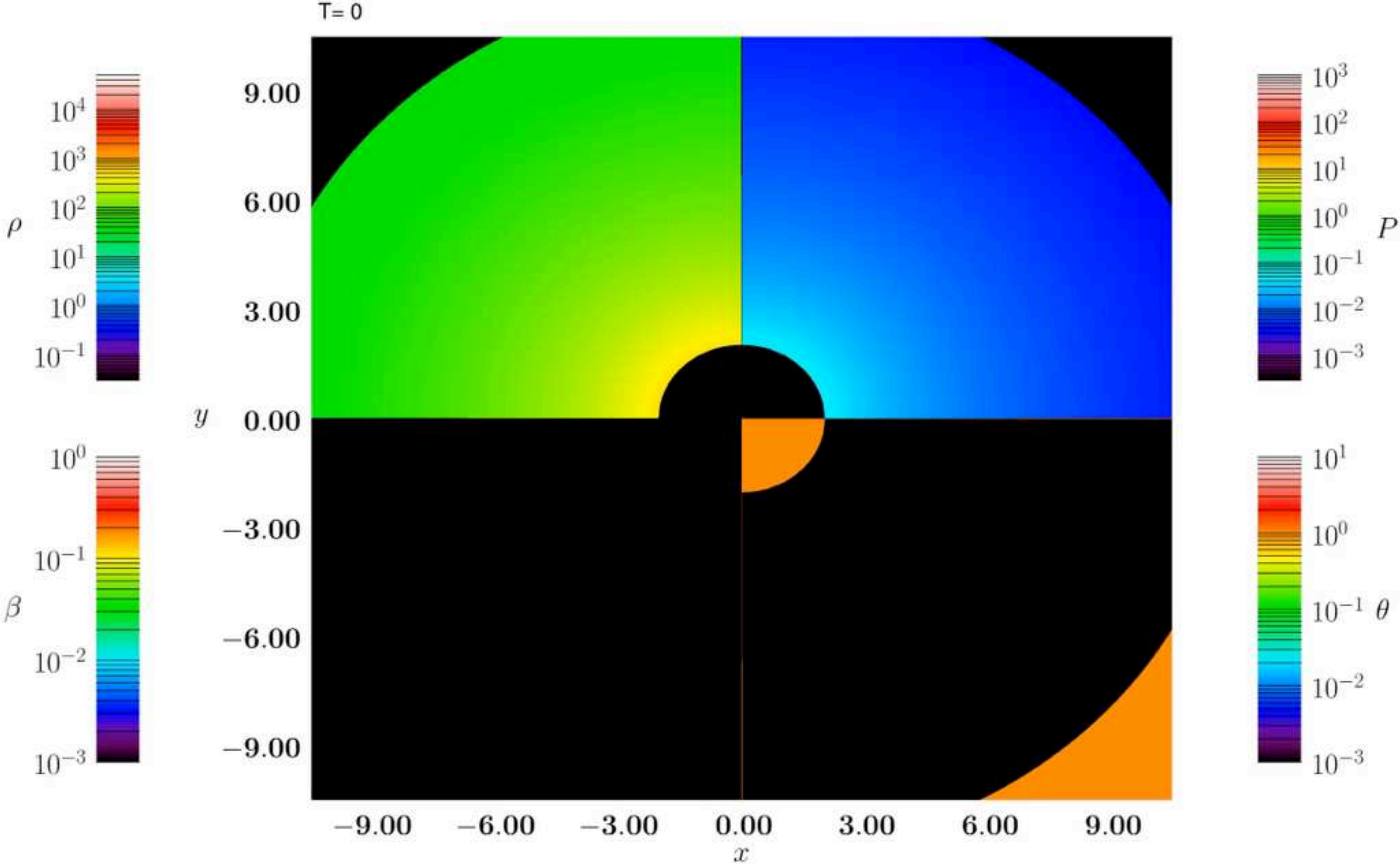

2D Simulations *(preliminary)*

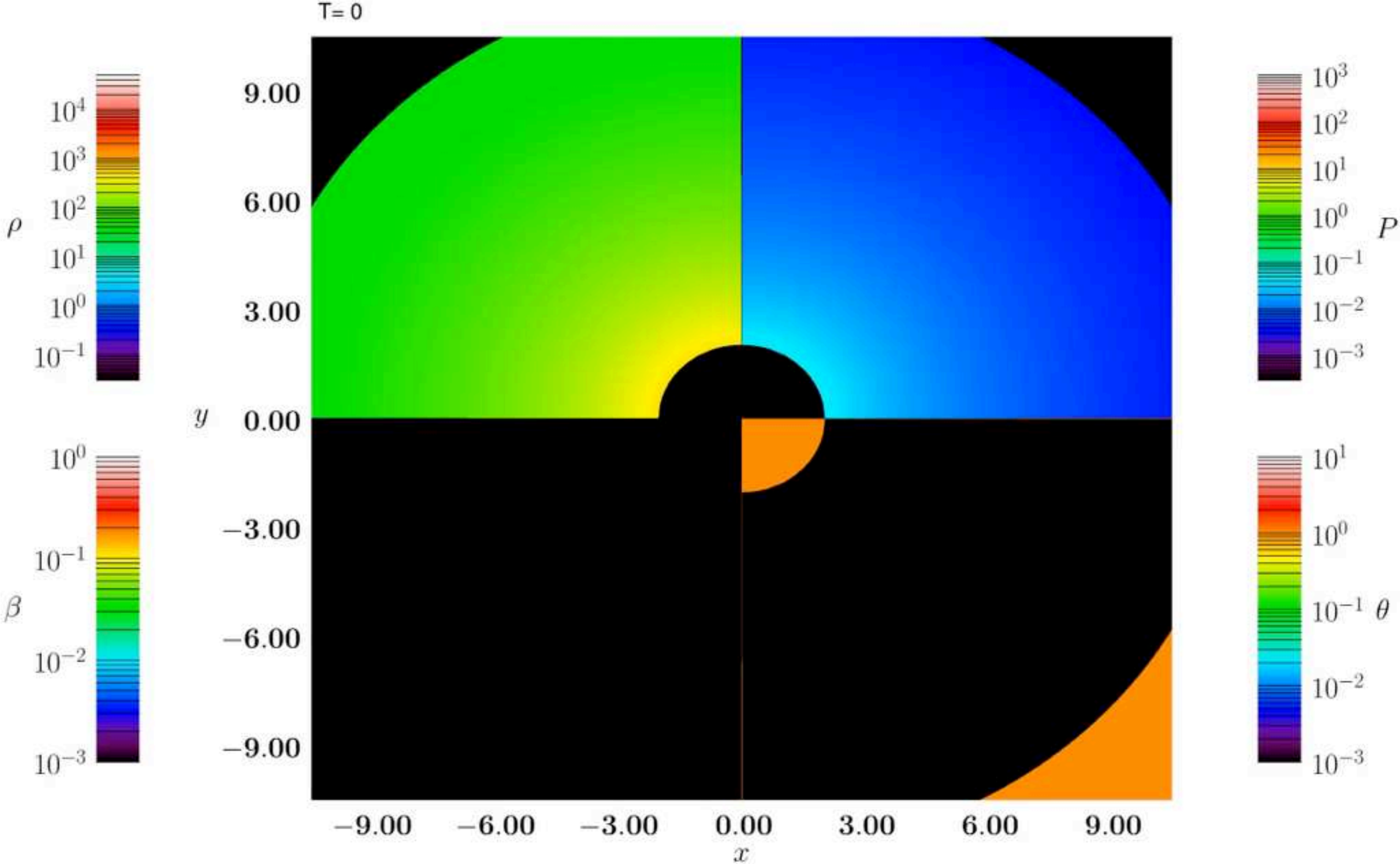

2D Simulations *(preliminary)*

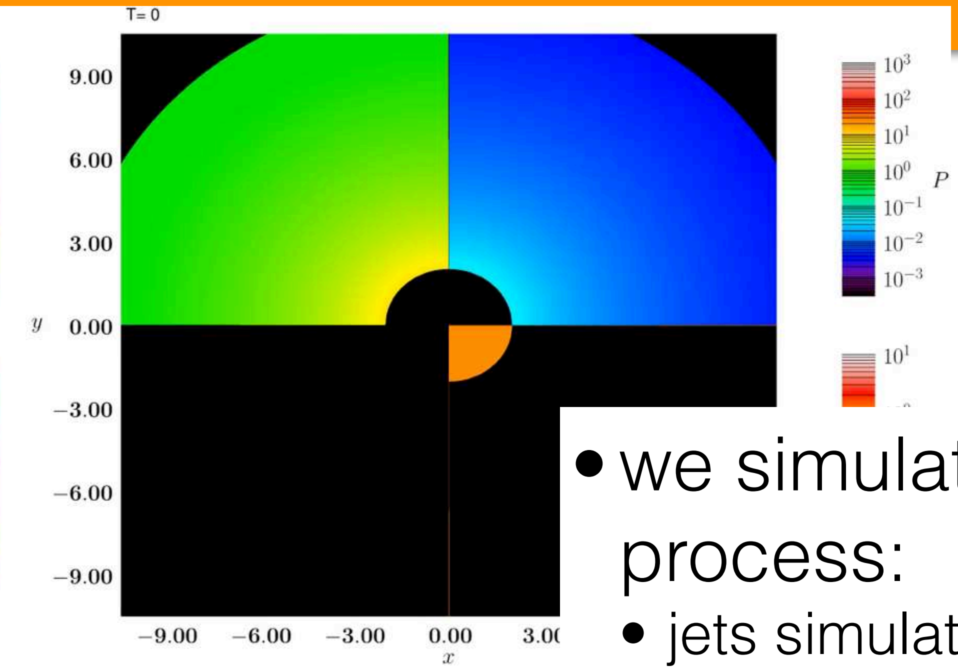

- we simulate jet dynamics and emission using an iterative process:
  - jets simulated using 1D and 2D RHD simulations
  - non-thermal and thermal emission computed by post-processing a large number (~10^3) simulation snapshots
  - emission, absorption, intensity analysed in observer frame
- GRB 101225A:
  - modelled as jet interacting with progenitor outer layers and interstellar medium
  - secondary star ejects CE-shell which disrupts the jet (no classical afterglow)
  - thermal emission predominantly emitted from jet/CE-shell interaction region
  - non-thermal emission comes from the bubble forward shock
- Swift J1644+53 (in progress):
  - modelled as TDE-powered jet interacting with circumnuclear medium
  - unexpected late-time increase in radio emission
  - single-component jet models: probably excluded
  - early-time X-ray cooling: probably excluded
  - external medium structure: probably excluded
  - most promising model: two-component jet